Use of Lightweight Sand for Internal Curing to Improve Performance of Concrete Infrastructure

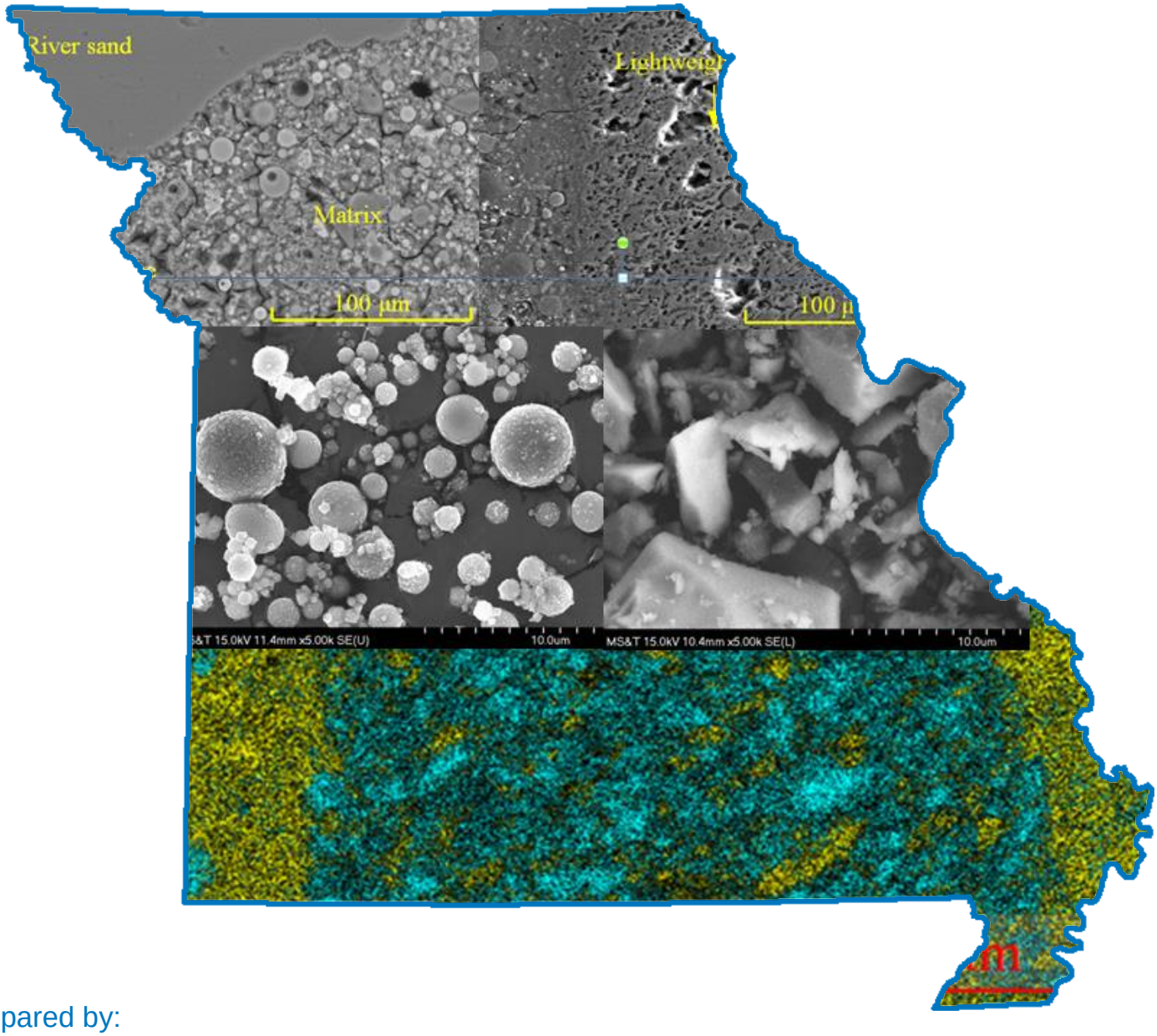

Prepared by:
Kamal H. Khayat, P. Eng., Ph.D.
Weina Meng, Ph.D., Post-doctoral Fellow
Mahdi Valipour, Ph.D., Post-doctoral Fellow
Matthew Hopkins, Ph.D. Candidate
Missouri University of Science and Technology, Department of Civil, Architectural and Environmental Engineering

Final Report Prepared for Missouri Department of Transportation
March 2018 Project TR201701 Report cmr18-005

TECHNICAL REPORT DOCUMENTATION PAGE

1. Report No.	2. Government Accession No.	3. Recipient's Catalog No.
cmr 18-005		

4. Title and Subtitle	5. Report Date
Use of Lightweight Sand for Internal Curing to Improve Performance of Concrete Infrastructure	February 2018 Published: March 2018
	6. Performing Organization Code

7. Author(s)	8. Performing Organization Report No.
Kamal H. Khayat, P. Eng., Ph.D. https://orcid.org/0000-0003-1431-0715 Weina Meng, Ph.D., Post-doctoral Fellow https://orcid.org/0000-0001-6195-0518 Mahdi Valipour, Ph.D., Post-doctoral Fellow https://orcid.org/0000-0002-0739-0211 Matthew Hopkins, Ph.D. Candidate	

9. Performing Organization Name and Address	10. Work Unit No.
Department of Civil, Architectural and Environmental Engineering Missouri University of Science and Technology 1401 N. Pine St., Rolla, MO 65409	**11. Contract or Grant No.** MoDOT project # TR201701

12. Sponsoring Agency Name and Address	13. Type of Report and Period Covered
Missouri Department of Transportation (SPR) Construction and Materials Division P.O. Box 270 Jefferson City, MO 65102	Final Report (July 2016-January 2018)
	14. Sponsoring Agency Code

15. Supplementary Notes

Conducted in cooperation with the U.S. Department of Transportation, Federal Highway Administration. MoDOT research reports are available in the Innovation Library at http://www.modot.org/services/or/byDate.htm.

16. Abstract

The project presented in this report aimed to develop an effective methodology to use saturated lightweight sand (LWS) for internal curing to enhance concrete performance and prolong service life of concrete structures. High-performance concrete (HPC) mixtures approved by MoDOT for pavement and bridge deck structures were used for the baseline mixtures. Five different types of saturated LWS employed at various contents were investigated to evaluate the optimum dosage of LWS and maximize its effectiveness on enhancing concrete performance. The content of LWS was varied to ensure the introduction of internal curing water that can secure up to 150% of the water consumed by chemical shrinkage during cement hydration (As per ASTM C1761). Performance improvement from the LWS focused mainly on reducing autogenous and drying shrinkage and the resulting cracking potential without sacrificing durability and cost competence. Proper combinations of internal and external curing were found to enhance shrinkage mitigation. Under 7 days of initial moisture curing, HPC made with the LWS3 resulted in the lowest overall shrinkage. The Bridge-LWS2-150% exhibited the best performance in mitigating autogenous shrinkage where the concrete maintained 160 micro-strain of expansion even after 175 days of age. The lowest drying shrinkage was obtained with the Bridge-LWS3-50% mixture (340 micro-strain) at 175 days subjected to 28 days of moist curing. For the paving HPC, the lowest drying shrinkage at 155 days was obtained with the Paving-LWS3-150% mixture (265 micro-strain) subjected to 28 days of moist curing. Concrete proportioned with the LWS2 expanded shale LWS exhibited the best compressive strength, regardless of the curing regime. In terms of initial moisture curing duration, the application of 7 days of moisture curing resulted in the highest compressive strength compared with other curing conditions. The 56-day compressive strength of HPC designated for bridge deck construction that was made with the LWS1 was up to 10 MPa (1,450 psi) greater than the Bridge-Reference concrete made without any LWS. The Bridge-LWS2-100% and Bridge-LWS1-50% mixtures exhibited the highest 56-day MOE of 42.5 GPa (6,615 ksi) under Standard curing. The Bridge-LWS3-100% mixture cured under Standard conditions had the highest 56-day flexural strength of 5.5 MPa (800 psi). The mixtures made with LWS2 presented the lowest sorptivity, regardless of the curing condition and LWS content. The findings from this comprehensive project provided a basis for: (1) new mixture design methodology and guidelines for using LWS for internal curing for bridge deck and pavement applications; and (2) validation of performance improvement when using internal curing and cost competitiveness in the State of Missouri.

17. Key Words	18. Distribution Statement
Binder content; Concrete curing; Curing agents; Field tests; High performance concrete; Laboratory tests; Mix design	No restrictions. This document is available through the National Technical Information Service, Springfield, VA 22161.

19. Security Classif. (of this report)	20. Security Classif. (of this page)	21. No. of Pages	22. Price
Unclassified.	Unclassified.	92	

USE OF LIGHTWEIGHT SAND FOR INTERNAL CURING TO IMPROVE PERFORMANCE OF CONCRETE INFRASTRUCTURE

By

Kamal H. Khayat, P. Eng., Ph.D.

Vernon and Maralee Jones Professor

Department of Civil, Architectural, and Environmental Engineering

Missouri University of Science and Technology

Weina Meng, Ph.D., Post-doctoral Fellow

Department of Civil, Architectural, and Environmental Engineering

Missouri University of Science and Technology

Mahdi Valipour, Ph.D., Post-doctoral Fellow

Department of Civil, Architectural, and Environmental Engineering

Missouri University of Science and Technology

Matthew Hopkins, Ph.D. Candidate

Department of Civil, Architectural, and Environmental Engineering

Missouri University of Science and Technology

Table of Contents

List of Illustrations

List of Tables

1. Introduction

1.1 Research objective

The project presented in this report seeks to develop a proper methodology to use saturated lightweight sand (LWS) to improve the performance and prolong the service life of concrete mixtures. High-performance concrete (HPC) approved by MoDOT was used for the baseline mixture and was modified with different types and contents of saturated LWS used for internal curing. This was done to evaluate the optimum dosage of LWSs and maximize their effectiveness on enhancing performance. The performance improvement from the LWS mainly focused on reducing shrinkage and resulting cracking potential without sacrificing durability and cost competence of the HPC.

The project established new mixture design and curing recommendations for concrete made with LWS and validated their performance through laboratory investigation. The results obtained in this work are expected to provide a basis for: (1) New mixture design methodology and guidelines for using LWS for bridge and pavement applications; and (2) Validation of performance improvement when using internal curing and cost competitiveness in the State of Missouri.

1.2 Research background

HPC is typically characterized by high binder content and low water-to-cementitious materials ratio (w/cm). The binder often contains some substitution of cement with supplementary cementitious materials (SCMs). Low w/cm and high binder content are necessary to ensure high strength and durability. The use of relatively low w/cm can lead to an increase in autogenous shrinkage and risk of cracking, unless the concrete is continuously maintained in saturated conditions by proper curing at early age.

Internal curing provided by different types of water-saturated materials can provide an internal source of water that can replace the water consumed by chemical shrinkage during hydration. Greater additions of water through internal curing can further reduce shrinkage. Crack width resulting from plastic shrinkage can also be reduced as the replacement volume of these water-saturated materials is increased. The major benefit of the internal curing is the reduction of cracking potential by reducing autogenous and/or drying shrinkage. In general, for a given period

of moist curing, concrete made with saturated LWS can exhibit significantly lower shrinkage than concrete without any LWS. A previous investigation on internal curing by LWS proved that concrete made with 30% LWS and 6 days of initial moist curing can exhibit total shrinkage of 640 microstrain at 91 days compared to 865 to 1,630 microstrain for similar concrete made without any LWS (Hwang et al., 2013).

In addition to the contribution to reducing autogenous shrinkage, for a given w/cm, the use of LWS can increase strength at later ages. The level of strength improvement resulting from the use of LWS depends on the w/cm. In the case of concrete made with 0.40 w/cm, compressive strength increase of concrete subjected to 6 days of moist curing was larger than that incorporating 30% LWS and 1 day of moist curing (Hwang et al., 2013). On the contrary, mixtures made with 0.30 w/cm exhibited larger strength increase due to the use of LWS than extended duration of moist curing. This indicates that the effect of internal curing through the use of saturated LWS is more significant for concrete with low w/cm that has less water available for cement hydration. The strength increase by the use of LWS makes it possible to reduce cement content, which could compensate for the additional cost increase by the use of LWS.

In order to achieve similar shrinkage, concrete made with LWS requires shorter moist curing compared to similar concrete without any water-saturated LWS. The reduction in the moist curing period can reduce the cost of curing in the field and enhance performance of the concrete that may not receive adequate moist curing in the field. For example, a previous study (Hwang et al., 2013) found that drying shrinkage reduction associated with the use of LWS was much greater in the case of air-dried concrete compared to concrete subjected to 6 days of moist curing (47% and 45% reduction for air-dried concrete vs. 34% and 30% reduction for moist-cured concrete).

The strength and durability requirments can limit the maximum allowable content of materials used for internal curing, such as saturated LWS. The effect of type and content of LWS can affect durability. For example, Hwang et al. (2013) compared the rapid chloride permeability (RCP) values of two similar concrete mixtures made with and without 30% LWS and found that for a given moist curing period, concrete made with 30% LWS replacement, by volume of total sand, exhibited slightly higher RCP values than concrete prepared without any LWS. However, the RCP spread between the two mixtures was limited to approximately 400 Coulomb, which is wihin the repeatability limited of the RCP test method.

ASTM C1761 recommends the use of a given content of LWS that can compensate for the chemical shrinkage of the cement paste. The chemical shrinkage of the paste differs from that of concrete. The efficiency of the LWS may vary with the type of concrete and application, w/cm, binder type, etc. It is important to provide adequate content range of LWS to secure the best cost-effectiveness. Thus, it is important to investigate the effect of LWS on "cost per performance" basis. The performance should include workability, mechanical properties, shrinkage and cracking potential, as well as durability.

1.3 Scope of work

The ***work plan*** that is presented in this study includes the following tasks:

Task I: Literature review

Task II: Laboratory investigation

Sub-task II-1: Materials characterization

Sub-task II-2: Investigation of curing regimes

Sub-task II-3: Dosage optimization and durability performance

Further descriptions of the tasks are described below.

Task I: Literature review

The purpose of Task I was to collect and review relevant literature, specifications, research findings, current practices, and other information relative to the use of internal curing for high performance concrete (HPC). Literature review was focused on mixture design methodology, and the effect of LWS on the cost-to-performance ratio.

Task II: Laboratory testing

The information reviewed in Task 1 was analyzed to finalize the laboratory testing program. A comprehensive investigation was undertaken and is described in the following sections.

Sub-task II-1: Material characterization of LWS

In this task, the absorption and desorption capacity of the material were investigated using simulated pore solution. Absorption was measured using the "tea bag" method (based on EDANA Standards). Then, desorption was measured using a method similar to ASTM 1761 for lightweight aggregates (LWA). Here, a thin layer of material saturated with pore water solution was subjected to a constant relative humidity of 94% produced by a salt solution using potassium nitrate.

Sub-task II-2: Investigation of curing conditions

The purpose of this task was to investigate the necessary moisture curing time for various concrete mixtures, while maintaining the required workability and mechanical properties. The optimum dosage established in Task II-1 was used in this investigation. The optimized mixture(s) was initially used, and testing was performed to reduce the binder content to secure workability and mechanical performance that are similar to the control mixture. The optimized mixture was subjected to multiple curing regimens to determine the most suitable moisture curing time.

Sub-task II-3: Dosage optimization and durability performance

The focus of this sub-task was to establish the optimum dosage of LWS required to mitigate shrinkage without compromising mechanical properties. This was followed by the evaluation of the optimized mixture and comparing them to concrete made with different types and dosages of LWS. Multiple concrete mixtures were considered, including HPC mixtures for pavement and bridge decks, as well as high-strength self-consolidating concrete for structural purposes.

The test program was performed in two blocks. The first block focused on the effect of the dosage of LWS on essential properties, i.e. workability, shrinkage, and compressive strength. A parametric approach was carried out for this task using LWS levels that were normalized to the theoretical water contents required to counteract chemical shrinkage. This was done using the Power's Model with a method established by Jensen and Hansen (2001). Four levels of LWS (0, 50%, 100%, and 150% of the theoretical requirement) were used to secure internal curing water content that can compensate for chemical shrinkage. Then, a second block of testing matrix was undertaken to focus primarily on durability performance and transport properties of the investigated optimized mixtures from Block 1. The outline of the project is presented in Figure 1.1.

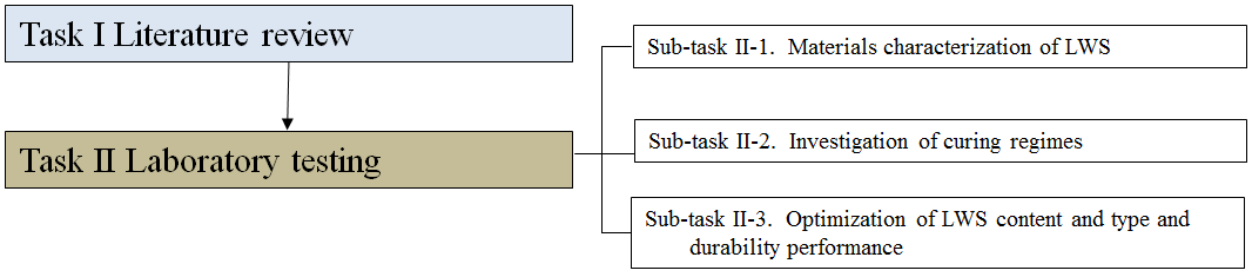

Figure 1.1: Outline of the research project

2. Literature Review

2.1 Introduction

The concept of internal curing has gained a lot of interest in recent decades, and it has become a useful tool that engineers can use to improve the performance of concrete structures. Formally, it is defined by the American Concrete Institute (ACI) as "a process by which the hydration of cement continues because of the availability of internal water that is not part of the mixing water". In practice, this means adding a material to concrete which acts as a vessel to hold internal water. The intent is to release the internal water after mixing and placement when the concrete has begun to harden. Normally, concrete can lose capillary water through external drying processes, such as evaporation at a surface exposed to air or suction from a surface exposed to an absorbent material. Also, in mixtures with low w/cm $\leq$ *0.42*, the hydration of the cementitious materials can consume enough capillary water to cause internal drying or self-desiccation at very low w/cm values. These losses of water can cause significant shrinkage, especially when external curing is limited, allowing the concrete to dry faster at early age. In these circumstances, internal curing can be used to replenish the loss of capillary water, which can allow hydration to continue, promote strength gain, reduce and/or delay shrinkage, and improve the overall durability of the structure. Many materials can be used to provide internal curing, but the primary focus of this work was to expand on the use of saturated LWS.

One of the primary incentives of internal curing is that it can counteract shrinkage that can occur in cement paste by replenishing the capillary water that is lost due to internal or external processes. Therefore, this discussion will begin with a summary of the mechanisms that cause shrinkage of the hydrated cement paste.

2.2 Shrinkage mechanisms

Typically, shrinkage due to water loss of the hardened concrete can be divided into two categories: autogenous shrinkage and drying shrinkage. Autogenous shrinkage refers to the volume that is lost during the chemical reaction between cement and water during hydration as well as volume change due to self-desiccation at low w/cm. This type of shrinkage occurs in both the fresh and hardened states; and if the w/cm is sufficiently low, chemical shrinkage that occurs after the

concrete has set can lead to significant self-desiccation. Drying shrinkage typically refers to the strain in the hardened concrete produced by the loss of capillary water through external processes. For example, in concrete slabs water is lost through evaporation at the surface which is open to air. For slabs on grade, water can be lost through suction from direct contact with a dry base material. Drying shrinkage can also occur in the fresh state, i.e. plastic shrinkage, which can cause plastic shrinkage cracking. The mechanisms driving each of the various shrinkage types, as well as some of the practical consequences of each, are discussed in the following sections.

2.2.1 Drying shrinkage

The underlying cause of drying shrinkage in concrete is primarily the loss of water through evaporation at the surface of the concrete. This results in a decrease in internal relative humidity of the cement paste, which produces internal stresses that cause the concrete to shrink. In the case of concrete slabs (i.e., pavement and bridge decks), such shrinkage has many practical consequences. Upon drying, a moisture gradient typically forms through the thickness of the slab, which produces non-uniform stresses that can cause the slab to warp. Specifically, the edges of the slab will tend to curl in the direction of lower relative humidity. Furthermore, when the deformations caused by shrinkage are restrained, which is the case for the bottom side of nearly all slabs, this can cause cracking in the hardened concrete. This has serious implications on the durability performance of a concrete slab, therefore understanding this type of shrinkage and the mechanisms that cause it are important.

Three mechanisms are thought to produce stresses that cause drying shrinkage; capillary stress, disjoining pressure, and changes in the surface free energy. Capillary stresses arise from the formation of menisci in the pores of the cement paste which are primarily formed due to the evaporation of the pore water. Evaporation cannot remove the pore water without a decrease in the relative humidity (RH), which is related to the radius of curvature of the meniscus (r) that forms in the pore upon the removal of water, and the surface tension of the pore water (γ). The simplest form of this relationship can be represented by the Kelvin equation, Eq. (1).

$$ln(RH) = \frac{2\gamma V_m}{rRT} \tag{1}$$

where R is the universal gas constant, T is the temperature (°C, °F), and V_m is the molar volume of the pore water. The radius of curvature of the meniscus (r) is oftentimes considered to be the same as the pore radius, i.e. the contact angle between the fluid and pore walls is near 90° (Ferraris and Wittman 1987, Mindess et al. 2003, Wei 2008). The capillary pressure (P_{cap}) that develops can be represented by Eq. (2), a simplification of the Young-Laplace equation. Combining Eqs. (1) and (2) the capillary pressure can also be related to the relative humidity by Eq. (3) (Mindess 2003, Wei 2008).

$$P_{cap} = \frac{-2\gamma}{r} \tag{2}$$

$$P_{cap} = \frac{-RT\,ln(RH)}{V_m} \tag{3}$$

Since the pore water is in a state of hydrostatic tension, it exerts a net compressive stress on the cement paste causing it to shrink. At high RH (*>95%*) this mechanism has a smaller effect due to the fact that only the large capillaries (macro-pores) can be emptied. These macro-pores have a relatively low surface-to-volume ratio, and the meniscus that forms in them when they are emptied has a relatively large radius of curvature. Therefore the stresses produced are small. At lower humidity levels, smaller capillaries (meso- and micro-pores) begin to empty. Here the volume of the pores being emptied decreases, but the surface-to-volume ratio increases. Furthermore, the radius of curvature of the meniscus that forms is decreasing, and the capillary stresses rise quite rapidly. This results in a greater contribution to shrinkage in the range of 45%-95% RH. Below *45%* RH, menisci become unstable, and the contribution of capillary stresses disappears. This release of capillary stress can cause expansion in some materials, but for cement paste, this is often negated by other factors, e.g. the shrinkage due to the change in free surface energy (Mindess et al. 2003).

Disjoining pressure primarily originates in the calcium silicate hydrate (C-S-H) gel that forms during the hydration of the cement paste. Due to the high surface area of C-S-H crystals, a significant amount of water adsorbs to their surface forming a film or interlayer space between crystals. This film consists of multiple layers of water molecules, which exerts a disjoining

pressure (P_{dis}) on the surfaces between crystals. This pressure is the result of Van der Waals' attraction forces, double layer repulsion forces, and structural repulsion forces (Ferraris and Whitman 1987, Wei 2008). The disjoining pressure increases as the thickness of the layer and the RH increase. When C-S-H crystals form during hydration, the repulsion forces typically exceed the attraction forces causing it to form in a dilated state. Therefore, when the cement paste dries, the decrease in relative humidity will cause a subsequent decrease in disjoining pressure in the cement paste. This allows the Van der Waals' attraction forces to bring C-S-H formations closer together, causing the cement paste to shrink. The decrease in disjoining pressure has a relative humidity dependency, which is similar to that of the capillary stresses, and it contributes significantly to drying shrinkage until the relative humidity decreases to about 45%. Below this value, it has a relatively small effect (Ferraris and Whitman 1987, Mindess et al. 2003).

Changes in the surface free energy account for the shrinkage that occurs below 45% relative humidity. When the final few layers of adsorbed water molecules are being removed from the surface of the C-S-H formations, their surface free energy begins to increase substantially. This exerts a mean pressure (P_{sfe}) on the C-S-H that is proportional to the surface energy (γ) and the specific surface area (S). This relationship can be represented by Eq. (4) (Mindess et al., 2003).

$$P_{sfe} = \frac{-2\gamma S}{3} \tag{4}$$

Since the specific surface area of C-S-H is relatively large, this phenomenon can cause significant compression of the cement paste. The resulting strain ($\Delta l/l$) can be represented by the Bangham equation, Eq. 5, which was originally developed using experiments related to the expansion of wood charcoal (Bangham and Fakhoury 1931, Ferraris and Whitman 1987; Mindess et al. 2003, Wei 2008).

$$\frac{\Delta l}{l} = k\Delta\gamma \tag{5}$$

Here, the strain is the proportion to the change in surface energy ($\Delta\gamma$) by a constant (k). The proportionality constant (k) depends on the internal surface of the pores, the density of the solid, and the elastic modulus of the porous material (Hiller, 1964; Ferraris and Whitman, 1987; Wei,

2008). The change in surface energy ($\Delta\gamma$) is dependent on the natural log of the RH, but in the range of 20% to 45% RH, the relationship is approximately linear. Above 45% the effect of this phenomenon is negligible, and below 20% RH, the effect becomes much greater (Mindess et al. 2003). It should be emphasized that the drying shrinkage caused by three mechanisms elaborated here is in part reversible upon re-wetting of the material. The irreversible component primarily occurs within the first drying cycle, from 100% to 0% RH, and it is typically attributed to the amorphous nature of the C-S-H gel. When the micro-pores of the cement paste are emptied, the large capillary stresses that are produced will cause the particles in the gel to re-arrange. This will alter the bond between the C-S-H fibers, and consequently, the pore structure will change. Specifically, some micro-pores will collapse causing the formation of new interlayer spaces and the enlargement of neighboring pores, which can create new meso-pores and enlarge existing ones. This process stabilizes the C-S-H gel and makes it less susceptible to expansion upon re-wetting (Mindess et al. 2003).

Irreversible shrinkage is affected by many factors, including the total porosity and the pore structure of the cement paste. Generally speaking, an increase in total porosity can increase the influence of capillary stresses and consequently increase the level of irreversible shrinkage. The total porosity is a function of the w/cm, the degree of hydration, and the volume of air in the cement paste; details of this relationship can be found in the section on chemical shrinkage. The size distribution and connectivity of the pore structure also plays a significant role because it influences the magnitude of the capillary stresses. That is a pore structure that enhances capillary stresses, e.g. one with a larger proportion of micro-pores that are loosely connected, will increase irreversible shrinkage and vice versa. As a result, external factors that influence the pore structure, such as the curing temperature and the drying history, will also influence irreversible shrinkage. For example, an increase in moist curing temperature will decrease the irreversible shrinkage. A slow rate of drying will also decrease the irreversible shrinkage, while quick drying can have the opposite effect. Also, prolonged drying at a constant low RH will increase the level of irreversible shrinkage (Helmuth and Turk 1967, Mindess et al. 2003).

It should be emphasized that drying shrinkage is an artifact of the cement paste, and the concepts discussed above are formulated in the context of measurements for small cement paste samples. Therefore, there are additional concerns related to concrete that are worth noting. First,

the incorporation of aggregates, that are dimensionally stable, will reduce drying shrinkage significantly. This is because the paste content is reduced, and the aggregates act as a restraint that limits the shrinkage. Furthermore, the size and stiffness of the aggregates play a significant role. Larger sized aggregates can develop greater stress concentrations at the interface between the paste and aggregate, which increases the likelihood of cracking.

2.2.2 Plastic drying shrinkage and plastic shrinkage cracking

Plastic shrinkage is the result of capillary stresses, identical to those previously discussed, which can develop in the fresh concrete when the rate of surface evaporation exceeds the rate at which bleed water can reach the surface. Under such conditions, the capillary pressure and the rate of plastic drying shrinkage will increase until a critical break-through pressure is reached in the capillary pore water. Once the break-through pressure is achieved, water near the surface will agglomerate into zones with boundaries of little to no moisture between them. Beyond the break-through pressure, capillary stresses will continue to rise, but any shrinkage that occurs beyond this point will be relatively negligible. Nonetheless, at the boundaries between these zones, plastic shrinkage cracking can occur, which can degrade the surface quality and cause durability issues (Wittman 1976, Mindess et al. 2003).

Plastic drying shrinkage and plastic shrinkage cracking are influenced by several factors, including environmental conditions, concrete temperature and composition, and surface area in contact with the air. Hot, arid, and windy environmental conditions, high concrete temperature, or a large surface area exposed to the air will promote the evaporation of water from the surface of the concrete and increase the potential of plastic shrinkage cracking. Low w/cm and the use of fine particles, like silica fume, will increase the capillary pressure and promote plastic shrinkage cracking as well (Wittman 1976, Cohen et al. 1990, Mindess et al. 2003). Like drying shrinkage in the hardened state, plastic drying shrinkage is significantly reduced by the incorporation of aggregates. Therefore, concrete will exhibit significantly less plastic shrinkage than pure cement paste (L'Hermite 1960, Mindess et al. 2003).

2.2.3 Autogenous shrinkage

Autogenous shrinkage is contributed to by chemical shrinkage and self-desiccation of

cementitious materials. The hydration of the Portland cement involves chemical reactions when the resulting hydration byproducts occupy less volume than the reactants, and the volume loss that occurs is commonly referred to as chemical shrinkage. Chemical shrinkage occurs in both the plastic and hardened states. In the plastic state, it results in measurable change in the bulk volume. After the paste begins to set, the increase in rigidity will restrain changes in the bulk volume, but chemical shrinkage can still continue to decrease the solid volume and produce vapor filled voids in the paste. As capillary water is consumed by the hydration reactions, the RH of these vapor filled voids can drop below 100%, thus resulting in a phenomenon known as self-desiccation.

The kinetics behind this can be explained by the Powers' model for the phase distribution of cement paste. This model is largely based on experimental measurements and can be seen from some perspectives as an over simplification, but it has proven to be very useful in describing many phenomena related to the hydration of Portland cement. The basis of this model can be found in papers by Powers and Brownyard (1946) and Powers (1947 and 1960). The version of the model presented here was used by Jenson and Hansen (2001) for the purposes of quantifying the water required to internally cure concrete using superabsorbent polymers, and it is also the same theoretical basis of the method developed by Bentz and Snyder (1999) for saturated expanded lightweight aggregate. It is very useful for quantifying the water demand for internal curing, in general, and explains the mechanism of self-desiccation adequately.

In the model, the water in the cement paste is classified by three phases: capillary water; gel water; and chemically bound water. Capillary water is the free water that is readily consumed by the hydration, and is easily evaporable. Gel water is physically bound water that is adsorbed by the gel solid. It cannot be consumed easily by hydration, and it does not evaporate as easily as the capillary water. Chemically bound water is the water consumed by hydration, and it is part of the gel solid's structure. It is generally considered to be non-evaporable because it requires temperatures above the boiling point of water to be evaporated. The volumetric proportions of each of these phases, in fully hydrated Portland cement, was measured by Powers. According to Jenson and Henson (2001), these measurements showed that approximately 0.23 grams (0.00805 oz) of water per gram (oz) of cement are bound chemically, approximately 0.19 grams (0.00665 oz) of water per gram (oz) of cement is adsorbed to the gel solid, and the volume loss due to chemical shrinkage is approximately 6.4 milliliters (0.2176 fl oz) per 100 grams (3.5 oz) of cement. It should

be noted that these numbers will change based on the composition of the cement and whether or not supplementary cementitious materials are used.

The effect of cement composition on chemical shrinkage has been modelled in the work of Paulini (1992). Also, the phase distribution for the pozzolanic reaction of silica fume was investigated in the work of Sellevold et al. (1982) and Jensen (1993). Nevertheless, if we use these three estimates (for chemically bound water, physically bound water, and chemical shrinkage), one can calculate the approximate volume proportions that develop during the hydration of cement. If a closed system of air-free cement paste is considered, the following equations can be used to calculate the volume of chemical shrinkage (V_{cs}), the volume of capillary water (V_{cw}), the volume of gel water (V_{gw}), the volume of gel solid (V_{gs}), and the volume of unhydrated cement (V_{uc}):

$$V_{cs} = 6.4\times10^{-5}\rho_c(1 - p)\alpha = 0.20(1 - p)\alpha \tag{6}$$

$$V_{cw} = p - (0.19 + 0.23)\left(\rho_c/\rho_w\right)(1 - p)\alpha = p - 1.32(1 - p)\alpha \tag{7}$$

$$V_{gw} = 0.19\left(\rho_c/\rho_w\right)(1 - p)\alpha = 0.60(1 - p)\alpha \tag{8}$$

$$V_{gs} = \left(1 - 6.4\times10^{-5}\rho_c + 0.23\left(\rho_c/\rho_w\right)\right)(1 - p)\alpha = 1.52(1 - p)\alpha \tag{9}$$

$$V_{uc} = (1 - p)(1 - \alpha) \tag{10}$$

Here, the density of the cement ($\rho_c = 3{,}150\ kg/m^3$) ($\rho_c = 5{,}309.5\ lb/yd^3$), and the density of the water ($\rho_w = 1{,}000\ kg/m^3$) ($\rho_w = 1{,}685.5\ lb/yd^3$) are constants. Therefore, the volumes can be expressed simply as a function of the degree of hydration (α) and the initial porosity (p). The initial porosity can be estimated using Eq. (11).

$$p = V_{cw.0} = \frac{(w/c)}{\left(w/c + \rho_w/\rho_c\right)} \tag{11}$$

The Eq. (11) is simply considered to be the initial volume of capillary water ($V_{cw.0}$), which is

a function of w/cm, by mass, and the densities of water (ρ_w) and cement (ρ_c). According to these relationships, the minimum w/c required for full unimpeded hydration is $0.42\ (= 0.19 + 0.23)$. Therefore, when the w/c is equal to or greater than this threshold, there will be excess capillary water and complete hydration is theoretically possible. This can be seen visually in Figure 2.1, which displays the phase distribution for a cement paste with $w/c = 0.6$, which is calculated using Eqs. (6) to (11). Since this is a closed system with no entrapped or entrained air, the vapor filled pores that develop are a direct result of chemical shrinkage. It should also be noted that, for this model, any RH depression caused by the dissolution of salts in the pore water is ignored. Therefore, the capillary water and the vapor filled pores are thought to be in equilibrium with a RH of 100%.

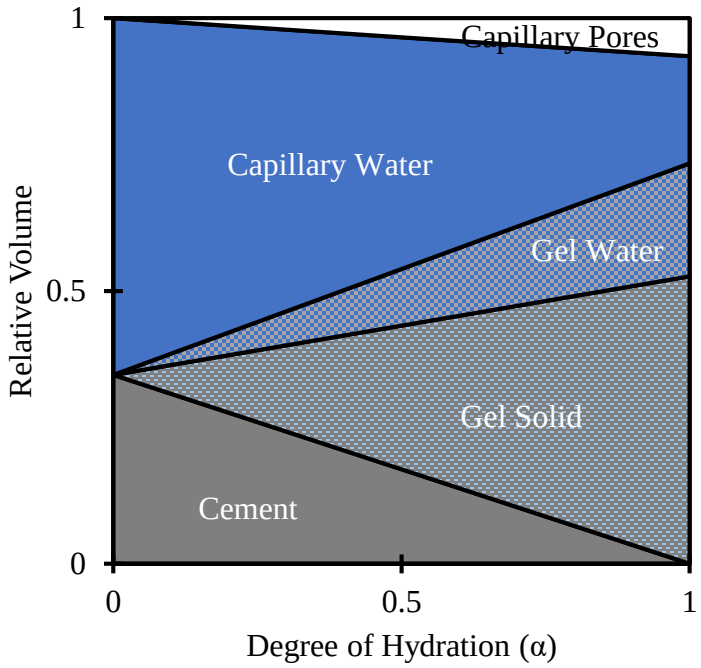

Figure 2.1: Volumetric phase distribution of cement paste as a function of the degree of hydration, α, with $w/c = 0.6$, adapted from (Jensen and Hansen, 2001)

When the w/cm is low ($w/cm < 0.42$), the capillary water will be consumed before the cement has completely hydrated. Once this occurs, the hydration reactions will attempt to consume some of the physically bound gel water, which slows the hydration process significantly. This can be visualized in Figure 2.2, which displays the phase distribution for a cement paste with $w/c = 0.3$, which again is calculated using Eqs. (6) to (11). Consumption of the gel water can occur until a minimum porosity is reached in the cement gel. According to the measurements of

Powers' this limit is *26%-28%* porosity (Powers and Brownyard 1946; Powers 1960). When this limit is reached, hydration will stop. Therefore, if the w/cm is sufficiently low, as in Figure 2.2, there is a maximum obtainable degree of hydration (α_{max}).

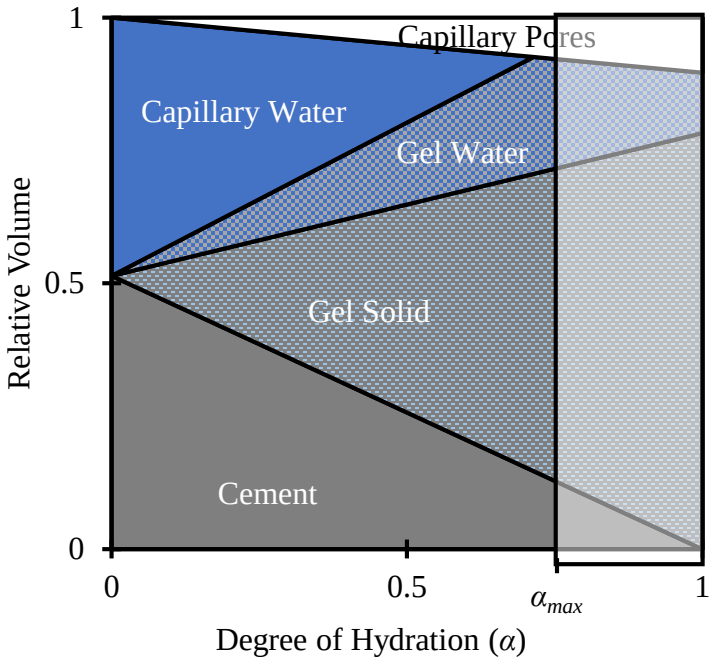

Figure 2.2: Volumetric phase distribution of cement paste as a function of the degree of hydration, α, with $w/c = 0.3$, adapted from (Jensen and Hansen, 2001)

Theoretically, in an open system with access to external curing water, self-desiccation is avoidable, and the maximum level of hydration is obtainable. However, in practice, concrete with a low w/cm ($<< 0.42$) will have a low porosity, which can impede the penetration of external curing water to the point that self-desiccation could occur regardless. If the hardened cement paste is allowed to self-desiccate, significant autogenous shrinkage will occur.

2.3 Mixture proportioning strategies of LWS concrete

The incorporation of LWS in a concrete mixture requires special considerations when determining the mixture proportions. First, the amount of LWS necessary for internal curing must be calculated, which is often done using some form of the Powers' model described previously. Then, one must decide how to incorporate the material into the mixture because the volume the material occupies must be considered. Specifically, the material must partially replace one or more

of the other ingredients, which is usually the normal weight sand.

A theoretical model was presented in ASTM C1761 to predict the minimum amount of LWS or superabsorbent polymer required to provide additional water to counteract the effects of self-desiccation and chemical shrinkage during the hydration of cement paste (Bentz and Snyder 1999). Water introduced by LWS is gradually released to sustain a relatively high internal relative humidity. This can ensure that the capillary porosity in the cement paste is water-filled at the maximum degree of hydration. The hydration reactions of cement can be terminated due to lack of space for precipitation of hydration products (Jensen and Hansen 2001, Bentz and Snyder 1999). The model has been applied in various concretes and demonstrated great effectiveness (De la Varga and Graybeal 2015, Bentz and Weiss 2011). However, Justs et al. (2015) claimed that the model for the determination of LWS content might not allow appropriate prediction for that of high or ultra-high performance concrete (UHPC). This is because the amount of internal curing agent calculated using the model can be insufficient to prevent self-desiccation and compensate for chemical shrinkage (Justs et al. 2015). The reason was likely because the pores of the internal curing agent that provided additional space for precipitation of hydration products were not taken into account in the model. The space introduced by the internal curing agent might be insignificant for normal concrete, but for HPC that has very low w/cm, such as UHPC, and limited space for precipitation, the additional space could allow a higher degree of hydration, which should not be neglected. For this reason, a greater amount of internal curing agent, such as LWS, may be required. In addition, the travel distance of internal curing water is limited in HPC due to the low permeability associated with the very low w/cm. The content of internal curing agent may then need to be carefully considered to ensure that a majority of the paste is within the travel distance of the internal curing water. Under such circumstances, investigations on LWS with high volume fraction for internal curing of HPC are highly desired. Therefore, a wide range of LWS content was considered in this study.

In HPC, lack of water and capillary pore space can compromise the precipitation of hydration products, thus resulting in low degree of hydration of cement (Justs et al. 2014). The unhydrated cement particles can then exist as “expensive” fillers. Moreover, the low w/cm leads to significant autogenous shrinkage, which tends to cause cracks in concrete (Bao et al. 2015). Bentz et al. (2005) claimed that small inclusions dispersed in the matrix store water during mixing and setting and

then progressively release water for internal curing in the later hydration reactions. De la Varga and Graybeal (2014) reported that supplying internal curing by utilizing pre-saturated lightweight aggregates resulted in a significant reduction in autogenous shrinkage of cementitious composites. Justs et al. (2015) used superabsorbent polymer for the internal curing agent to reduce autogenous shrinkage of concrete. Rice husk ash also proved to be a good internal curing agent and pozzolanic material (Van et al. 2014, Nguyen 2011).

Internal curing has been gaining wide acceptance as an effective way to reduce shrinkage of HPC (Hwang et al. 2013, Bentur et al. 2001). However, employment of superabsorbent polymers was reported to significantly reduce workability (Beushausen and Gillmer 2014) and compressive strength (Justs et al. 2015). Mechtcherine et al. (2009) reported complete autogenous shrinkage reduction using superabsorbent polymers in high strength concrete that experienced very high autogenous shrinkage of about 1100 μm/m (0.0011 ft/ft) at 7 days. However, the high dosage of superabsorbent polymer necessary to significantly reduce such shrinkage reduced the compressive strength from 150 MPa (21,755 psi) to less than 100 MPa (14,505 psi). Zhutovsky and Kovler (2009) reported that the presence of excessive additional pores in internally cured concrete may cause reduction in compressive strength. Habeeb and Fayyadh (2009) stated that fine rice husk ash increased compressive strength of concrete but it also increased the autogenous shrinkage. Past studies in the literature indicate a trade-off between the mechanical properties and autogenous shrinkage of concrete with use of superabsorbent polymer or rice husk ash. On the other hand, lightweight aggregates were found to offer more effective and longer internal curing effects than superabsorbent polymers (Weiss et al. 2012). Limited information is available on the effectiveness of LWS for internal curing of HPC. There is a concern that the relatively large particle size of LWS can potentially have an adverse effect on mechanical properties of HPC. In this literature review, existing studies on the effect of LWS on performance of concrete was elucidated.

2.3.1 Hardened properties

Increase in strength: In addition to the contribution to reduce autogenous shrinkage of concrete, for a given w/cm, the use of internal curing can increase strength of concrete at later age. It is important to note that the effect of LWS replacement on compressive strength depends on the w/cm. For example, in the case of mixtures made with relatively high w/cm of 0.40, compressive

strength increase resulting from 6 days of moist curing was much larger than strength gain due to the incorporation of 30% LWS. On the contrary, mixtures made with 0.30 w/cm exhibited larger strength increase due to LWS replacement than the extended duration of moist curing. This indicates that the effect of internal curing through the use of LWS is more significant for concrete with low w/cm that has less water available for cement hydration (Hwang et al. 2013). The compressive strength increase by the use of LWS in turn, indicates the possibility of reducing cement content, which may compensate for cost increase due to the use of LWS. Similar effect of other LWS, such as super-absorbent polymer, on strength is expected but still needs to be verified.

2.3.2 Shrinkage

Reduction in shrinkage and cracking potential: Water-saturated materials, including pre-saturated fine and coarse aggregates, provide an internal source of water necessary to replace the water consumed by chemical shrinkage during hydration and perhaps a greater amount of water demand to maintain high RH. Crack width resulting from plastic shrinkage can also be reduced as the replacement volume of these water-saturated materials is increased. A major advantage of the internal curing is the reduction of cracking potential by reducing autogenous and/or drying shrinkage. The efficiency of the LWA varies with the pore structure of the aggregate. Generally, larger LWA particles have larger pore structures, which results in more efficient internal curing (Hammer et al., 2004). However, it should be noted that well dispersed LWA is needed to provide efficient internal curing. This is similar to the case that properly dispersed air voids can improve frost durability. Several studies proved that smaller LWA particles can achieve better distribution than larger LWA particles (Bentz and Snyder, 1999, Bentz et al., 2005). Henkensiefken et al. (2009) investigated the influence of replacement rates of saturated LWA on the performance of self-curing concrete. The inclusion of a sufficient volume of pre-wetted LWA can significantly reduce free drying shrinkage and delay the elapsed time to cracking. In the case of mixture with 0.30 w/cm and cement content of 700 kg/m^3 (1,180 lb/yd^3), mortar mixture containing low volume of LWA of 7.3%, by volume, was reported to exhibit similar free drying shrinkage and cracking behavior to that of the control mixture made without any LWA. This may be due to the fact that in the case of low replacement rate, the LWA particles are dispersed too far from each other to effectively supply internal curing water to the paste.

Şahmaran et al. (2009) studied the effect of replacement rate of LWS as an internal curing agent on the shrinkage and mechanical behavior of engineered cementitious composites. The addition of saturated LWS was found to be very beneficial in controlling the development of autogenous shrinkage for mixtures made with w/cm of 0.27. A 67% reduction in autogenous shrinkage at 28 days compared to the control mixture can be attained with 20% substitution of normal sand by saturated LWS. In addition, the use of 20% LWS delivered 37% reduction in drying shrinkage after 90 days of drying compared to control specimens. De la Varga et al. (2012) investigated the application of internal curing for mixtures containing low w/cm of 0.30 and high volume of Class C fly ash (up to 60%), which are more susceptible to high shrinkage and cracking. They reported that the slower hydration reaction in the high volume fly ash mixtures results in less initial autogenous shrinkage deformations at early ages. However, due to the pozzolanic reaction and refining the porosity, the rate of autogenous shrinkage increases in the fly ash mixtures at later ages. This behavior can lead to higher risk of shrinkage cracking potential at later ages. Their results showed that the use of 15% LWA, by volume, can be a beneficial method to provide internal curing and reduce tensile stress development caused by restrained shrinkage. Golias et al. (2012) studied the performance of LWA with different initial moisture contents. Their results indicated that the oven-dried LWA is able to absorb water from the paste prior to setting, then absorbed water will be returned to the system as internal curing water. When mixture proportion adjustments are properly made to account for the water absorbed by the ovendried LWA before setting, the mixture can provide internal curing benefits.

In general, for a given period of moist curing, concrete mixture made with LWS can exhibit significantly lower shrinkage than concrete without any LWS. Our previous investigation on the internal curing by LWS proved that concrete made with 30% LWS and 6 days of initial moist curing period exhibited lower total shrinkage of 640 microstrains at 91 days compared to 865 to 1,630 microstrains for non-LWS mixtures. One of the impressive benefits of the LWS is that regardless of the w/cm, concrete made with 30% LWS replacement that did not receive any moist curing exhibited lower shrinkage than moist-cured concrete prepared without any LWS. For a given w/cm and initial moist curing period of 6 days, the use of 30% LWS led to 30% to 47% decrease in the total shrinkage at 91 days compared to values of corresponding concrete made without LWS (see Figure 2.3).

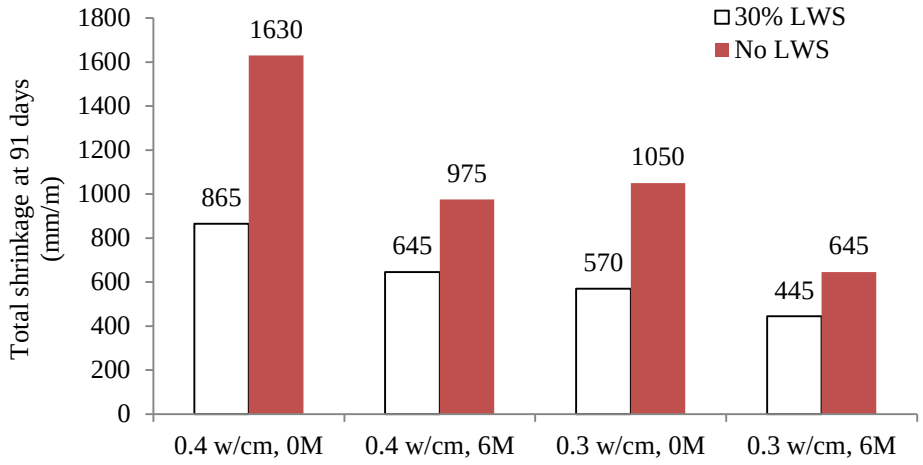

Figure 2.3: Shrinkage comparison of concrete made with 30% LWS and without any LWS subjected to 6 days of initial moist curing (Hwang et al. 2013)

Possible reduction in moist curing period: In order to achieve similar level of shrinkage or cracking potential, concrete made with LWS/LWA requires shorter period of moist curing compared to similar concrete without any water-saturated materials. The reduction in the moist curing period can reduce cost of curing practice in the field. For example, previous study carried by Hwang et al. (2013) found that shrinkage reduction associated with the use of LWS was much greater in the case of air-dried concrete compared to that moist-cured for 6 days (47% and 45% reduction for air-dried concrete vs. 34% and 30% reduction for moist-cured concrete). Moist-cured concrete made with low w/cm of 0.3 had 200 microstrains shrinkage reduction by 30% LWS. On the other hand, air-dried concrete prepared with 0.4 w/cm and 30% LWS exhibited 765 microstrains lower shrinkage than similar concrete made with any LWS. The impact of using super-absorbent polymer on the reduction in moist curing period still needs to be clarified.

2.3.3 Durability

In most cases, some detrimental effect of using LWS on early-age strength is reported (Bentur et al. 1999, Lura and Breugel 2000). However, HPC is often used for its superior durability. The addition of LWS into the dense cement matrix increases the porosity, and thus permeability and diffusivity of HPC. The properties most-used in both industry and research to characterize durability of concrete are water permeability and sorptivity (Hooton 1993). However, LWS may have a positive effect on durability. First, the cracking due to autogenous shrinkage is eliminated

or reduced by internal curing. Second, LWS has an improved elastic compatibility with cement paste that would result in lower microcracking (Bremner and Holm 1986). Third, the improved interfacial transition zone (ITZ) between the LWS and cement paste matrix (Wasserman and Bentur 1996) would have a positive effect on permeability. Higher replacement of LWS can reduce chloride diffusivity (Chia and Zhang 2002). The size of LWS influences chloride diffusivity as well, lowering diffusivity for the finer LWA. Mortar made with LWS for internal curing was reported to reduce chloride penetration (Bentz 2009) and sorptivity (Henkenseifken et al. 2009), and its use in concrete was shown to improve scaling resistance (Jozwiak-Niedzwiedzka 2005).

A survey of HPC bridge decks provides evidence that LWS has a beneficial effect on service life as well (Cusson et al. 2010). The amount, type, particle size and degree of saturation of LWS have considerable effect on internal curing (Zhutovsky et al. 2002). Moreover, the internal curing effectiveness depends on the permeability of the cement paste matrix, and thus on the w/cm (Zhutovsky et al. 2004). The effect of LWS on durability of HPC made at different w/cm is extremely important, since w/cm is the primary factor that affects durability. However, a systematic study of different types and volumes of LWS on durability is still very limited.

2.3.4 Microstructure

To better understand of effect of LWS on internal curing of concrete, several researchers have focused their work on the microstructure (Bents et al. 2006). Lam (2005) reported that "the interfacial transition zone (ITZ) of lightweight aggregate concrete was superior to that of normal weight aggregate concrete due to the interlocking exhibited by the paste with the pores at the surface of the LWA." This observation is in agreement with the results of Zhang and Gjørv (1990) who observed a dense and homogeneous ITZ between cement paste and LWA with a porous outer layer. By investigating the long-term (120 days) microstructures of high-performance mortars based on scanning electron microscopy (SEM) analysis, Bentz (2008) found that the increased hydration and absence of large empty pores (hollow-shell or partly hollow-shell pores) by LWS within the hydrating cement paste can contribute to the later age strength increase. The emptying of the larger pores within the LWS as opposed to much smaller pores within the hydrating cement paste should result in a substantial reduction in the capillary stresses, resulting from autogenous shrinkage of the cement paste. Ultimately, this reduces the risk of early-age cracking.

Figure 2.4 shows the pore size distribution and cumulative porosity of the UHPC mixtures made with a w/cm of 0.20 (Meng and Khayat 2017), as the LWS contents was increased from 0 to 50%. The total capillary porosity was shown to decrease by about 20% as the LWS content was increased from 0 to 25%, and the total porosity is increased by about 110% as the LWS content is increased from 25% to 50%. The reduction in total porosity can be caused by three mechanisms: (1) LWS promoted the hydration reaction and led to refined microstructure; (2) the hydration products filled a significant part, if not all, of the pores introduced by the LWS; and (3) the hydration products partially sealed the surface pores of the LWS, thus preventing intrusion of mercury in the MIP measurement and leading to a reduction in measured porosity.

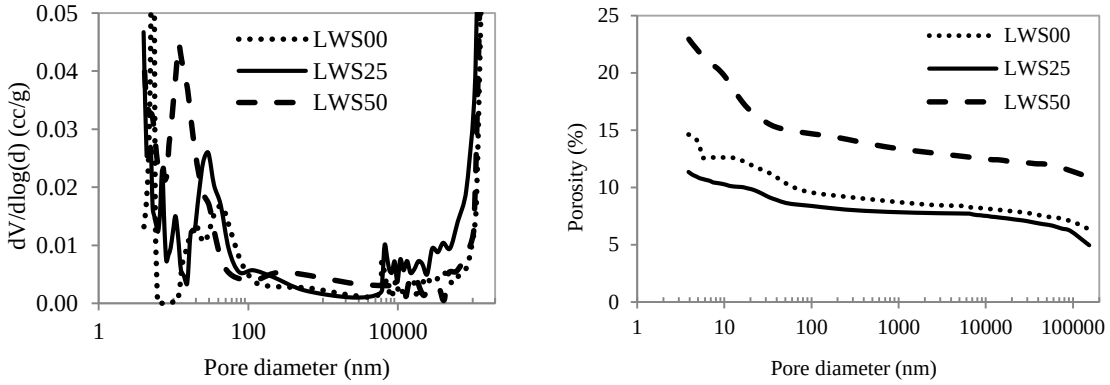

(a) (b)

Figure 2.4: Effect of LWS content on (a) pore size distribution, and (b) porosity of UHPC at 28 days. (Meng and Khayat 2017) (1 nm = 3.94×10^{-8} in.)

As the LWS content was increased from 25% to 50%, the total porosity was increased by 110%. The effect of LWS to reduce total porosity and the level of macro pores were overwhelmed by the effect of LWS to increase porosity, given the porous structure of the excessive amount of LWS. Figures 2.5 illustrates the interface between the cementitious matrix and sand particles embedded in concrete made with optimum LWS content (Meng and Khayat 2017). Compared with river sand, LWS is porous. While a distinct interface can be observed between the relatively smooth river sand and the matrix, there is not a well-defined interface between the LWS and the matrix given the uneven and porous surface of LWS. The matrix seems to encapsulate the LWS, forming a well-integrated sand-matrix interface. The existence of large quantities of voids indicates that the hydration products did not fill all the internal voids of the LWS. The energy dispersive spectroscopy (EDS) image enables the observation of SiO_2 content in the LWS and paste. It was

observed that the SiO_2 in LWS pores is much higher than that in the cement paste. The chemical composition of cement paste is dominated by CaO. Therefore, elementary mappings of Si (representing LWS) and Ca (representing cement matrix) could enable a clearer observation of the interaction between these two phases, cement paste and LWS. The hydration products of cement, most likely C-S-H gel, protrude into the micro-pores in the LWS. On one hand, the nano-porous C-S-H gel tends to seal the surface of the LWS particles, and separate the micro-pores inside from the well-connected capillary network in the matrix. On the other hand, such an inter-penetrated microstructure eliminates the ITZ between the LWS and the matrix, strengthens the LWS, and tends to enhance the interfacial bonding strength, thus enhancing mechanical properties of the cementitious materials.

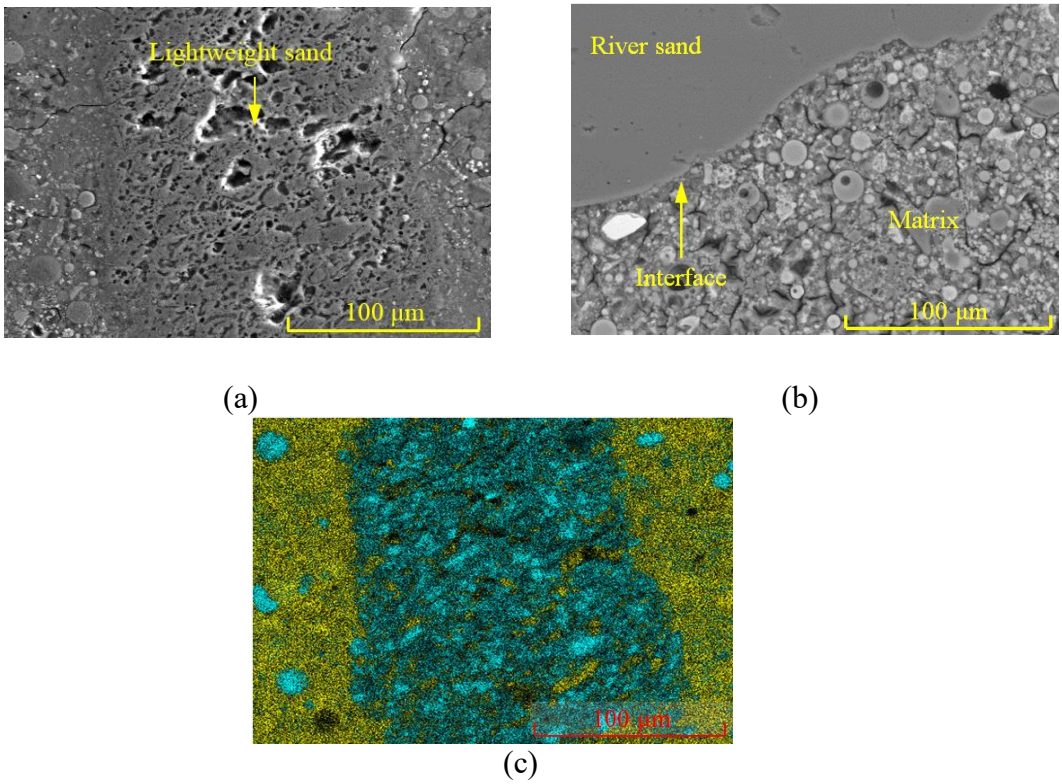

(a) (b)

(c)

Figure 2.5: SEM of interfaces between sand and matrix of LWS25: (a) LWS at 500X; (b) river sand at 500X; (c) elementary mapping of (a): cyan and yellow colors indicate Si and Ca. (Meng and Khayat 2017) (1 µm = 3.94×10^{-5} in.)

2.4 Remaining work to be investigated for internal curing of concrete

The following section presents some of the key issues regarding the use of LWS in concrete that need to be addressed.

What is the maximum dosage of LWS that can be used without reducing mechanical properties and durability? ASTM C1761 specifies the content of LWS that can compensate for only chemical shrinkage of cement paste. The chemical shrinkage of paste differs from that of concrete. Furthermore, the efficiency of the LWS may vary with the type of concrete and application, w/cm, binder type, etc. It is important to provide adequate dosage range of the LWS, which results in the best overall performance and cost-effectiveness. Such analysis should consider cost per performance comparison.

How can we measure desorption capacity of materials faster and easier? The efficiency of internal curing and dosage of the saturated LWS are closely related to the desorption capacity, which is tricky to determine without specific testing apparatus. Desorption capacity of the LWS to be used should be provided.

Can the increase in material cost be compensated for by performance enhancement? It is important to investigate the effect of internal curing material on cost per unit of performance. The performance should include workability, mechanical properties, and durability aspects. Is internal curing enough, or should it be used along with other shrinkage compensating materials, such as shrinkage reducing agent (SRA) or expansive agent? Is there any combination that yields synergy (to recommend), or is there specific combinations that reduces individual benefits (to prevent those)?

How can we ensure better moisture control of LWS? In general, a water sprinkler is used to ensure high moisture content of the materials is above the SSD condition. However, there is no guidance about how many days of water sprinkling would be required to ensure saturation of the LWS. It is important to suggest easy and cost-effective ways to pre-saturate the LWS and determine its moisture content for the correction of the batching water.

Is there any issue with durability when using LWS? The effect of the type and content of LWS on durability, including chloride ion permeability and frost durability, should be verified.

Hwang et al. (2013) compared the rapid chloride permeability (RCP) values of two similar concretes made with and without 30% LWS and found that for a given moist curing period, mixtures made with 30% LWS replacement exhibited slightly higher RCP values than similar concrete prepared without any LWS (see Figure 2.6), even if the RCP spreads between the two mixtures are quite small (maximum 410 Coulomb). The durability performance should be considered to limit the maximum allowable dosage of the LWS.

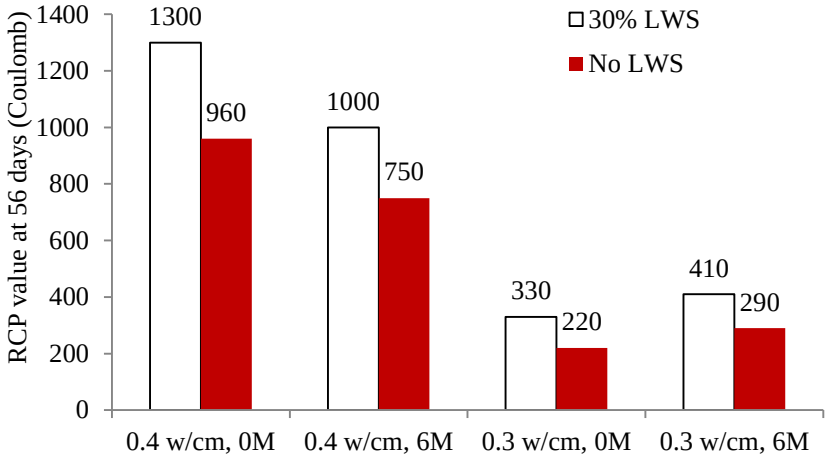

Figure 2.6: Comparison of RCP values for concrete made with 30% LWS and without LWS (Hwang et al., 2013)

Effect of LWS on elastic modulus of concrete? In general (except for repair application), reduction in elastic modulus of concrete should be avoided for structural performance. The use of adequate content of LWS results in a slight increase in elastic modulus (Hwang et al, 2017). Generally speaking, the use of highly porous materials (water-absorbent materials) can reduce elastic modulus of concrete, in particular at early ages. Therefore, their effect on the modulus of elasticity of concrete should be clarified.

3. Materials, Test Methods, and Experimental Program

3.1 Sources of selected LWS

Expanded lightweight aggregate (LWA) is prepared by expanding and vitrifying selected minerals (e.g., shale, clay, or slate) in a rotary kiln at temperatures above 1000 °C (1832 °F). This forms a ceramic material that is structurally sound, dimensionally stable, durable, environmentally inert, non-toxic, low in density, and absorptive. This material is then crushed and sifted into different gradations, both coarse and fine. In order to provide internal curing, expanded LWS absorbs a significant amount of water and retains it during the mixing and placement period. The low density and absorptive capacity of these aggregates are attributed to its cellular pore structure. The pores close to the surface of the particles can readily absorb water and become filled within the first few hours or few days of submersion in water. After casting of the concrete, the material must be able to release this water when the relative humidity in the capillary pores drops below 100%. Therefore, when selecting a LWS, the absorption and desorption characteristics are very important. The absorption and desorption tests are carried out according to ASTM C128 and ASTM C1761, respectively.

Five types of LWS produced or distributed in the Midwest have been selected for this study. Table 3.1 provides a summary of these LWS materials.

Table 3.1: Investigated LWS types

Code	Type	Company	Plant location	Stockpile location
LWS 1	Expanded Shale	Buildex	New Market, MO	
LWS 2	Expanded Shale	Northeast Solite	Shepardsville, KY	
LWS 3	Expanded Shale	Trinity Lightweight	Erwinville, LA	St. Louis, MO
LWS 4	Expanded Shale	Buildex	New Market, MO	
LWS 5	Expanded Clay	Trinity Lightweight	Erwinville, LA	Memphis, TN

3.2 Physical properties of LWS

Table 3.2 provides a summary of the physical properties, including specific gravity saturated surface dry (SG_{SSD}), specific gravity oven dry (SG_{OD}), absorption (ABS), and fineness modulus (FM). Two methods were used for the characterization: (1) the paper towel method, detailed in ASTM 1761; and (2) the centrifuge method, detailed by Miller et al. (2014). The results for all five LWS types can be found in Table 3.2. Both methods seem to produce similar results, but the centrifuge method is much quicker and fundamentally less subjective than the paper towel method. Specifically, the centrifuge method takes minutes, while the paper towel method can take hours. The paper towel method is highly dependent on the technique and judgement of the operator. Therefore, the centrifuge method has been adopted as the primary method to achieve surface dry conditions in future tests.

Table 3.2: Physical Properties at 72 hours of submersion of LWS

Code	Paper Towel Method			Centrifuge Method			F.M.
	SGSSD	SGOD	ABS.	SGSSD	SGOD	ABS.	
LWS 1	1.97	1.74	13.6%	1.95	1.72	13.1%	3.62
LWS 2	1.80	1.52	18.4%	1.81	1.51	19.8%	3.17
LWS 3	1.69	1.52	19.7%	1.71	1.51	19.8%	3.17
LWS 4	1.96	1.47	17.5%	1.98	1.41	19.7%	3.80
LWS 5	1.66	1.38	20.0%	1.68	1.41	19.3%	3.66

3.3 Particle size distribution of investigated LWS types

The particle size distribution, in terms of cumulative percent retained and percent passing, for the selected LWS can be seen in Figure 3.1 (a) and (b), respectively.

3.4 Absorption and desorption of investigated LWS materials

The variation of water absorption with time was measured using the volumetric flask method described by Castro et al. (2011). The results can be found in Figure 3.2; here the relative absorption was determined with respect to the 72-hour absorption value.

It can be observed that LWS 1 and LWS 4 absorb water at a slower initial rate, but continue to absorb water at a faster rate beyond 72 hours. Nonetheless, the overall absorption characteristics of the investigated LWS materials were similar. Within 10 minutes of submersion, more than 50%

of relative absorption was achieved and within 48 hours of submersion, more than 90% of relative absorption was achieved for the five investigated LWS materials.

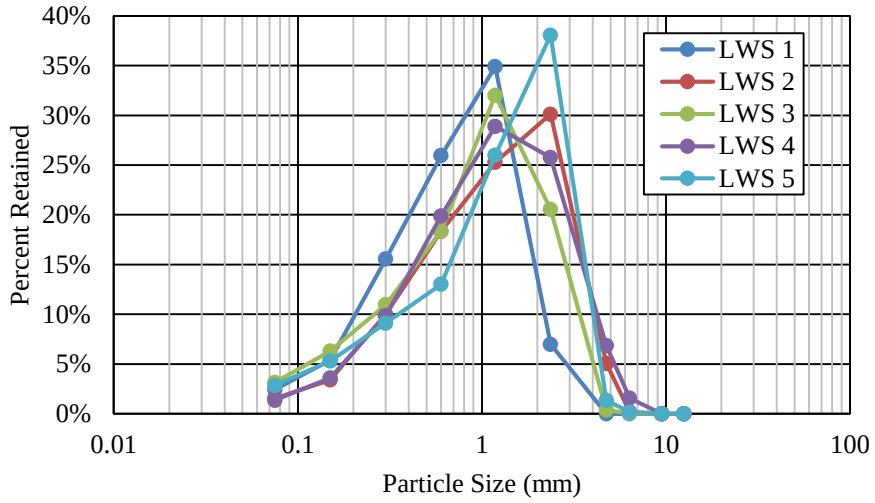

(a) Percent retained

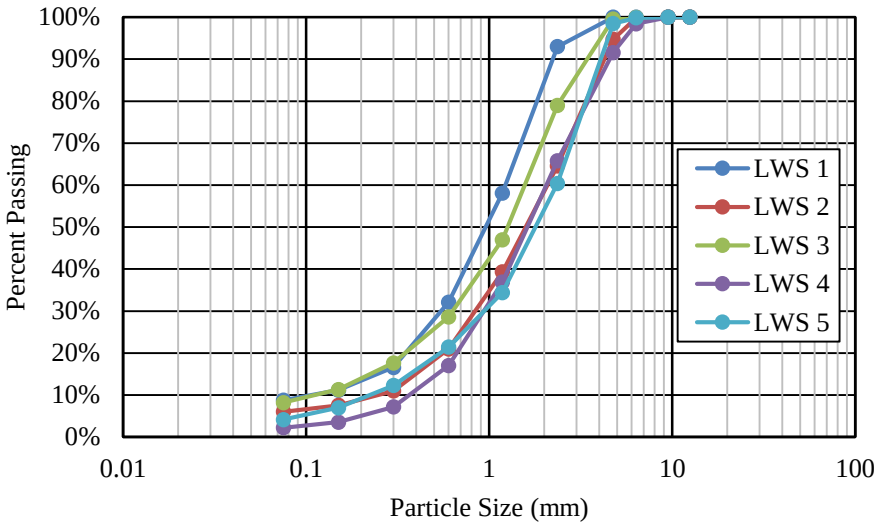

(b) Percent passing

Figure 3.1: Particle size distribution of the investigated LWS materials (1 mm = 0.0394 in.)

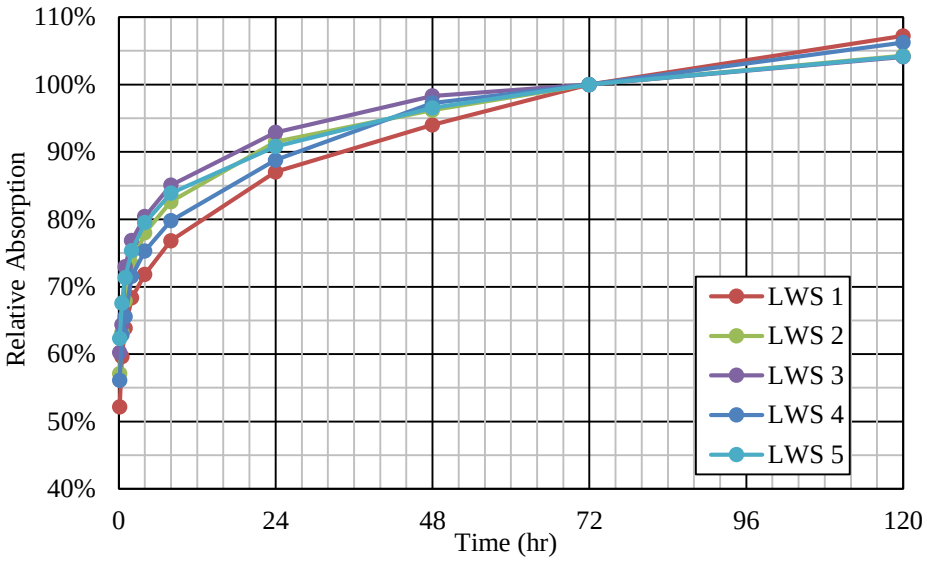

Figure 3.2: Relative absorption as a function of time

The relative desorption, with respect to the 72-hour absorption value, was also measured. The method was based on ASTM C1761, but some modifications were made. The container size was reduced by half, from one gallon to a half of a gallon, as well as the quantity of salt solution, from 300 g (10.5 oz) to 150 g (5.25 oz). On the other hand, the sample size (approx. 5 g (0.175 oz)) and mass tolerance (± 0.01 g (0.00035 oz)) were maintained. The containers were stored in standard ambient conditions at 21 ± 1 ºC (69.8 ± 33.8 ºF) and 50% ± 4% relative humidity. The weight of each sample was measured daily for 2 to 4 weeks until the mass of the sample reached equilibrium and did not change by more than 0.01 g (0.00035 oz) over a 3-day period. Multiple humidity levels were tested using different salt solutions, with the standard being 94% using potassium nitrate (ASTM 1761). The results can be found in Table 3.3 and Figure 3.3.

Table 3.3: Relative desorption results

Salt solution	R.H.*	Relative desorption				
		LWS1	LWS2	LWS3	LWS4	LWS5
Sodium Chloride	75%	99.6%	98.9%	96.2%	-	-
Potassium Chloride	85%	99.1%	98.4%	93.4%	-	-
Potassium Nitrate	94%	97.3%	96.4%	88.0%	97.5%	87.0%
Potassium Sulfate	97%	91.8%	85.0%	77.5%	-	-

Note: These values are based on literature by Greenspan, 1977 and Rockland, 1960.

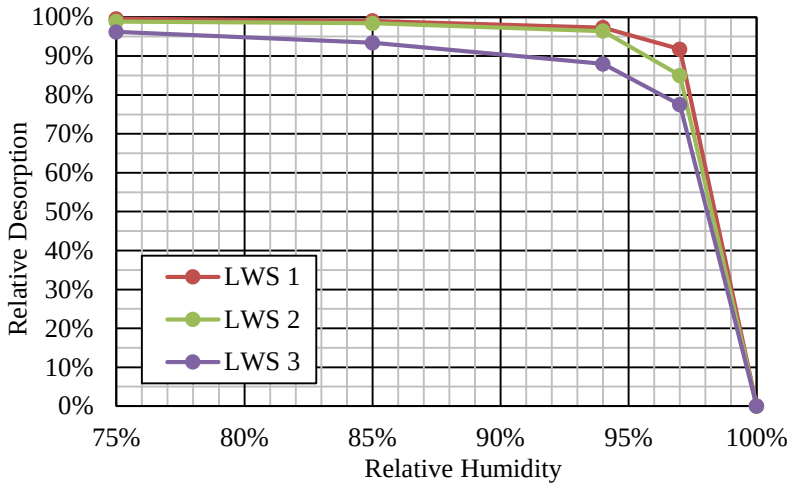

Figure 3.3: Desorption isotherms

The LWS 3 and LWS 5 materials are shown to have a lower relative desorption, while the remaining LWS have excellent desorption characteristics. The threshold for acceptance set by ASTM 1761 is 85% relative desorption at 94% RH. The LWS 3 does not technically meet this requirement, but it can still be used as an effective internal curing material, as long as the lower relative desorption value is taken into account.

3.5 Other constituent materials

Commercially available Type I/II ordinary Portland cement (OPC) was used in this study. Class C fly ash was employed in the binary cementitious systems. The scanning electron microscope (SEM) images of the investigated cementitious materials are presented in Figure 3.4. Missouri River sand (0-4.75 mm) was used under saturated surface dry (SSD) condition. The water absorption and specific gravity of the river sand is 0.14% and 2.65, respectively. The coarse aggregates are a 3/4” dolomitic limestone (MoDOT Gradation D or ASTM Gradation 67). The physical and chemical characteristics of the cementitious materials used in this investigation are presented in Table 3.4.

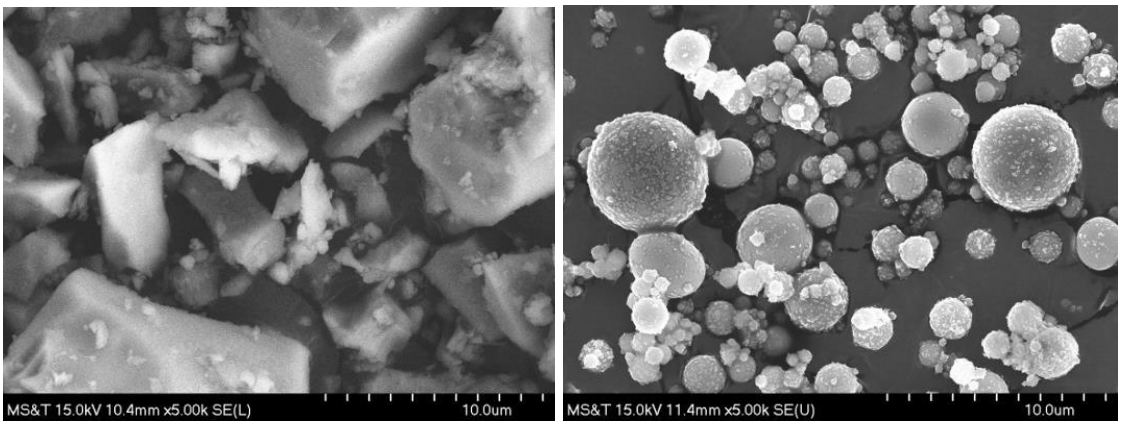

(a) OPC (b) Class C fly ash

Figure 3.4: SEM images of cementitious materials with magnification of 5000X

The chemical admixtures used in this study included a polycarboxylate-based mid-range water reducer (MRWR) and a synthetic-based air-entraining agent (AEA) (solid content of 12.5%, specific gravity of 1.01). The AEA dosage was adjusted to secure an air volume of 5% ± 2%. The MRWR dosages were varied to obtain initial slump consistencies of 50-100 mm (1.95-3.9 in.) for concrete targeted for pavement construction and 100-200 mm (3.9-7.8 in.) for concrete targeted for bridge deck applications.

Table 3.4 Chemical and physical properties of cementitious materials

	Type I/II cement	Class C fly ash
SiO_2(%)	19.72	36.50
Al_2O_3(%)	5.10	24.80
Fe_2O_3(%)	2.76	5.20
CaO (%)	64.50	28.10
MgO(%)	2.30	5.00
SO_3(%)	3.25	2.50
Na_2O eq. (%)	0.33	–
C_3S (%)	65.23	–
C_2S (%)	7.33	–
C_3A (%)	8.85	–
C_4AF (%)	8.40	–
Loss of Ignition (%)	1.50	0.50
Blaine surface area (m^2/kg)	562	465
Specific gravity, SSD	3.15	2.70

Note: 1 kg/m^2 = 0.2048 lb/ft^2

3.6 Experimental program

3.6.1 Optimization of curing strategies of HPC with LWS (Sub-task II-2)

As discussed earlier, the test program was performed in two blocks. The first block of testing matrix focused on the effect of the dosage of LWS on workability, shrinkage, and compressive strength. The second block focused on the effect of LWS content on mechanical properties, shrinkage, and transport properties of concrete made with optimized mixtures from the first block.

The test matrix of the experimental work undertaken in the first block is shown in Table 3.5. Four mixtures made with different types of LWS and without any LWS were investigated. For each mixture, different initial moist curing regimes were adopted. As shown in Table 3.6, the mixing regimes consisted of subjecting the concrete to initial moist curing periods of 1, 3, and 7 days as well as Standard curing. Standard curing was 28 days of moist curing in the case of drying shrinkage followed by air drying at 50% RH and continuous moist curing until the time of testing for samples used to determine mechanical properties. Table 3.7 summarizes the testing program considered in the first block of the experimental work.

Table 3.5: Test matrix for the first block

Concrete type	LWS type	LWS content	Curing regime
Bridge Deck	Ref.	-	1D, 3D, 7D, and Standard curing (continuous moist curing until time of testing for mechanical properties and 28 days followed by air drying for drying shrinkage testing)
	LWS 1	100% of suggested content	
	LWS 2		
	LWS 3		

Table 3.6: Proposed curing regimens

Moist curing duration	Detail
Dry curing (1D)	1 day in mold, then air drying at 23 °C and 50% RH
3 days curing (3D)	1 day in mold, then 2 days moist curing, then air drying at 23 °C and 50% RH
7 days curing (7D)	1 day in mold, then 6 days moist curing, then air drying at 23 °C and 50% RH
Standard: Continuous moist curing for mechanical properties	1 day in mold, then moist curing until the age of testing
Standard: 28 days of moist curing for drying shrinkage	1 day in mold, then 27 days moist curing followed by air drying at 23 °C and 50% RH

Note: °F = (°C × 1.8) + 32

Table 3.7: Test methods for the first block

Property type	Test method
Fresh Properties	Unit weight (ASTM C 138), air content (ASTM C 173), and slump (ASTM C143)
Mechanical properties	Compressive strength (ASTM C 39) at 3, 7, 28, 56 days
Shrinkage	Drying shrinkage (ASTM C 157)

Table 3.8 shows the Reference mixture proportioning, which was modified based on the MoDOT B-2 mixture. The normal weight coarse aggregates used for this block was 19 mm (¾") dolomitic limestone (MoDOT Gradation D or ASTM Gradation 67) from Sullivan, MO. The normal weight sand was a Missouri River sand meeting the requirements of MoDOT Section 1005 or ASTM C33. The LWS content was calculated using the method presented in ASTM 1761.

Table 3.8: Reference mixture proportions and targeted slump consistencies

Proportions and requirements	Bridge deck	Paving
Cement (kg/m^3)	281	244
Class C Fly ash (kg/m^3)	94	81
w/cm	0.40	0.40
Water (kg/m^3)	150	130
Sand (kg/m^3)	898	780
Coarse Aggregate (kg/m^3)	898	1122
Air Content (%)	6 ± 1	6 ± 1
Slump (mm)	100 ± 25	50 ± 15

Note: 1 kg/m^3=1.686 lb/yd^3, 1 mm=0.039 in.

3.6.2 Optimization of dosage and type of LWS for pavement and bridge deck (Sub-task II-2)

The second block of experiments was carried out to optimize the content of each of the three selected LWS types. A parametric approach using LWS contents that are normalized to the theoretical content of saturated LWS providing enough water to counteract the chemical shrinkage was used. The theoretical content was calculated according to the ASTM C 1761.

The test matrix is shown in Table 3.9. The experimental program was done for both paving and bridge deck concrete mixtures. Three LWS types (LWS 1, LWS 2, and LWS 3) were chosen.

The LWS was added at three different levels varying from 50% to 150% of the required content of the LWS to compensate for chemical shrinkage. Two moist curing regimes of 3 days of moisture curing and Standard moist curing were employed. Table 3.10 shows the test methods considered in this testing program.

Table 3.9: Test matrix for the second test block

Concrete type	Lightweight sand type	Content, % of volume of total sand	Curing
Bridge Deck	Reference	0	3 days of moisture curing Standard curing (continuous moist curing until time of testing for mechanical properties and 28 days followed by air drying for drying shrinkage testing)
	LWS 1	50	
		100	
		150	
	LWS 2	50	
		100	
		150	
	LWS 3	50	
		100	
		150	
Paving	Reference	0	
	LWS 1	50	
		100	
		150	
	LWS 2	50	
		100	
		150	
	LWS 3	50	
		100	
		150	

Table 3.10: Test methods for the second block

Property	Test method
Fresh Properties	Unit weight (ASTM C 138), air content (ASTM C 173), slump (ASTM C143), setting time (ASTM C403)
Mechanical properties	Compressive strength (ASTM C 39) at 3, 7, 28, 56, 91 days
	Modulus of elasticity (ASTM C 469) at 56 and 91days
	Flexural strength (ASTM C 78) at 56 and 91 days
Shrinkage	Drying shrinkage (ASTM C 157)
	Autogenous shrinkage (ASTM C 1698)
Durability	Sorptivity (ASTM C 1585) at 56 days
	Surface Resistivity (AASHTO T95) at 56 and 91 days
	Bulk electrical conductivity (ASTM C 1760) at 56 and 91 days

3.6.3 Test methods

The test methods to determine the various fresh and hardened properties, shrinkage, and durability of the investigated mixtures are detailed below.

Mixing procedure

The concrete mixtures were prepared using a drum mixer with 150-L (39.6-gal) capacity. Before batching, the moisture content of the bulk LWS was measured in accordance with ASTM C128. The rest amount of water to be added in the LWS was calculated by subtracting the water content in the LWS from the total water demand of the LWS to secure a saturated-surface-dry (SSD) condition. After adding the rest amount of water to the LWS, the LWS was homogenized with water and then placed in a sealed plastic bag for 24 h before batching to secure the SSD condition. The mixing procedure was as follows:

1) add aggregates and mix for 1 minute to homogenize;

2) add approximately half the batch water (add the AEA to this water) and mix for 1 minute;

3) add cement and supplementary cementitious materials (this is the initialization point for hydration) and mix for 30 seconds;

4) add the remaining half of the batch water gradually while maintaining mixing for an 2.5 minutes (add the MRWR to the water if applicable, also if only adding part of the MRWR, hold back a small amount of water to assist in adding the remaining water reducer later);

5) allow the concrete to rest for 3 minutes and verify the slump concrete and air content if needed; then

6) remix for 3 minutes (add MRWR or AEA to adjust slump or air content if needed).

Fresh properties

The unit weight and fresh properties of the concrete were determined in accordance with ASTM C138 and ASTM C1611, respectively. Three samples replicates were prepared for each test. The average results are reported.

Mechanical properties

Cylindrical specimens measuring 100 × 200 mm (3.9 × 7.8 in.) were cast to determine compressive strength (ASTM C39) and modulus of elasticity (ASTM C469) at 3, 28, 56, and 91 days. For each testing age, three 100 × 200 mm (3.9 × 7.8 in.) cylindrical specimens were used for determining the compressive strength and modulus of elasticity. Specimen end surfaces were grinded to ensure uniform load distribution over the specimen surfaces to evaluate the modulus of elasticity. Prismatic specimens measuring 75 × 75 × 400 mm (2.93 × 2.93 × 15.6 in.) were cast to determine the flexural strength of concrete according to ASTM C1609.

Shrinkage

Drying shrinkage of concrete (ASTM C157) was determined with a digital type extensometer using prismatic specimens measuring 75 × 75 × 285 mm (2.93 × 2.93 × 11.12 in.). After demolding at 24 hr, the prismatic specimens were immersed in water for 6 days. The samples were then stored in a temperature and humidity controlled room at 23 ± 1°C (73.4 ± 33.8 °F) and 50% ± 3% RH. Shrinkage was then measured until stabilization of shrinkage readings.

Autogenous shrinkage of mortars made with different LWS was determined according to ASTM C1698. The mortar specimens were prepared by screening the coarse aggregate out of the concrete mixtures. According to ASTM C1698, the initial reading for the autogenous shrinkage of a mortar sample should be carried out at the final setting time of the mortar. Therefore, the final setting time of mortar mixtures was determined according to ASTM C403. Figure 3.5 shows the shrinkage setup used for unsealed and sealed specimens. For each mixture, three specimens were prepared.

Figure 3.5: Drying shrinkage (left) and autogenous shrinkage (right)

Durability

The electrical resistivity was used to classify the concrete according to the corrosion rate. The measurement of electrical resistivity was determined using two different methods: the direct two-electrode method (ASTM C1760) and the four-point Wenner probe method (AASHTO TP 95-11), corresponding to bulk electrical conductivity and surface resistivity, respectively (Figure 3.6). The electrical resistivity was measured using cylindrical samples measuring 100 mm (3.9 in.) in diameter and 200 mm (7.8 in.) in height that were cured in lime-saturated water until the age of testing. The electrical resistivity is calculated as follows:

$$\rho = R \times k \tag{1}$$

where ρ is the resistivity, and R and k refer to measured resistance and geometry correction factor, respectively. The geometry correction factor for surface resistivity and bulk electrical conductivity can be calculated as:

$$k \text{ (surface resistivity)} = \frac{2\pi a}{1.1 - \frac{0.73}{d/a} + \frac{7.82}{(d/a)^2}} \tag{2}$$

$$k \text{ (bulk electrical conductivity)} = \frac{A}{L} \tag{2}$$

where d, A, a, and L refer to the diameter, cross section area, probe spacing, and length of the specimen, respectively.

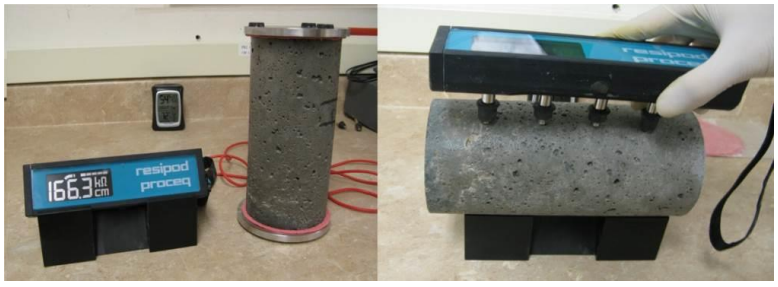

Figure 3.6: Bulk electrical conductivity (left) and surface resistivity (right)

The sorptivity of concrete mixtures was determined in compliance with ASTM C1585. The

test consisted of measuring the increase in mass of a disc specimen at given intervals of time when permitted to absorb water by capillary suction. After 56 days of moist curing, cylinder samples from each mixture were cut in three disc specimens measuring 50 mm (1.95 in.) in height. The specimens were then placed in an environmental chamber at 50°C (122 °F) and 80% RH for 3 days. Each specimen was then placed inside a sealable container and stored at a 23 ± 2°C (73.4 ± 35.6°F) for at least 15 days until it reached equilibrium mass when the moisture distribution is consistent within the test specimen. Prior to absorption testing, the side surface of the samples was sealed with aluminum tape, and the top surface was covered with plastic wrap. This was done to prevent drying of the sample from these surfaces. The test procedure is schematically illustrated in Figure 3.7. The amount of absorbed water was normalized by the cross-section area of the specimen exposed to the fluid, as shown in equation (3):

$$I = \frac{m_t}{a \times d} \tag{3}$$

where I is the absorption, m_t is the specimen mass at time t (gr); a is the exposed area of the specimen (mm^2), and d is the density of the water. The absorbed fluid volume is plotted as a function of the square root of time. The initial sorptivity is determined from the slope of the curve during the first 6 h according to ASTM C1585. The secondary sorptivity is determined using the slope of the same measurements between 1 and 7 days, as outlined in ASTM C1585.

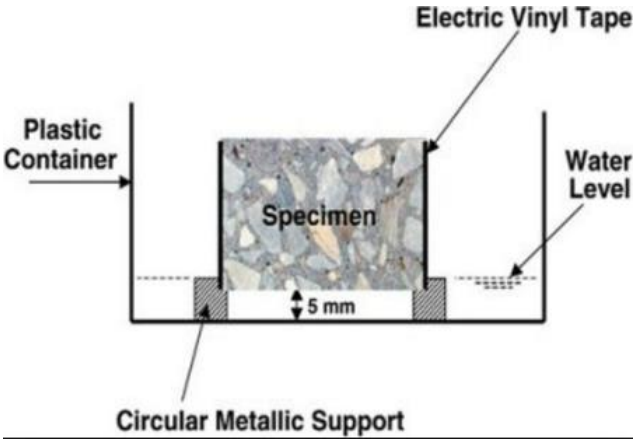

Figure 3.7: Illustration of sorptivity test

4. Optimization of Curing Strategies of Concrete Containing LWS for Pavement and Bridge Deck

4.1 Mixture design of investigated concrete

This chapter presents the results of the investigation of the coupled effect of LWS and moist curing duration on key properties of concrete that can be used in bridge deck construction. The MoDOT bridge deck mixture was used for the Reference mixture. The investigated concrete mixtures were prepared with various types of LWS subjected to different moist curing durations. As presented before, various LWS materials available in Missouri and/or surrounding states were used. The test matrix and test methods used in this investigation were introduced in Chapter 3. The mixture compositions of the investigated concrete are presented in Table 4.1. The replacement ratio of normal sand by LWS were calculated according to ASTM 1761.

Table 4.1: Mixture design of selected concrete for bridge deck construction

	Reference	LWS1	LWS2	LWS3
Cement (kg/m^3)	281	281	281	281
Fly ash (kg/m^3)	93	93	93	93
Coarse aggregate (kg/m^3)	919	919	919	919
Fine aggregate (kg/m^3)	882	587	678	611
Lightweight sand (kg/m^3)	-	233	158	190
MRWR (g/m^3)	814	814	814	814
AEA(g/m^3)	303	303	303	303
Total Water (kg/m^3)	147	134	134	133

Note: 1 kg/m^3 = 1.686 lb/yd^3, 1000 g/m^3 = 1 kg/m^3

A vibrating rod was used to facilitate the consolidation of the fresh concrete. Molded samples were kept under wet burlap and covered by plastic sheets for 24 hr before demolding. The samples for 3D, 7D, and Standard moist curing were then placed in lime-saturated water at 23 ± 1 °C (73.4 ± 33.8 °F) to allow moist curing for the desired durations followed by air drying at 23 °C (73.4 °F) and 50% RH. The samples prepared for Dry curing conditions were exposed to air drying at 23 °C (73.4 °F) and 50% RH right after demolding.

A batch of 120 liters (31.7 gal) of concrete was prepared to evaluate the various properties of each mixture. The targeted slump was 100 ± 25 mm (3.9 ± 0.975 in.), and the targeted air content was 6% ± 1%. As shown in Table 4.2, the slump varied from 80 mm (3.12 in.) for the LWS3

mixture to 120 mm (4.68 in.) for the LWS1 mixture. The unit weight ranged from 2,278 kg/m^3 (3,840 lb/yd^3) (LWS1 concrete) to 2,337 kg/m^3 (3,940 lb/yd^3) (Reference concrete). The LWS3 and Reference mixtures with 5% and 6.2% had the lowest and highest air contents, respectively.

Table 4.2: Fresh properties of investigated mixtures for bridge deck

	Reference	LWS1	LWS2	LWS3
Slump (mm)	85	120	85	80
Unit weight (kg/m^3)	2337	2278	2318	2292
Air content (%)	6.2	5.9	5.1	5.0

Note: 1 kg/m^3 = 1.686 lb/yd^3, 1 mm = 0.039 in.

4.2 Compressive strength under different curing conditions

The compressive strength results of the investigated mixtures evaluated up to 56 days under different curing durations are presented in Table 4.3. For each age, three 100×200 mm (3.9 × 7.8 in.) cylindrical specimens were tested. At early age, the compressive strength with different curing regimes exhibited similar results, regardless of the LWS type. However, at later ages, mixtures with LWS2 and 7-day moisture curing had the highest strength. In other words, the combination of LWS2 and 7 days of moisture curing can provide the most effective curing condition. The use of LWS2 enabled the most effective internal curing given its high desorption rate.

Table 4.3: Compressive strength results

Curing condition	Testing age (day)	Reference	LWS1	LWS2	LWS3
Dry	3	31.0	31.4	32.9	31.9
	7	35.5	35.9	38.6	38.1
	28	41.8	44.2	48.9	45.8
	56	43.3	46.5	51.6	47.6
3 days of moisture curing	3	30.4	30.3	32.5	32.7
	7	37.4	37.2	40.3	38.9
	28	44.5	46.0	50.7	49.1
	56	47.5	49.3	52.7	50.4
7 days of moisture curing	3	30.7	31.1	32.5	31.5
	7	35.4	36.5	38.3	37.6
	28	46.8	47.8	52.1	49.6
	56	49.4	52.8	55.4	52.0
Standard curing	3	30.3	31.3	32.5	31.6
	7	34.9	36.3	39.1	38.3
	28	43.6	46.4	48.8	46.7
	56	48.0	50.5	53.7	50.2

Notes: 1 MPa = 145 psi

As summarized in Table 4.3, the highest strength development rate occurred between 7 and 28 days in all investigated mixtures. For example, the LWS1, LWS2, and LWS3 mixtures exhibited sharp increase in compressive strength, respectively, between 7 to 28 days of 8.5, 10, 9.5, and 8.5 MPa (1,235, 1,450, 1,380, and 1,235 psi). However, such increase was limited to 4.5, 4, 5, and 3.5 MPa (655, 580, 725, and 510 psi), respectively, between 28 and 56 days.

Figures 4.1 and 4.2 compare the 28-day and 56-day results, respectively, of mixtures containing different types of LWS cured under various curing durations. The 56-day compressive strength values varied from 43 to 56 MPa (6,235 to 8,120 psi). The lowest and highest values corresponded to the Reference bridge deck concrete mixture subjected to Dry curing condition and the LWS2 mixture under 7D curing condition, respectively.

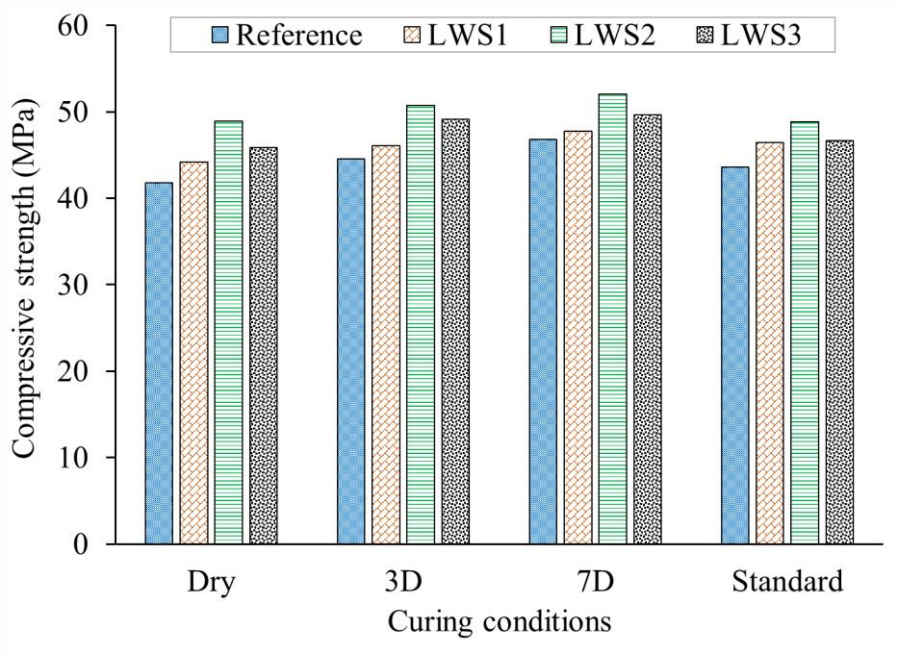

Figure 4.1: Compressive strengths of investigated mixtures at 28 days (1 MPa=145 psi)

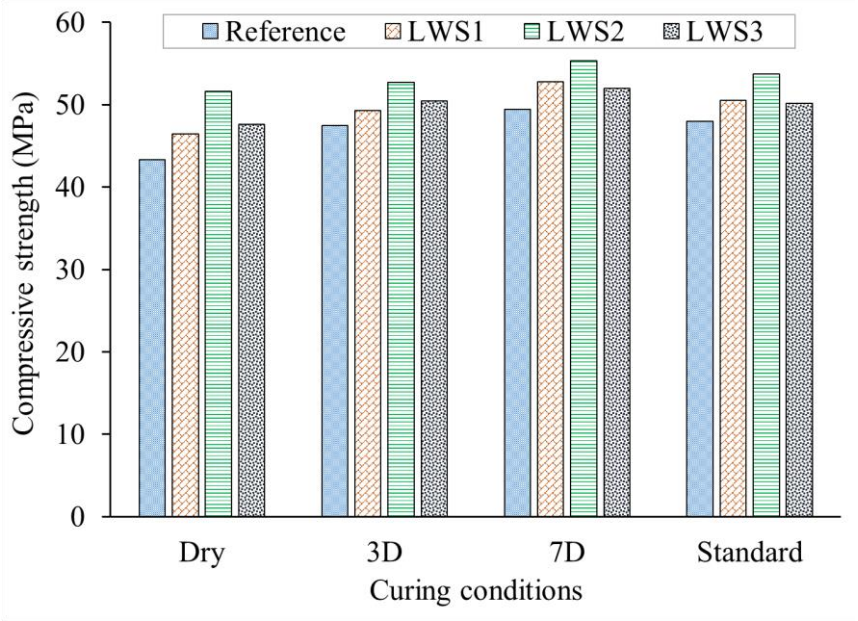

Figure 4.2: Compressive strengths of investigated mixtures at 56 days (1 MPa=145 psi)

4.2.1 Effect of curing condition

Increasing the moist curing duration up to 7 days led to the enhancement of compressive strength. Slight reduction in strength was observed when moist curing continued after 7 days. For example, the Reference, LWS1, LWS2, and LWS3 mixtures showed the highest compressive strength values at 56 days of approximately 50, 53, 56, and 52 MPa (7,250, 7,690, 8,120, and 7,540 psi), respectively, under the 7D curing condition. These values were 2, 4, 3, and 2 MPa (290, 580, 435, and 290 psi) higher and 1.5, 2.5, 2, and 2 MPa (218, 363, 290, and 290 psi) lower than similar mixtures subjected to the 3D and Standard curing conditions, respectively.

4.2.2 Effect of LWS type

The LWS2 mixture exhibited better performance in terms of compressive strength compared to the other mixtures. For example, the 56-day compressive strength of the LWS2 mixture was 12% higher than the Reference mixture under the 7D curing condition where the LWS1 and LWS3 mixtures had 7% and 5% higher compressive strengths, respectively, compared to the Reference mixture under the same curing condition. All mixtures proportioned with LWS had their greatest level of improvement in performance compared to the Reference mixtures when no moist curing was applied initially (Dry curing condition). For example, the incorporation of LWS2 led to a 19%

increase in the 56-day compressive strength under Dry curing condition compared to only 7%, 10%, and 9% when the same concrete was subjected to 3D, 7D, and Standard curing conditions, respectively. Under drying condition, the quick drop of internal relative humidity can stimulate the efficiency of internal curing by LWS. In particular, the LWS2 with relatively high absorption and desorption capacities exhibited the best performance in internal curing, which provided more water for cement hydration and resulted in the highest compressive strength.

4.3 Drying shrinkage under different curing conditions

The decrease in internal relative humidity of the cement paste produces internal stresses and causes the concrete to shrink. Large shrinkage can lead to severe cracking of concrete structures. The drying shrinkage in concrete is primarily due to the loss of water through evaporation at the surface of the concrete. Evaporation removes the pore water, thus decreasing the RH of concrete. When concrete maintains at high RH (*>95%*), the drying shrinkage is very limited. However, at lower RH condition, the empty rate of smaller capillary pores of concrete dominates the drying shrinkage. The empty rate is mainly controlled by the total porosity and the pore structure of the cement paste. Increase in total porosity may increase the drying shrinkage. The loosely connected pore structure can also increase the drying shrinkage. As a result, external factors that influence the pore structure, such as the curing conditions and type of LWS incorporated, can significantly influence the result of drying shrinkage.

Figures 4.3 to 4.6 show the variations in drying shrinkage of the investigated mixtures that were subjected to Dry, 3D, 7D, and Standard curing conditions, respectively. As expected, none of the investigated mixtures showed drying shrinkage variations during moist curing, i.e. the initial period of moisture curing (RH > *95%*). However, the different initial curing regimes and LWS types led to different shrinkage behaviors, as elaborated further in the following sections.

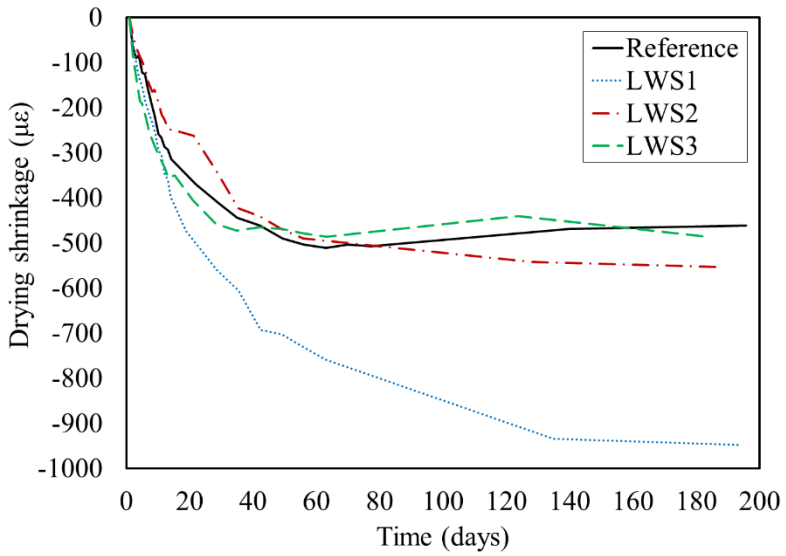

Figure 4.3: Drying shrinkage variations for mixtures under Dry curing condition

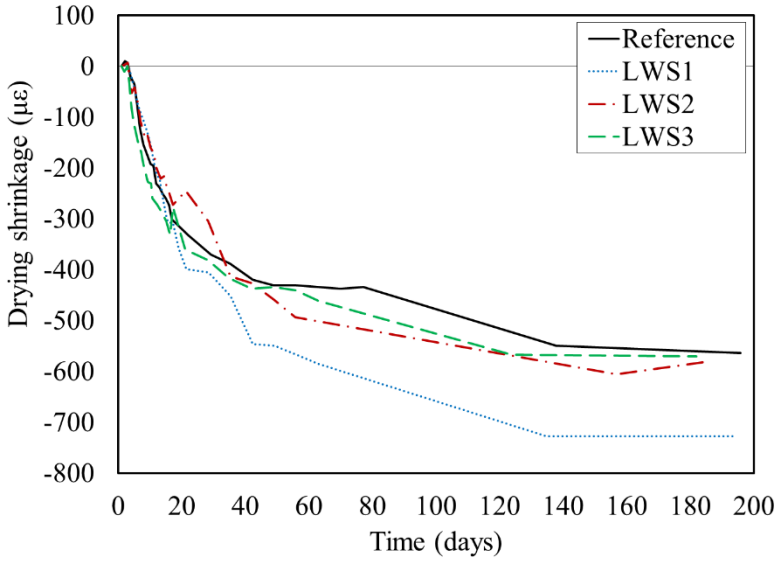

Figure 4.4: Drying shrinkage variations for mixtures under 3D curing condition

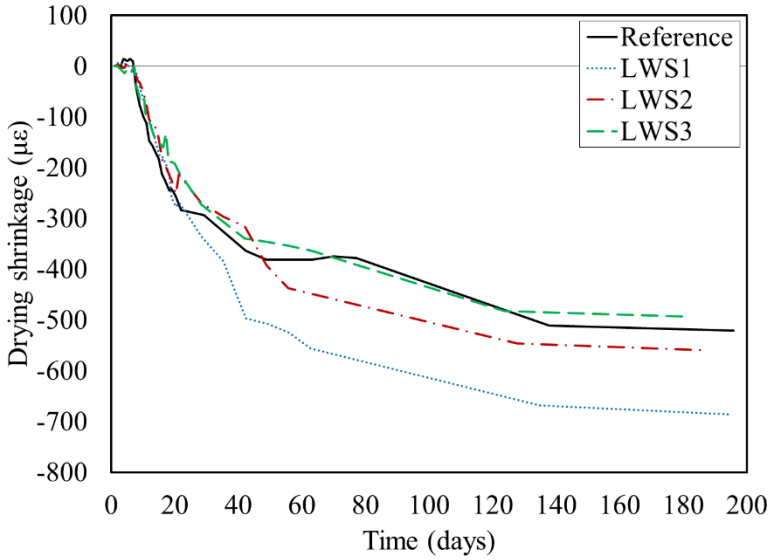

Figure 4.5: Drying shrinkage variations for mixtures under 7D curing condition

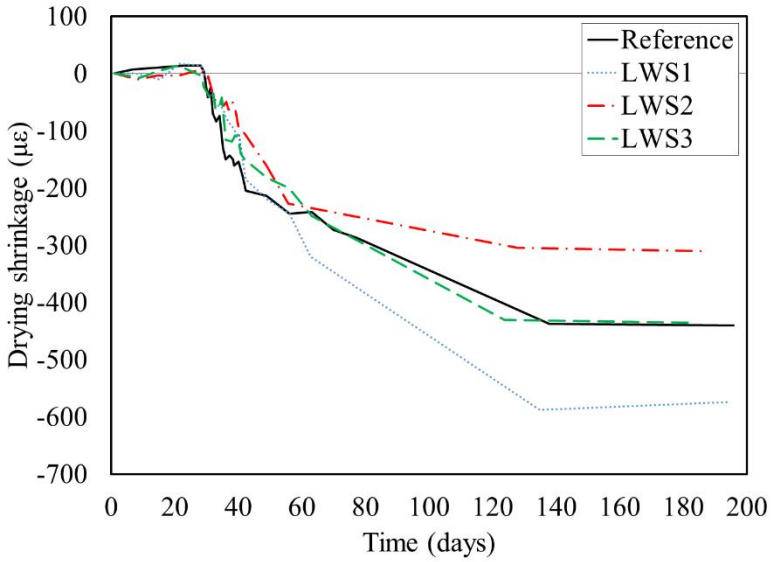

Figure 4.6: Drying shrinkage variations for mixtures under Standard curing condition (28 days of moist curing)

4.3.1 Effect of initial moisture curing duration on drying shrinkage

The increase in moisture curing duration resulted in a reduction of drying shrinkage regardless of the LWS type. For example, the drying shrinkage of the LWS1, LWS2, and LWS3 mixtures

decreased from 730 to 670, 600 to 550, and 570 to 480 micro-strain at 190 days when the initial moisture curing was extended from 3 to 7 days. Further shrinkage reduction, of 80, 250, and 50 micro-strain was obtained for the LWS1, LWS2, and LWS3 mixtures when the Standard curing condition was applied compared to the 7D curing condition.

All of the investigated mixtures exhibited their lowest drying shrinkage values under the Standard curing condition, as expected, where the Reference, LWS1, LWS2, and LWS3 mixtures had shrinkage values of 440, 590, 300, and 430 micro-strain at 190 days. The Reference, LWS2, and LWS3 mixtures had their highest shrinkage values when cured under 3D curing condition that resulted in shrinkage values of 550, 600, and 560 micro-strain at 190 days, respectively. The LWS1 mixture exhibited its highest shrinkage value of 930 micro-strain under Dry curing condition.

4.3.2 Effect of LWS type on drying shrinkage

The LWS1 mixture exhibited the highest drying shrinkage regardless of the curing condition. The increase in drying shrinkage associated with the use of LWS can be due to the lower stiffness of the LWS compared to the normal weight sand that is being replaced.

The shrinkage values at 190 days were 930, 730, 670, and 590 micro-strain for concrete subjected to the Dry, 3D, 7D, and Standard curing conditions, respectively. As shown in Figure 4.3, under Dry curing condition, the LWS3 mixture showed the lowest drying shrinkage of 440 micro-strain which indicated a shrinkage mitigation of 60 micro-strain compared to 500 micro-strain for the Reference mixture.

Under the 3D curing condition, the mixtures incorporating LWS did not exhibit lower shrinkage than the Reference mixture that had 550 micro-strain after 190 days (Figure 4.4). Under the 7D curing condition, the LWS3 mixture with 480 micro-strain at 190 days showed the lowest drying shrinkage compared to the Reference mixture with 510 micro-strain (Figure 4.5). As shown in Figure 4.6, the LWS1, LWS2, and LWS3 mixtures exhibited shrinkage values of 590, 300, and 430 micro-strain, respectively, compared to the Reference mixture with 440 micro-strain under Standard curing condition at 190 days.

4.4 Summary

In this chapter, three types of saturated LWS materials were used at specific replacement

values of normal weight sand that can enable the compensation for chemical shrinkage. The testing involved subjecting the mixtures to different initial moisture curing durations and evaluate the coupled effect of LWS type and external moist curing on compressive strength development and drying shrinkage.

The overall performance of the various mixtures is compared in Table 4.4. The results are normalized by those of the Reference bridge deck mixture of MoDOT subjected to the Dry curing condition. For compressive strength, the values which are greater than 100% show improvement in certain performance characteristics. In the case of drying shrinkage, the lower percentage values indicate better performance. It is important to note that the effect of LWS on autogeneous shrinkage was not evaluated here and will be the subject of detailed evaluation in the next chapter along with durability.

Table 4.4: Comparison of compressive strength and drying shrinkage of concrete with different LWS and curing conditions (best performance is highlighted in **red**)

Curing condition	Properties	Reference	LWS1	LWS2	LWS3
Dry	f'c at 28 days	100%	106%	117%	110%
	f'c at 56 days	100%	107%	119%	110%
	Drying shrinkage at 190 days	100%	186%	108%	88%
3 days of moisture curing	f'c at 28 days	106%	110%	121%	117%
	f'c at 56 days	110%	114%	122%	116%
	Drying shrinkage at 190 days	110%	146%	120%	114%
7 days of moisture curing	f'c at 28 days	112%	114%	**125%**	119%
	f'c at 56 days	114%	122%	**128%**	120%
	Drying shrinkage at 190 days	102%	134%	110%	96%
Standard curing	f'c at 28 days	104%	111%	117%	112%
	f'c at 56 days	111%	117%	124%	116%
	Drying shrinkage at 190 days	88%	118%	**60%**	86%

The following conclusions can be made:

(1) Concrete mixtures proportioned with LWS had better performance in terms of 28 and 56 days compressive strength regardless of the curing regime.

(2) The LWS2 mixture exhibited better performance in terms of compressive strength at later ages compared with mixtures made with LWS1 or LWS3, regardless of the curing regime.

(3) In terms of initial moisture curing duration, 7 days of moisture curing resulted in the highest compressive strength levels at 28 and 56 days compared with other curing methods. Slight reduction in strength was observed when the moist curing continued after 7 days.

(4) Regardless of the curing condition, concrete made with the LWS1 exhibited the highest drying shrinkage at 140 days. Under drying and 7-day moisture curing, the LWS3 mixture obtained the lowest shrinkage results, which can be attributed to high initial water absorption of LWS3 and proper external water absorbed for curing. However, under 3 days of moisture curing, the incorporation with LWS did not provide better performance in terms of drying shrinkage. Proper combination of external and internal curing can provide effective curing for concrete mixtures to reduce shrinkage.

(5) Increasing the duration of initial moisture curing can reduce drying shrinkage. The mixtures exhibited the lowest drying shrinkage values under Standard curing condition.

5. Optimization of Lightweight Sand Content and Type in Concrete for Pavement and Bridge Deck Applications

5.1 Mixture design of investigated concretes

This chapter deals with the results of Sub-task II-3, as identified in Chapter 1. The focus of this sub-task is to establish the optimum content of LWS required to mitigate shrinkage, especially autogeneous shrinkage, without compromising mechanical properties. The durability of the optimized mixtures was also assessed. Multiple paving and bridge deck concrete mixtures were considered. In total, 20 concrete mixtures were investigated. The mixture proportioning of the investigated mixtures are summarized in Table 5.1. The mixtures were prepared with the LWS1, LWS2, and LWS3 materials that were presented earlier. The content of each LWS type was increased to provide internal curing water that could compensate for 50%, 100%, and 150% of the chemical shrinkage, as estimated from ASTM 1761.

Table 5.1: Mixture proportions of bridge deck and paving concrete mixtures

	Cement (kg/m^3)	Fly ash (kg/m^3)	Coarse aggregate (kg/m^3)	Fine aggregate (kg/m^3)	LWS (kg/m^3)	Water (kg/m^3)	MRWR (g/m^3)	AEA (g/m^3)
Bridge-Reference	281	94	920	879	-	150	837	303
Bridge-LWS1-50%	281	94	920	743	120	132	837	313
Bridge-LWS1-100%	281	94	920	596	239	125	837	322
Bridge-LWS1-150%	281	94	920	449	359	118	837	308
Bridge-LWS2-50%	281	94	920	781	92	131	837	303
Bridge-LWS2-100%	281	94	920	677	184	117	837	313
Bridge-LWS2-150%	281	94	920	573	276	105	837	313
Bridge-LWS3-50%	281	94	920	753	98	134	837	303
Bridge-LWS3-100%	281	94	920	621	196	126	837	313
Bridge-LWS3-150%	281	94	920	489	294	117	837	313
Paving-Reference	244	81	1093	808	-	131	725	427
Paving-LWS1-50%	244	81	1096	688	107	112	725	427
Paving-LWS1-100%	244	81	1096	561	214	103	802	427
Paving-LWS1-150%	244	81	1096	434	321	94	802	427
Paving-LWS2-50%	244	81	1095	718	82	113	806	427
Paving-LWS2-100%	244	81	1095	622	164	103	806	427
Paving-LWS2-150%	244	81	1095	526	246	93	806	427
Paving-LWS3-50%	244	81	1095	698	83	117	725	427
Paving-LWS3-100%	244	81	1095	584	166	109	725	427
Paving-LWS3-150%	244	81	1095	469	249	101	725	427

Notes: 1 kg/m^3 = 1.686 lb/yd^3, 1000 g/m^3 = 1 kg/m^3

5.2 Results and discussion

5.2.1. Fresh properties

Table 5.2 summarizes the fresh properties of the investigated mixtures. The fresh concrete temperature was controlled between 20 and 21.5 °C (68 and 70.7°F). In general, the incorporation of LWS had no significant effect on fresh properties. For the bridge deck concrete, the slump values ranged from 85 to 125 mm (3.32 to 4.88 in.) with the Bridge-LWS3-150% and Bridge-LWS1-50% mixtures exhibiting the lowest and highest slump values, respectively.

Table 5.2: Fresh properties of investigated mixtures

	Temperature (°C)	Slump (mm)	Unit weight (kg/m^3)	Air content (%)	Initial setting time (hr)	Final setting time (hr)
Bridge-Reference	20.6	120	2320	6.2	6.3	8.4
Paving-Reference	20.3	75	2368	6.0	7.1	9.5
Bridge-LWS1-50%	20.4	125	2285	7.0	6.5	8.6
Bridge-LWS1-100%	20.1	125	2224	7.0	7.3	9.0
Bridge-LWS1-150%	20.5	100	2229	6.2	6.4	8.8
Bridge-LWS2-50%	20.4	85	2312	6.1	6.0	8.1
Bridge-LWS2-100%	20.4	90	2281	6.1	6.3	8.2
Bridge-LWS2-150%	20.3	85	2231	6.6	6.1	7.9
Bridge-LWS3-50%	20.4	85	2297	6.0	6.6	8.7
Bridge-LWS3-100%	20.3	90	2263	5.5	6.8	8.8
Bridge-LWS3-150%	20.6	85	2211	5.4	5.4	7.2
Paving-LWS1-50%	20.5	40	2345	6.1	5.8	7.7
Paving-LWS1-100%	20.8	45	2314	6.2	5.6	7.8
Paving-LWS1-150%	22.4	40	2310	5.7	5.9	7.7
Paving-LWS2-50%	20.8	40	2326	6.1	5.5	7.1
Paving-LWS2-100%	21.2	50	2265	6.9	6.0	7.8
Paving-LWS2-150%	21.4	55	2251	6.7	6.0	7.9
Paving-LWS3-50%	20.7	40	2281	6.9	5.4	7.1
Paving-LWS3-100%	21.5	45	2272	6.8	5.7	7.7
Paving-LWS3-150%	21.2	55	2238	6.9	5.5	7.7

Note: 1 °C = 33.8 °F, 1 mm = 0.0394 in, 1kg/m^3 = 1.686 Ib/yd^3

The Bridge-LWS3-150% mixture had the lowest air volume of 5.4% and the shortest initial and final setting times of 5.4 and 7.2 hr, respectively. The lower setting may be attributed to the faster connectivity of cement hydration product given the accelerated hydration rate provided by

the 150% internal curing of the LWS3 material. The Bridge-LWS1-100% mixture had the longest initial and final setting times of 7.3 and 9 hr, respectively. In the case of paving concrete, the slump values ranged from 40 to 75 mm (1.56 to 2.93 in.), air contents from 5.7% to 6.9%, initial setting times from 5.4 to 6 hr, and final setting times from 7.1 to 7.9 hr.

5.2.2. Compressive strength

Table 5.3 presents the compressive strengths at 3, 7, 28, and 56 days of the investigated mixtures subjected to 3D and Standard curing conditions. In Chapter 4, the 7D curing showed the best performance in terms of strength and shrinkage, and the results were not significantly different from those obtained with the 3D curing. Therefore, the shorter initial curing duration of 3 days was employed in this study for practical purposes.

Table 5.3: Compressive strength results of the investigated mixtures at different ages

	3D curing condition				Standard curing condition			
	3 days	7 days	28 days	56 days	3 days	7 days	28 days	56 days
Bridge-Reference	30.4	39.7	48.2	48.7	32.5	39.0	43.4	50.9
Bridge-LWS1-50%	30.7	38.6	51.0	51.4	32.7	36.8	46.9	53.0
Bridge-LWS1-100%	30.2	38.6	51.0	51.5	30.6	36.7	47.6	52.3
Bridge-LWS1-150%	34.3	41.6	56.0	58.5	34.0	40.1	55.1	59.3
Bridge-LWS2-50%	33.6	44.2	54.0	54.6	32.7	39.5	52.2	55.9
Bridge-LWS2-100%	33.9	38.5	53.4	57.0	34.1	38.9	53.0	54.9
Bridge-LWS2-150%	33.6	39.9	52.4	56.1	31.2	37.4	50.1	53.3
Bridge-LWS3-50%	33.7	43.5	53.2	55.3	34.1	41.1	48.8	54.5
Bridge-LWS3-100%	34.3	43.4	54.0	55.5	34.1	41.0	50.4	54.4
Bridge-LWS3-150%	30.3	36.8	47.5	48.4	29.2	34.6	44.9	48.9
Paving-Reference	28.2	37.7	48.3	47.4	29.6	35.4	46.5	48.2
Paving-LWS1-50%	36.7	47.6	52.6	55.2	32.3	41.5	51.5	55.2
Paving-LWS1-100%	38.2	47.2	58.4	61.3	37.6	42.2	52.1	56.3
Paving-LWS1-150%	39.7	47.5	60.4	64.2	40.0	44.0	56.5	59.8
Paving-LWS2-50%	34.2	42.9	53.7	57.2	34.6	39.8	49.2	53.6
Paving-LWS2-100%	33.0	39.3	51.9	54.6	32.3	37.2	45.6	50.2
Paving-LWS2-150%	34.4	42.4	54.3	58.0	35.0	40.5	51.3	55.2
Paving-LWS3-50%	32.7	43.5	53.4	57.5	33.2	38.7	49.9	53.6
Paving-LWS3-100%	32.1	40.4	53.1	58.1	32.9	39.6	49.9	55.8
Paving-LWS3-150%	30.8	38.2	49.1	55.0	30.3	36.2	46.3	49.9

Figures 5.1 and 5.2 compare the 28- and 56-day compressive strength results for the bridge deck mixtures, respectively. The Bridge-LWS1-150% mixture had the highest 56-day compressive value of 59 MPa (8,560 psi) (Standard curing condition), which was 8 MPa (1,160 psi) higher than

the Bridge-Reference mixture. For the LWS1 mixture, increasing the LWS content from 0 to 150% increased the 28-day and 56-day compressive strengths by approximately 20%. However, for the LWS2 and LWS3 mixtures, increasing the LWS content led to slight variation or even reduction in the 28- and 56-day compressive strengths. This could be attributed to the difference in total porosity introduced by the different types of LWS (Meng and Khayat 2017). The lower water absorption of the LWS1 compared with the LWS2 and LWS3 materials indicate that the LWS1 has the lowest total porosity. Therefore, with the increase in the content of LWS to secure more internal curing capacity, the total resulting porosity introduced by the LWS was the lowest for LWS1. Lower porosity can lead to greater strength. On the other hand, internal curing water is increased with the increase of LWS content. Therefore, the hydration degree of cement is promoted with the increase in LWS content. Additional hydration products can reduce capillary porosity and strengthen the microstructure of the concrete, thus improving strength. This explains why the strength of mixtures made with the less porous LWS1 was increased with the increase in LWS content. On the other hand, when the content of the more porous LWS2 or LWS3 was increased, the higher porosity introduced by the LWS was dominating, thus resulting in an overall reduction in compressive strength despite the additional internal curing potential.

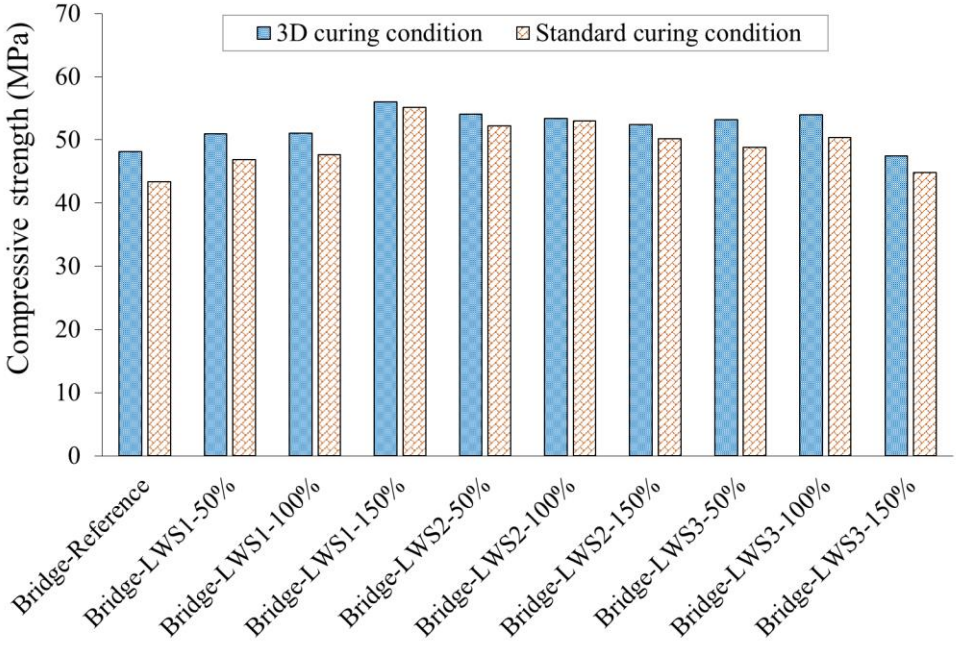

Figure 5.1: 28-day compressive strength results of bridge deck concrete mixtures containing different LWS types and contents (1MPa = 145 psi)

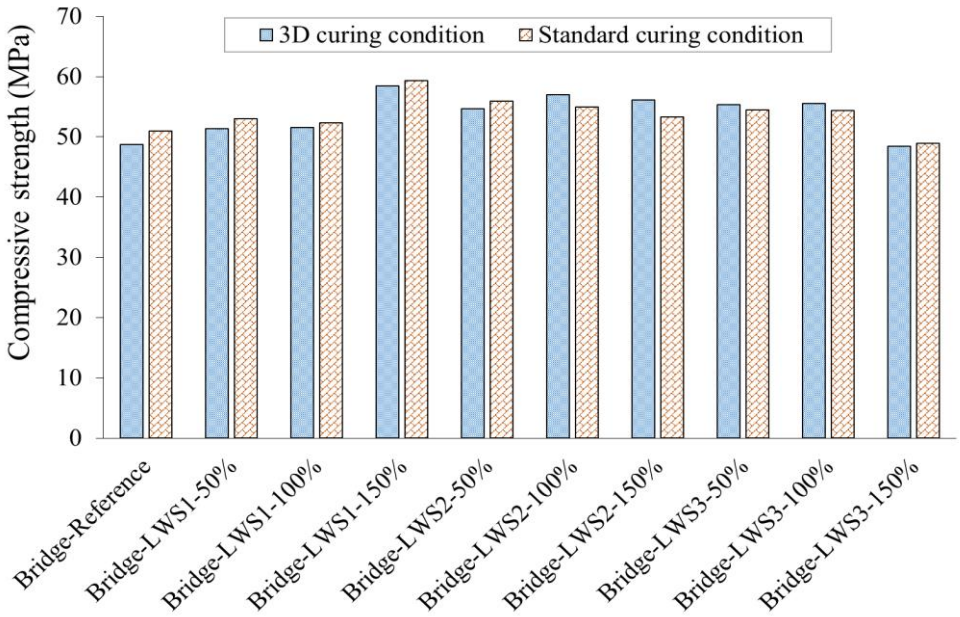

Figure 5.2: 56-day compressive strength results of bridge deck concrete mixtures containing different LWS types and contents (1MPa = 145 psi)

Figures 5.3 and 5.4 compare the 28- and 56-day compressive strengths for the paving mixtures, respectively. The highest 56-day compressive strength of 64 MPa (9,280 psi) was obtained for the Paving-LWS1-150% mixture subjected to 3 days of moist curing (3D). The Paving-Reference mixture subjected to the same curing condition had the lowest 56-day compressive strength of 47 MPa (6,815 psi).

Effect of curing condition

The bridge deck mixtures cured under 3D conditions exhibited slightly higher 28-day compressive strengths than those subjected to Standard curing, regardless of the LWS type and content. For example, the Bridge-Reference mixture showed the highest increase of 5 MPa (725 psi), and the Bridge-LWS2-100% exhibited the lowest increase of 1 MPa (145 psi). However, the 56-day compressive strength results showed no significant difference in terms of curing condition. For example, the Bridge-LWS2-150% exhibited only 3 MPa higher 56-day compressive strength under 3D compared to that of Standard curing condition, whereas the Bridge-LWS1-50% mixture had 2 MPa (290 psi) lower 56-compressive strength under 3D condition compared to the Standard condition.

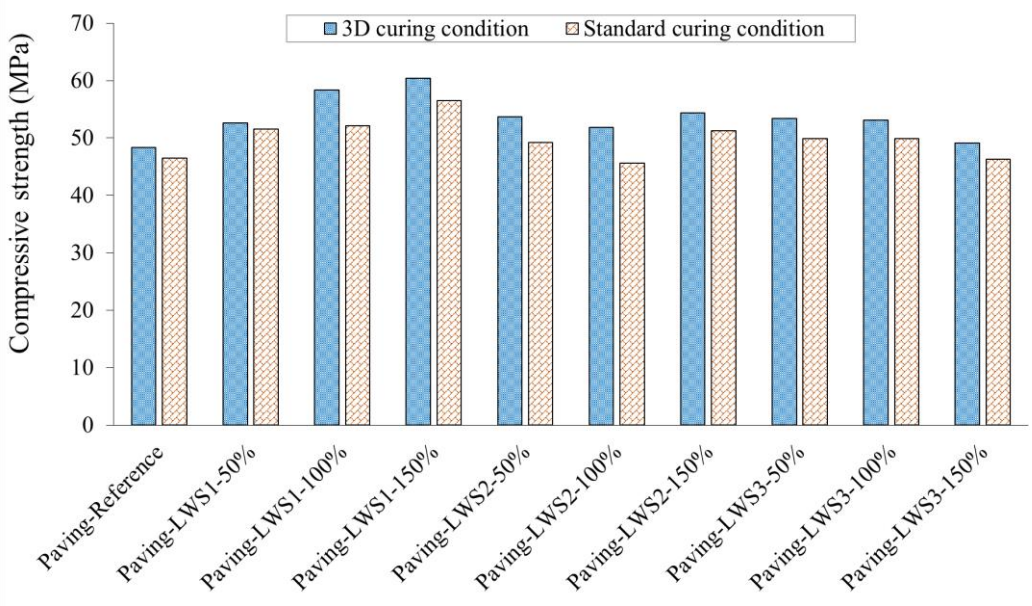

Figure 5.3: 28-day compressive strength results of paving concrete mixtures containing different LWS types and contents (1MPa = 145 psi)

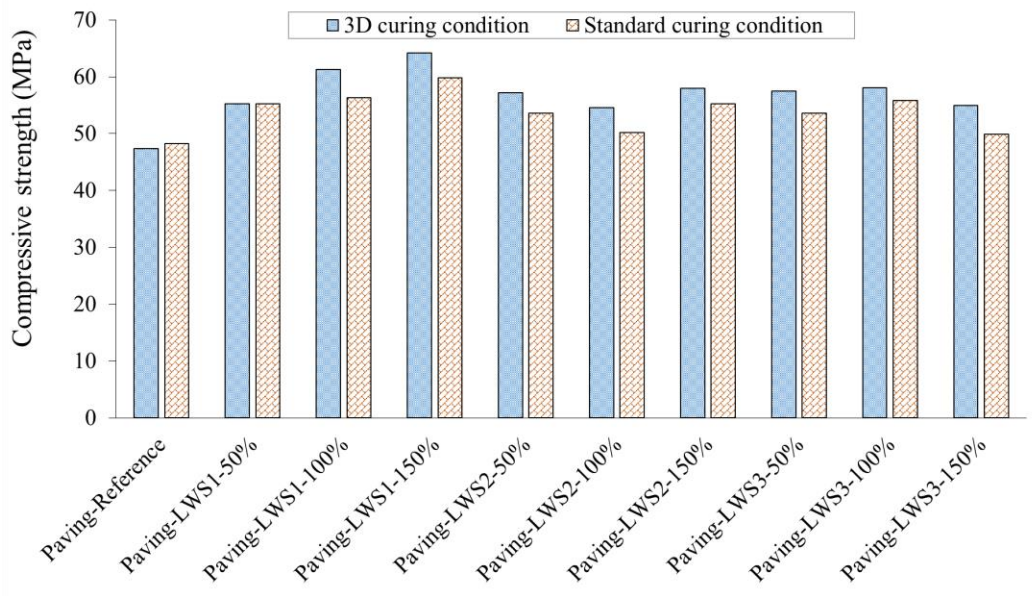

Figure 5.4: 56-day compressive strength results of paving concrete mixtures containing different LWS types and contents (1MPa = 145 psi)

In the case of paving concrete, the mixtures subjected to the 3D curing condition exhibited higher 28- and 56-day compressive strengths compared to those prepared under the Standard

curing condition, regardless of the LWS type and content. For example, the incorporation of 50%, 100%, and 150% LWS in the Paving-LWS2 concrete cured under 3D condition resulted in 4, 4, and 3 MPa (580, 580, and 435 psi), respectively, greater 56-day compressive strengths than those cured under the Standard condition. These values were 4, 6, and 3 MPa (580, 870, and 435 psi), respectively, for 28-day compressive strength for the same mixtures with the same curing conditions.

Effect of LWS content

In general, all of the mixtures proportioned with LWS exhibited higher compressive strengths compared to the Reference mixtures, regardless of concrete type and curing condition. However, no clear relationship was observed between compressive strength enhancement and the LWS type or content. For example, the 56-day compressive strengths of bridge deck mixtures made with 50%, 100%, and 150% LWS1 moist-cured for 3 days were 3, 3, and 10 MPa (435, 435, and 1,450 psi) greater than the Bridge-Reference mixture. These values were 6, 8, and 7 MPa (870, 1,160 and 1,015 psi) for the mixture proportioned with LWS2.

The paving concrete mixtures generally exhibited greater compressive strength gains than the bridge deck mixtures when compared to the Reference mixtures. However, no clear relationship was shown in terms of LWS type and content. For example, the Paving-LWS3-50%, Paving-LWS3-100%, and Paving-LWS3-150% mixtures subjected to 3 days of moist curing developed 10, 11, 8 MPa (1,450, 1,595, and 1,160 psi) greater compressive strength compared to the Paving-Reference mixture. These values were 5, 8, 2 MPa (725, 1,160, and 290 psi) for the Standard curing condition.

5.2.3. Modulus of elasticity

Figure 5.5 presents the 56-day modulus of elasticity (MOE) results of selected mixtures made with different LWS types and contents. In general, the Paving-Reference mixture exhibited the highest 56-d MOE values of 39 and 47.5 GPa (5,655 and 6,890 ksi) under the 3D and Standard curing conditions. In the case of the bridge deck mixtures, the Bridge-LW2-100% and Bridge-LWS1-50% mixtures (Standard) the highest MOE value of 42.5 GPa (6,165 ksi). The Bridge-LWS2-150% concrete had the lowest MOE of 27.5 GPa (3,990 ksi).

Most of the 56-day MOE values of the investigated mixtures were equal or lower than the Reference mixture. Only the Bridge-LWS1-150% (3D) and Bridge-LWS2-100% mixtures showed 2.5 and 1 GPa (363 and 145 ksi) higher MOE compared to the Bridge-Reference mixture.

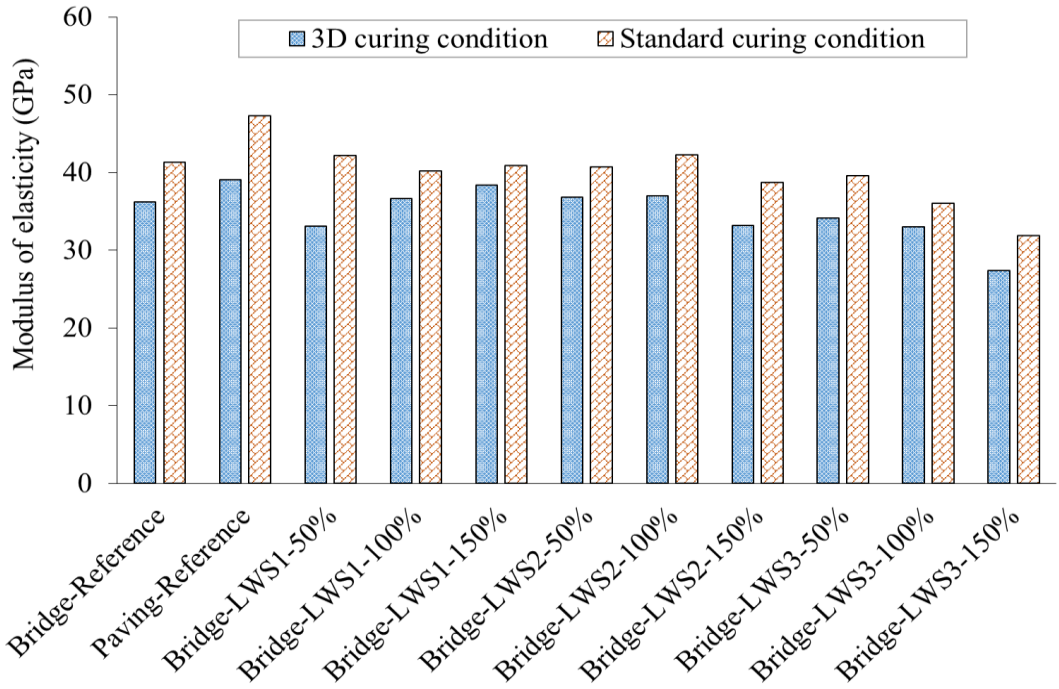

Figure 5.5: 56-day MOE results of various mixtures made with different LWS types and contents under 3D and Standard curing conditions (1GPa = 145 ksi)

Effect of LWS content

In the case of LWS3, the increase of LWS content reduced the MOE, regardless of curing condition. For example, the 50%, 100%, and 150% LWS3 mixtures subjected to 3D of curing resulted in MOE values of 34, 33, and 27.5 GPa (4,930, 4,785, and 3,990 ksi), respectively. These values were 39.5, 36, and 32 GPa (5,730, 5,220, and 4,640 ksi) for mixtures subjected to Standard curing. However, no clear trend was observed in terms of MOE development for the mixtures proportioned with LWS1 or LWS2.

Effect of LWS Type

No clear relationship was observed between the LWS type and MOE development.

Effect of curing condition

The mixtures cured under Standard condition obtained higher MOE compared to those under 3D curing condition. For example, the Bridge-LWS1-50%, Bridge-LWS1-100%, and Bridge-LWS1-150% mixtures developed the MOE values of 42, 40, and 41 GPa (6,090, 5,800, and 5,945 ksi), respectively, under Standard curing condition compared to 33, 36.5, 38.5 GPa (4,785, 5,295, and 5,585 ksi), respectively, under the 3D curing condition.

5.2.4. Flexural strength

The flexural strength results of the investigated mixtures are presented in Figure 5.6.

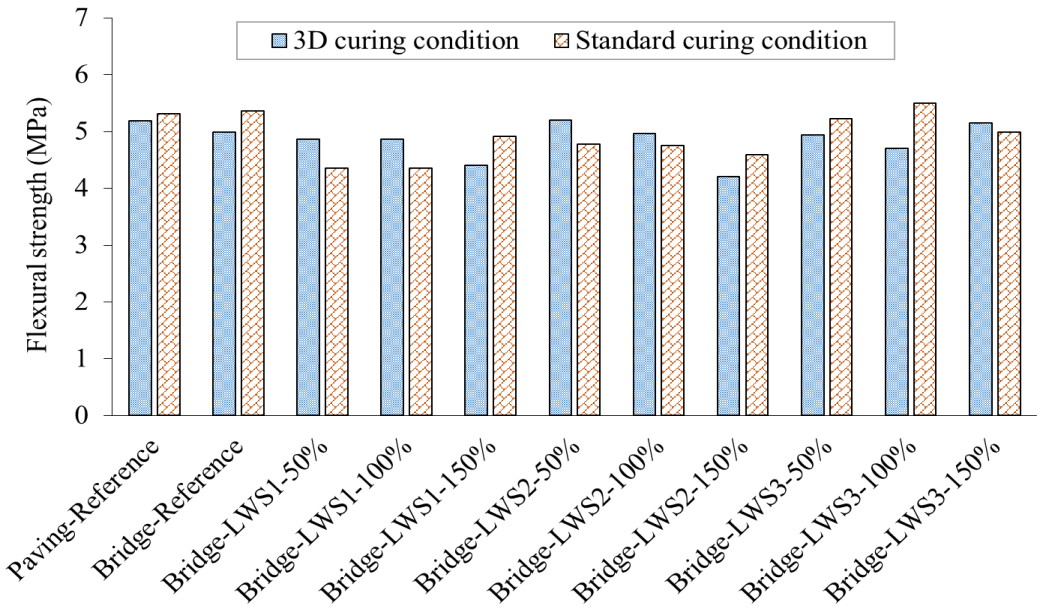

Figure 5.6: 56-day flexural strength results of the selected mixtures with different LWS types and contents under 3D and Standard curing conditions (1MPa = 145 psi)

The Bridge-LWS3-100% mixture cured under Standard condition had the highest flexural strength of 5.5 MPa (800 psi). On the other hand, the Bridge-LWS2-150% mixture with 4.2 MPa (580 psi) exhibited the lowest flexural strength when cured under the 3D curing condition. Compared to the Reference mixture, no clear relationship was observed between the flexural strength of the Reference mixture and the other mixtures made with LWS.

Effect of LWS content and Type

No clear relationship was observed between the flexural strength and LWS content. No clear

relationship was observed neither between the flexural strength development and the LWS type.

Effect of curing condition

No clear relationship was observed between the flexural strength and the curing condition.

5.2.5. Surface resistivity

Figure 5.7 compares the 56-day surface resistivity results of the bridge deck and paving concrete mixtures made with different LWS contents that were subjected to 3D and Standard curing conditions. As mentioned earlier, for each specimen, four separate readings were taken around the circumference of the cylinder at 90-degree increments (0°, 90°, 180°, and 270°). Measurements were repeated several times at each angle for the most reliable reading.

The longer initial moisture curing can provide denser microstructure, thus increasing surface resistivity. For example, the surface resistivity values for the Bridge-Reference mixture subjected to Standard and 3D curing conditions were 23.5 and 21.5 kΩ-cm (9.3 and 8.5 kΩ-in.), respectively. These values were 27.5 and 25.5 kΩ-cm (10.8 and 10.0 kΩ-in.) for Paving-Reference mixture.

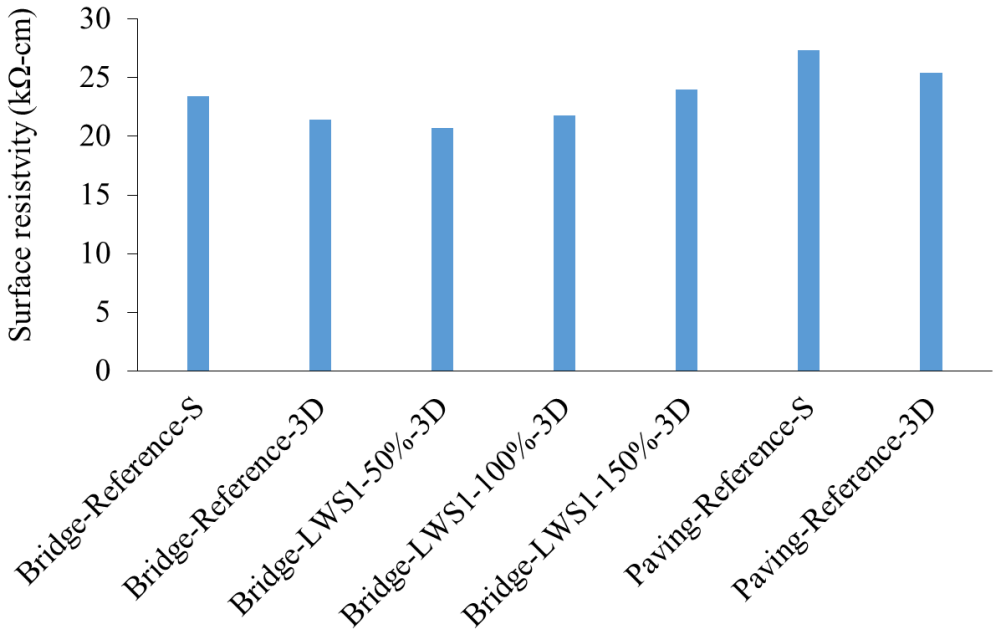

Figure 5.7: Surface resistivity results for bridge deck and paving concrete containing different LWS contents under 3D and Standard curing conditions at 56 days (1 kΩ-cm = 0.393 kΩ-in.)

Compared to the Reference mixture, the mixtures proportioned with LWS1 exhibited equal or higher surface resistivity values compared to the Reference mixture under 3D curing condition. Further, the increase of LWS1 content increased the surface resistivity. For example, the Bridge-LWS1-50% mixture had the same surface resistivity of 21 kΩ-cm (8.3 kΩ-in.) compared to the Bridge-Reference mixture under 3D curing condition while the Bridge-LWS1-100% and Bridge-LWS1-150% mixtures had 1 and 3 kΩ-cm (0.4 and 1.2 kΩ-in.) higher surface resistivity. As mentioned previously, the increase of the content of the saturated LWS1 led to greater cement hydration, thus reducing concrete porosity and increasing surface resistivity.

Effect of LWS content

The increase in LWS1 content enhanced the surface resistivity. The incorporation of 50%, 100%, and 150% LWS1 resulted in 21, 22, and 24 kΩ-cm (8.3, 8.7, and 9.5 kΩ-in.) surface resistivity for the Bridge-LWS1-50%, Bridge-LWS1-100%, and Bridge-LWS1-150% mixtures, respectively.

Effect of curing condition

The mixtures cured under Standard condition exhibited slightly higher surface resistivity values than those of the mixtures under 3D condition. For example, the Bridge-Reference and Paving-Reference mixtures cured under Standard curing condition exhibited 23.5 and 27.5 kΩ-cm (9.3 and 10.8 kΩ-in.) surface resistivity, which were 2 kΩ-cm (0.8 kΩ-in.) higher than the specimens cured under 3D curing condition.

5.2.6. Bulk electrical resistivity

In addition to the surface resistivity, the bulk resistivity of the specimens was measured. The same samples used for surface resistivity testing were used for measuring the bulk resistivity, according to ASTM C1760. Figure 5.8 presents the 56-day bulk resistivity results for bridge deck and paving concrete containing different LWS contents under 3D and Standard curing conditions.

Similar to surface resistivity results, the paving mixtures exhibited higher bulk resistivity values compared to bridge deck mixtures, regardless of curing condition. The Paving-Reference mixture with 91.5 kΩ-cm (36.2 kΩ-in.) had the highest bulk resistivity values compared to the other mixtures.

Effect of curing condition

The investigated mixtures under Standard conditions exhibited higher bulk resistivity values compared to those under 3D curing conditions. For example, the Bridge-Reference mixture with Standard curing condition had a bulk resistivity of 80 kΩ-cm (31.5 kΩ-in.) while this value was 68 kΩ-cm (26.8 kΩ-in.) for the Bridge-Reference mixture with 3D curing condition.

Effect of LWS content

Incorporation of LWS1 slightly increased bulk resistivity compared to the Reference mixture. For example, the Bridge-LWS1 mixture with 50% LWS with 70 kΩ-cm (27.6 kΩ-in.) had 2 kΩ-cm (0.8 kΩ-in.) higher values compared to that of the Bridge-Reference mixture. Increasing LWS content from 50% to 100% increased bulk resistivity by 4 kΩ-cm (1.6 kΩ-in.), under the same 3D curing condition.

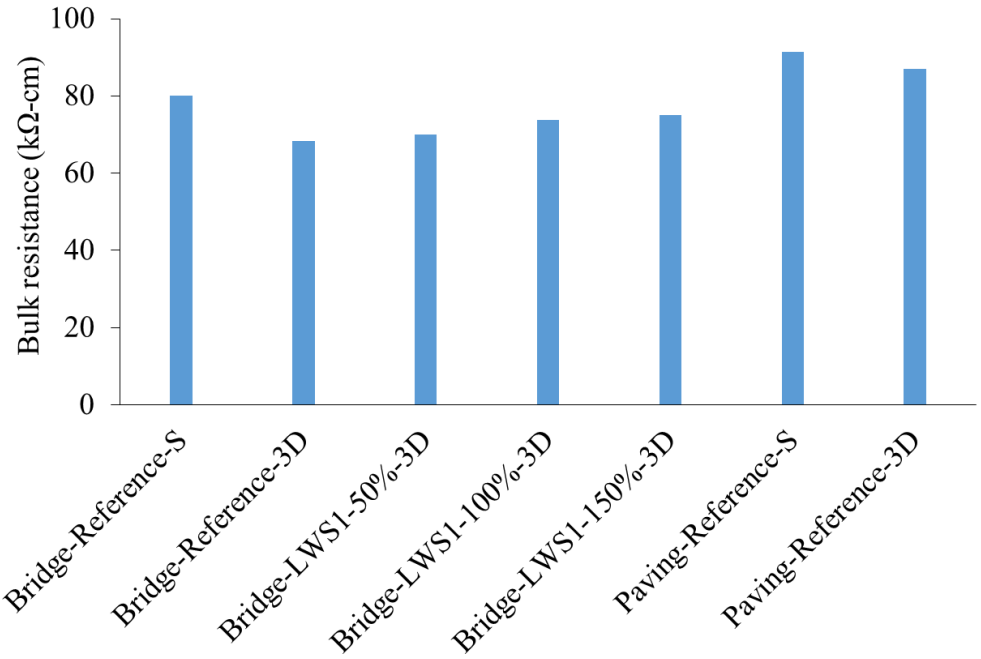

Figure 5.8: Bulk resistivity results for bridge deck and paving concrete containing different LWS contents under 3D and Standard curing conditions at 56 days (1 kΩ-cm = 0.393 kΩ-in.)

5.2.7. Sorptivity

The initial and secondary sorptivity results for bridge deck and paving concrete containing different LWS contents were determined. Results obtained from two curing regimes of 3D and

Standard curing conditions at 56 days are presented in Figures 5.9 and 5.10, respectively. The initial and secondary sorptivity results were determined based on the sorptivity measurements from 60 sec to 6 hour and from 24 hours to 7 days, respectively. As expected, the initial sorptivity values were greater than the secondary sorptivity values, regardless of the LWS type, LWS content, and curing conditions. The initial sorptivity values varied from 0.001 to 0.0017 mm/√s (3.94×10^{-5} and 6.69 x 10^{-5} in./√s) and from 0.0004 to 0.0007 mm/√s (1.57×10^{-5} and 2.76×10^{-5} in./√s) for the mixtures cured under 3D and Standard conditions, respectively. On the other hand, the secondary sorptivity values under 3D and Standard curing conditions ranged from 0.00045 to 0.00085 mm/√s (1.77×10^{-5} and 3.34×10^{-5} in./√s) and from 0.0002 to 0.0003 mm/√s (7.87×10^{-5} and 1.18×10^{-5} in./√s), respectively. The Paving-Reference mixture had 30% and 50% higher initial sorptivity values under 3D and Standard curing conditions, respectively, compared to those of the Bridge-Reference mixture.

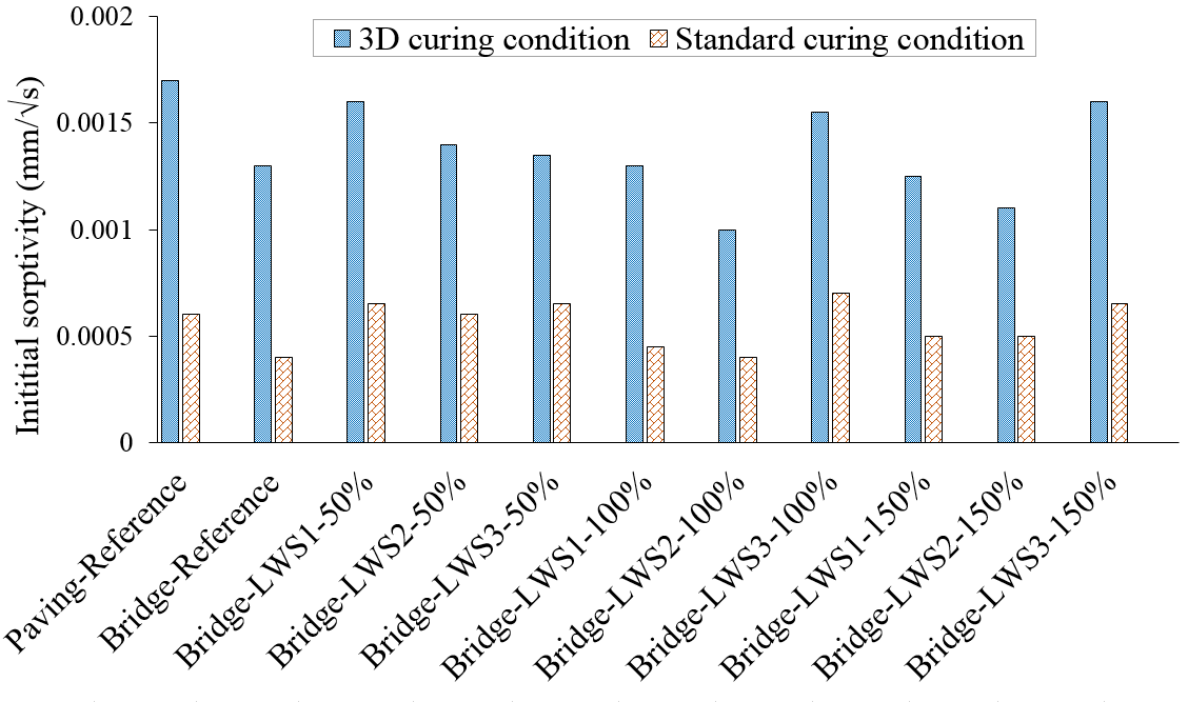

Figure 5.9: Initial sorptivity results for bridge deck and paving concrete containing different LWS contents under 3D and Standard curing conditions at 56 days (1 mm/√s = 0.039 in./√s)

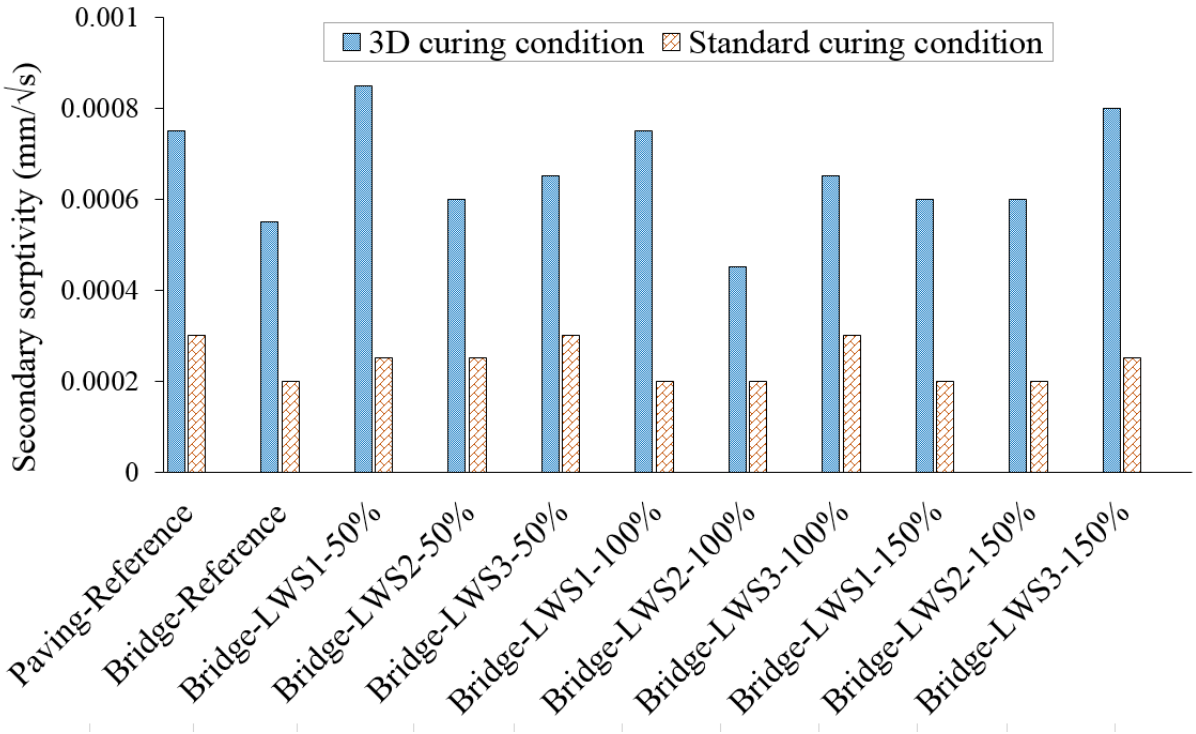

Figure 5.10: Secondary sorptivity results for bridge deck and paving concrete containing different LWS contents under 3D and Standard curing conditions at 56 days
(1 mm/√s = 0.039 in./√s)

Effect of curing condition

As shown in Figure 5.9 for the initial sorptivity results, and regardless of LWS type and content, the mixtures prepared under 3D curing condition exhibited significantly higher sorptivity values when compared to those under Standard curing condition. The same general trend was observed in the case of the secondary sorptivity values, as shown in Figure 5.10. For example, the second sorptivity of the Bridge-LWS1-50% mixture was 0.00085 mm/√s (3.34×10^{-5} in./√s) under 3D curing and 0.00025 mm/√s (9.84×10^{-5} in./√s) under Standard curing condition.

Effect of LWS type and content

At 50% LWS content under the 3D curing condition, the mixture made with LWS1 had the highest initial sorptivity of 0.0016 mm/√s (6.3×10^{-5} in./√s) followed by those proportioned with LWS2 and LWS3 with 0.0014 and 0.0013 mm/√s (5.51×10^{-5} and 5.12×10^{-5} in./√s) , respectively. However, at higher LWS contents of 100% and 150%, the mixtures containing LWS2 exhibited

the lowest initial sorptivity values of 0.0010 and 0.0011 mm/√s (3.93×10^{-5} and 4.33×10^{-5} in./√s), respectively, under the same curing condition of 3D. The same general trend was observed when the mixtures were cured under Standard curing condition. In the case of secondary sorptivity, the mixtures made with LWS2 exhibited the lowest secondary sorptivity values at 50%, 100%, and 150% LWS contents, regardless of curing condition.

In the case of LWS1, the initial sorptivity value decreased with an increase in LWS content. For instance, the mixtures made with 50, 100, and 150% LW1 exhibited the initial sorptivity values of 0.0016, 0.0013, and 0.00125 mm/√s (6.3×10^{-5}, 5.12×10^{-5}, and 4.92×10^{-5} in./√s), respectively, under 3D curing condition. However, the initial sorptivity value increased for higher LWS3 contents. For example, the Bridge-LWS3-50%, Bridge-LWS3-100%, and Bridge-LWS3-150% mixtures had initial sorptivity values 0.00135, 0.00155, 0.0016 mm/√s (5.31×10^{-5}, 6.1×10^{-5}, and 6.3×10^{-5} in./√s), respectively, under the same curing condition.

In the case of secondary sorptivity, the sorptivity decreased when the LWS1 content increased (under 3D curing condition). For example, the mixture proportioned with 150% LW1 exhibited the lowest secondary sorptivity of 0.0006 mm/√s (2.36×10^{-5} in./√s). However, no clear trend was observed with higher LWS2 and LWS3 contents.

5.2.8. Autogenous shrinkage

Figures 5.11 to 5.15 present the autogenous shrinkage developments of the investigated mixtures proportioned with different LWS contents. Results indicate that the incorporation of LWS at the level of 150% resulted in significant reduction in autogenous shrinkage compared to the Reference mixtures, followed by 100% and 50% LWS incorporation, regardless of LWS type. As expected, the Reference had the highest shrinkage values compared to other mixtures.

Figure 5.11 compares the autogenous shrinkage of the of bridge deck mixtures made with different contents of LWS1. The expansion increased with the LWS content where mixtures containing 50%, 100%, and 150% LWS exhibited maximum expansions of 3, 50 and 175 micro-strain, respectively, after 12 days. Following these peak values, the expansion gradually decreased in time. After 175 days of age, the mixture proportioned with 150% still had an expansion of 95 micro-strain, whereas those with 100% and 50% LWS exhibited autogenous shrinkage values of 150 and 200 micro-strain, respectively, compared to 420 micro-strain for the Reference mixture.

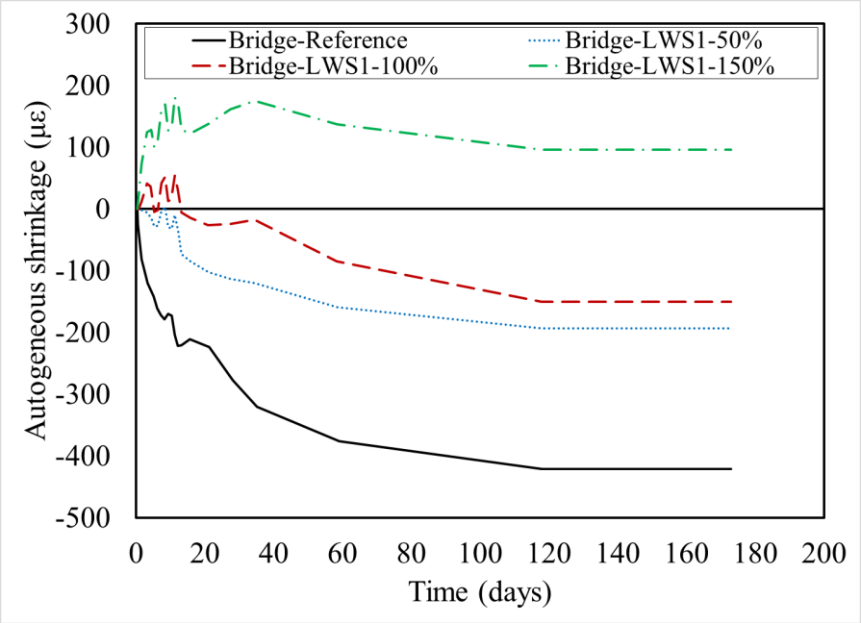

Figure 5.11: Autogenous shrinkage of bridge deck concrete with different LWS1 contents

Figures 5.12 and 5.13 compare the autogenous shrinkage variations for the bridge deck concrete mixtures containing LWS2 and LWS3, respectively. The same performance trend as LWS1 was observed. The Bridge-LWS2-150% and Bridge-LWS3-150% mixtures had the highest expansions of 190 and 200 micro-strain, respectively, at 7 days. These mixtures still exhibited an expansion after 175 days with strain values of 160 and 10 micro-strain. The mixtures proportioned with 50% and 100% of LWS2 resulted in low shrinkage values of 5 and 270 micro-strain. In the case of LW3, these values were 50 and 200 micro-strain at 175 days.

Similar to bridge deck concrete mixtures, the incorporation of LWS in the paving concrete mixtures had a significant effect on autogenous shrinkage. As shown in Figures 5.14 and 5.15, a greater content of LWS1 and LWS2 with 150% led to an expansion of 230 and 110 micro-strain at the ages of 5 and 20 days, respectively. The Paving-LWS1-150% mixture had an expansion of 20 micro-strain at 175 days where the Paving-LWS1-100% and Paving-LWS1-50% mixtures exhibited a shrinkage value of 65 and 150 micro-strain. As shown in Figure 5.15, the Paving-LWS2-150% and Paving-LWS2-100% mixtures still exhibited expansion of 50 and 20 micro-strain, respectively, after 175 days. The Paving-LWS2-50% mixture had a shrinkage value of 120 micro-strain at the same age. This shrinkage of the Paving-Reference mixture was 500 micro-strain under the same conditions. The autogenous shrinkage was not determined for paving concrete made

with LWS3 since the test results for bridge deck concrete made with LWS1 or LWS2 indicated that these LWS materials can secure lower shrinkage than concrete with LWS3.

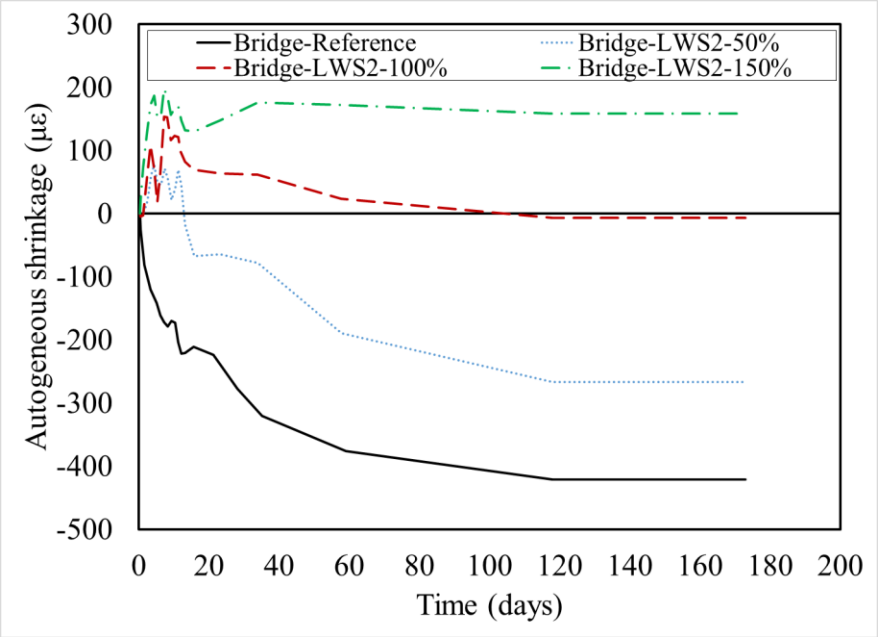

Figure 5.12: Autogenous shrinkage of bridge deck concrete with different LWS2 contents

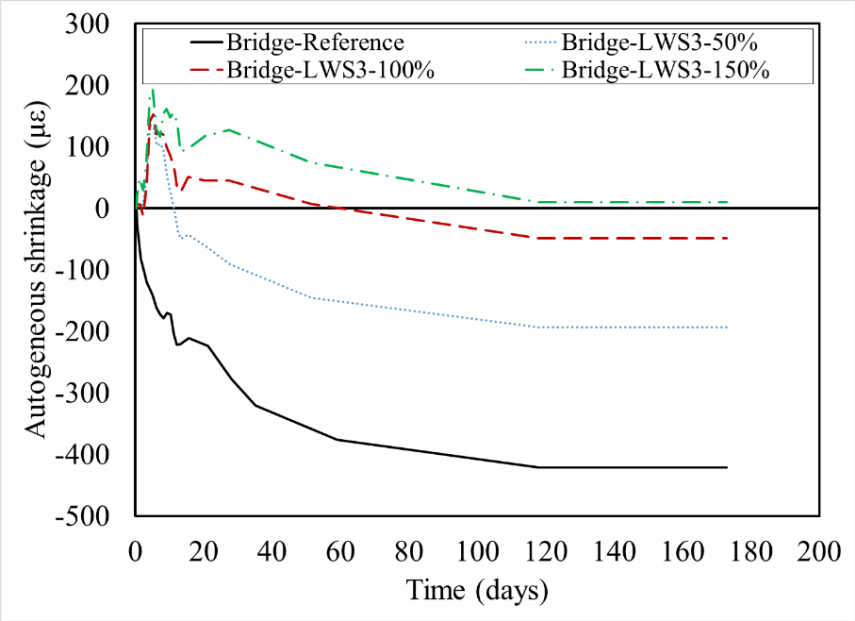

Figure 5.13: Autogenous shrinkage of bridge deck concrete with different LWS3 contents

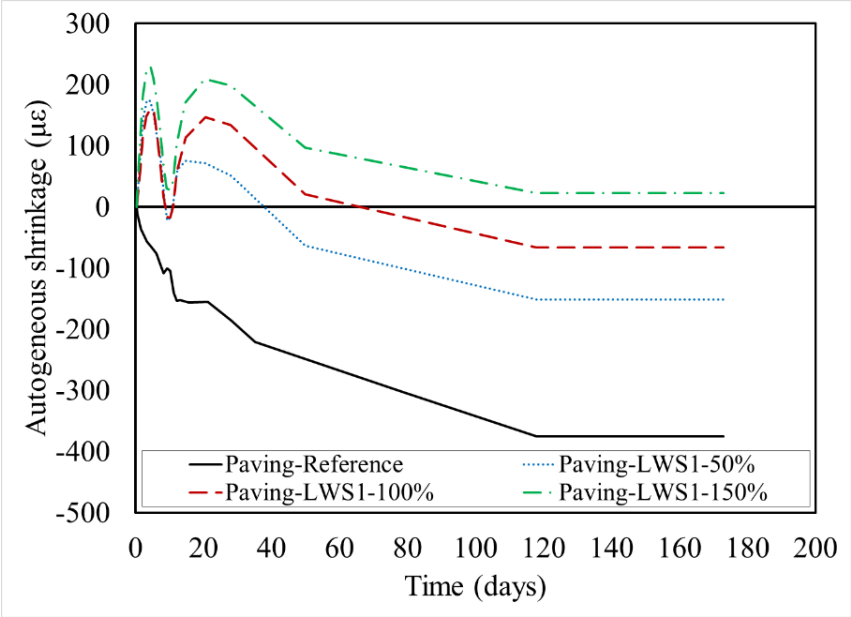

Figure 5.14: Autogenous shrinkage of paving concrete with different LWS1 contents

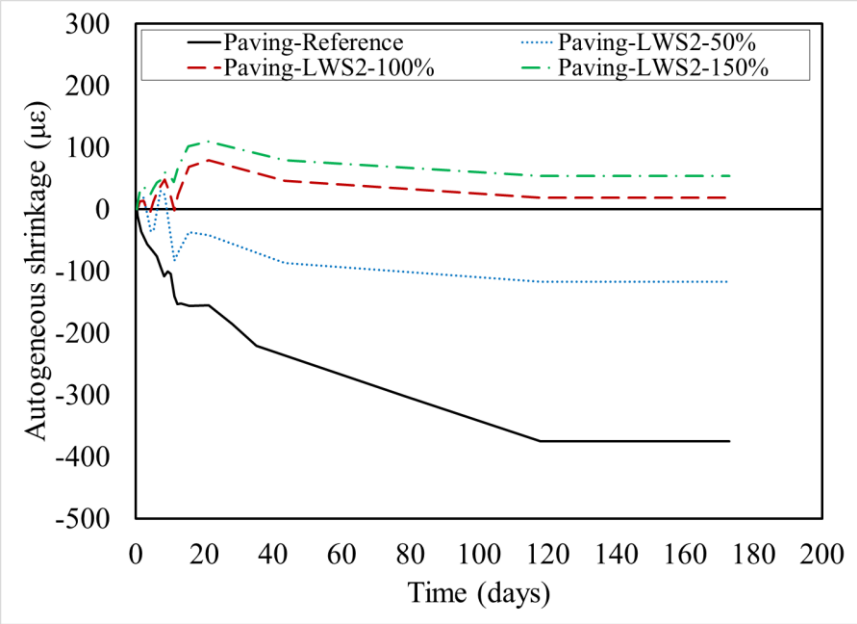

Figure 5.15: Autogenous shrinkage of paving concrete mixtures with different LWS2 contents

5.2.9. Drying shrinkage

Drying shrinkage was initiated following initial moist curing periods of either 3 or 28 days

corresponding to curing conditions of 3D and Standard, respectively. Figures 5.16 to 5.18 and 5.19 to 5.21 compare the variations of drying shrinkage for bridge deck concrete mixtures cured under 3D and Standard conditions, respectively.

The results indicate that all mixtures proportioned with LWS exhibited slight expansion (less than 100 micro-strain) during the moist curing period. The mixtures made with LWS3 showed the highest expansion values of 100 micro-strain compared to others. As shown in Figures 5.16 to 5.18 for bridge deck concrete mixtures, all mixtures proportioned with 50% and 150% LWS exhibited greater drying shrinkage than the Reference mixture, except the Bridge-LWS1-100% and the Bridge-LWS3-100% mixtures that had a shrinkage value of 420 micro-strain at 175 days. The Bridge-Reference mixture subjected to the 3D curing condition developed 490 micro-strain shrinkage at 175 days. For example, the drying shrinkage values at 175 days of the Bridge-LWS2-50%, Bridge-LWS2-100%, and Bridge-LWS2-150% mixtures were 520, 500, and 610 micro-strain, respectively.

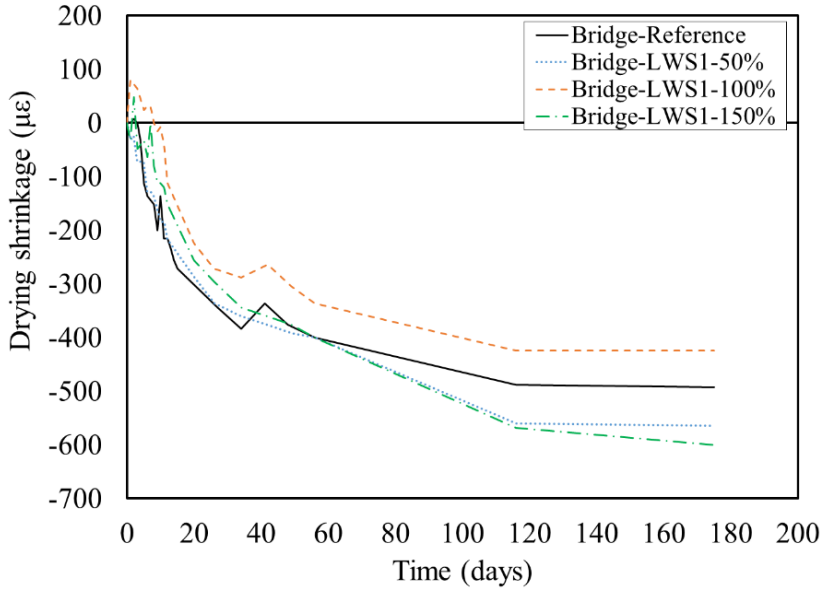

Figure 5.16: Drying shrinkage variations of bridge deck concrete mixtures with different LWS1 contents under 3D curing condition

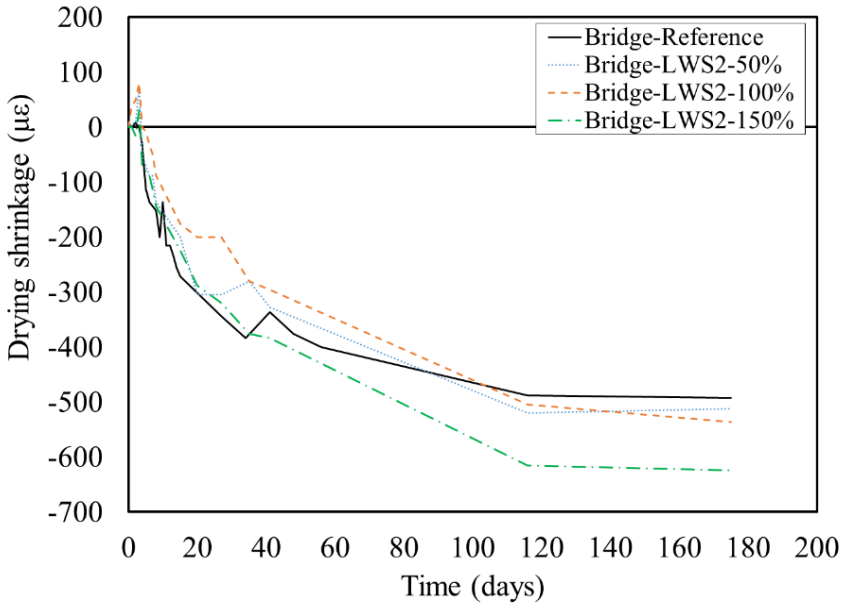

Figure 5.17: Drying shrinkage variations of bridge deck concrete mixtures with different LWS2 contents under 3D curing condition

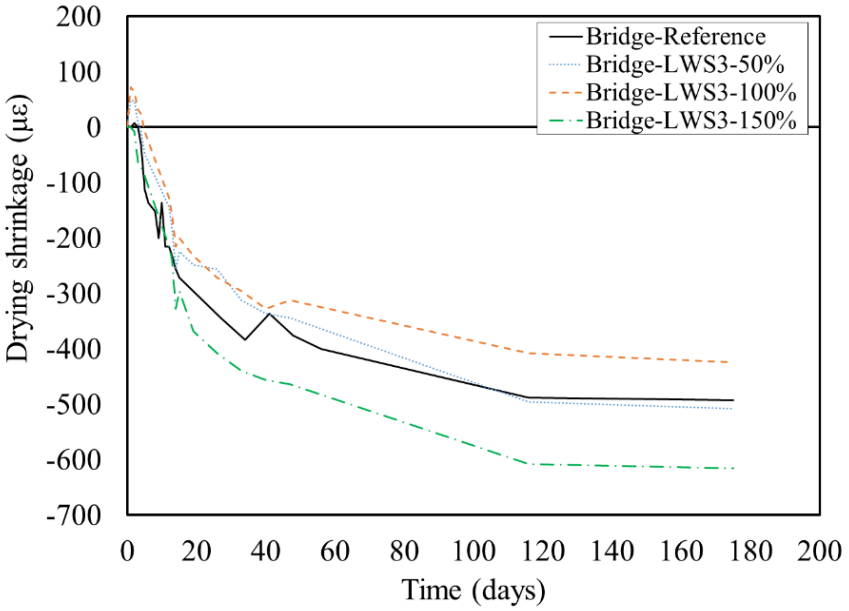

Figure 5.18: Drying shrinkage variations of bridge deck concrete mixtures with different LWS3 contents under 3D curing condition

All mixtures proportioned with LWS and cured under Standard condition exhibited lower drying shrinkage compared to those prepared under 3D curing condition. However, contrary to the

mixtures cured under 3D, the mixtures subjected to Standard curing condition had lower drying shrinkage compared to the Reference mixture that developed a drying shrinkage of 540 micro-strain at 175 days.

The increase in the LWS1 content reduced drying shrinkage. However, the mixtures incorporating LWS2 exhibited increase in drying shrinkage with the increase in LWS2 content. For example, after 175 days of Standard curing, the mixtures made with 50%, 100%, 150% LWS1 resulted in 450, 420, and 375 micro-strain, respectively, whereas those made with LWS2 were 410, 420, and 490 micro-strain, respectively.

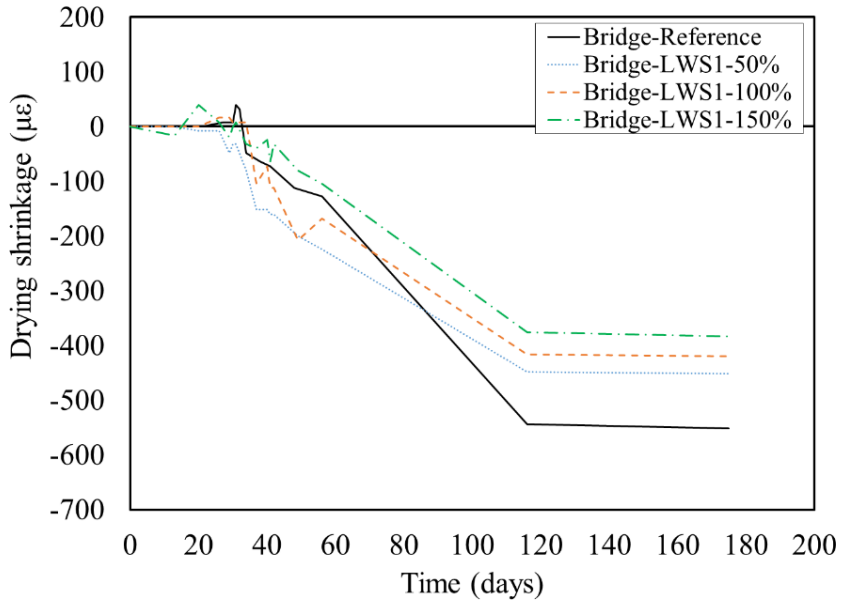

Figure 5.19: Drying shrinkage variations of bridge deck concrete mixtures with different LWS1 contents under Standard curing condition (28 days of moist curing)

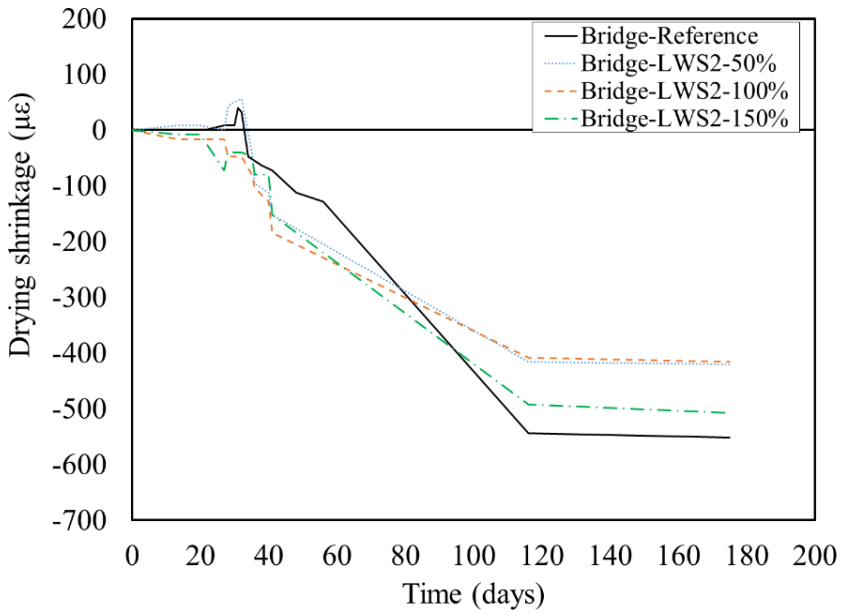

Figure 5.20: Drying shrinkage variations of bridge deck concrete mixtures with different LWS2 contents under Standard curing condition (28 days of moist curing)

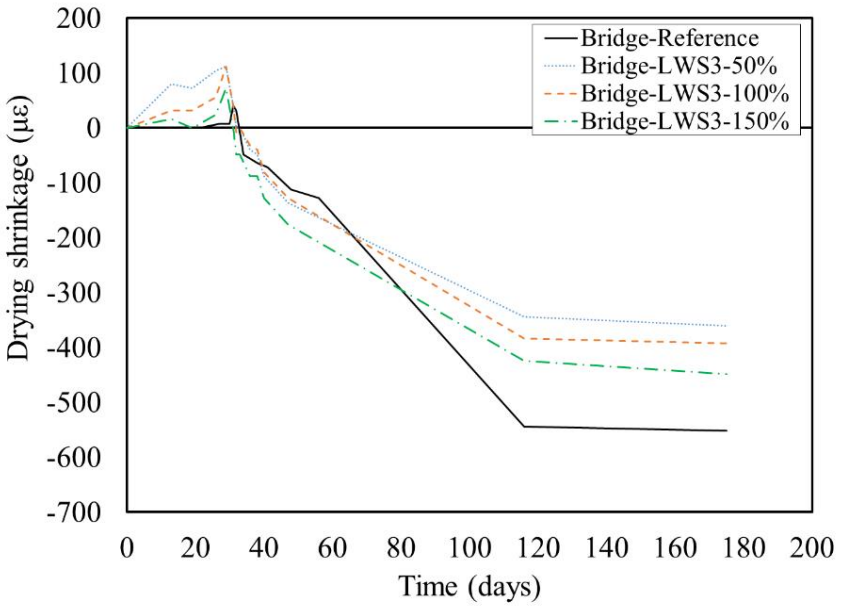

Figure 5.21: Drying shrinkage variations of bridge deck concrete mixtures with different LWS3 contents under Standard curing condition (28 days of moist curing)

In the case of the paving concrete, all 3D-cured mixtures made with LWS exhibited higher drying shrinkage values than that of the Reference mixture, except for the Paving-LWS2-100%

mixture that had a slight 35 micro-strain lower shrinkage. For example, the mixtures proportioned with 50%, 100%, and 150% LWS1 had drying shrinkage values of 500, 450, and 450 micro-strain, respectively, at 175 days compared to the Paving-Reference mixture that developed 410 micro-strain shrinkage under the 3D curing condition. The mixtures made with LWS3 had the highest drying shrinkage compared to those proportioned with LWS1 and LWS2. For example, for mixtures that had 3 days of initial moist curing condition, the 175-day drying shrinkage results of mixtures made with 50%, 100%, 150% LWS1 were 500, 450, and 450 micro-strain, respectively. These values were 550, 375, and 480 micro-strain, respectively, for mixtures with LWS2 and 640, 455, and 570 micro-strain, respectively, for those with LWS3.

Figures 5.22 to 5.24 present the drying shrinkage variations of paving concrete mixtures with different LWS contents with the 3D curing condition. Similarly, Figures 5.25 to 5.27 present the drying shrinkage variations of the paving concrete mixtures made with different LWS contents that received Standard curing. The results indicate a similar general trend for the 3D and the Standard curing conditions.

All mixtures made with LWS developed higher drying shrinkage values compared to the Reference mixture that was Standard cured that had 290 micro-strain after 175 days; this was in exception of the Paving-LWS1-150% and Paving-LWS3-150% mixtures. In the case of LWS1, the increase in LWS1 content resulted in drying shrinkage reduction. For example, the Paving-LWS1-50%, Paving-LWS1-100%, Paving-LWS1-150% mixtures had 340, 310, and 280 micro-strain, respectively. The incorporation of 50%, 100%, and 150% LWS2 and LWS3 led to drying shrinkage values of 310, 290, and 345 micro-strain (LWS2), respectively, and 310, 310, and 265 micro-strain (LWS3), respectively, all under Standard curing condition at 155 days.

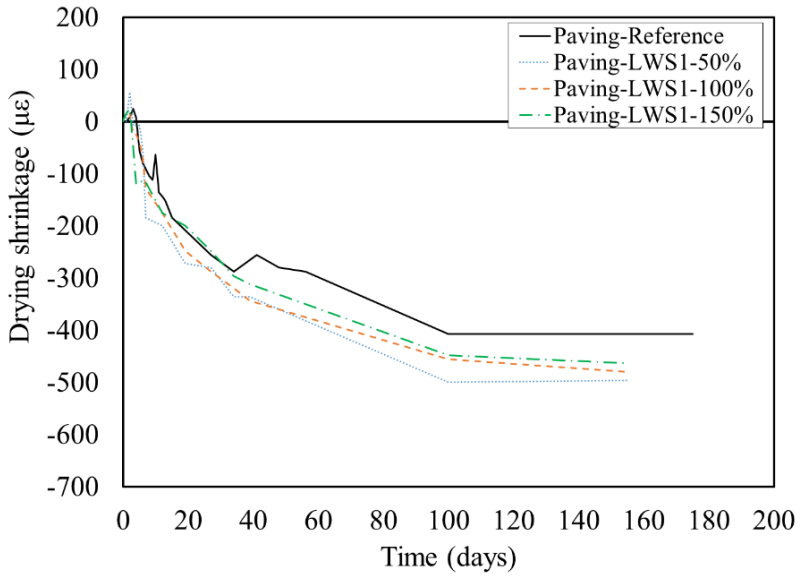

Figure 5.22: Drying shrinkage variations of paving concrete mixtures with different LWS1 contents under 3D curing condition

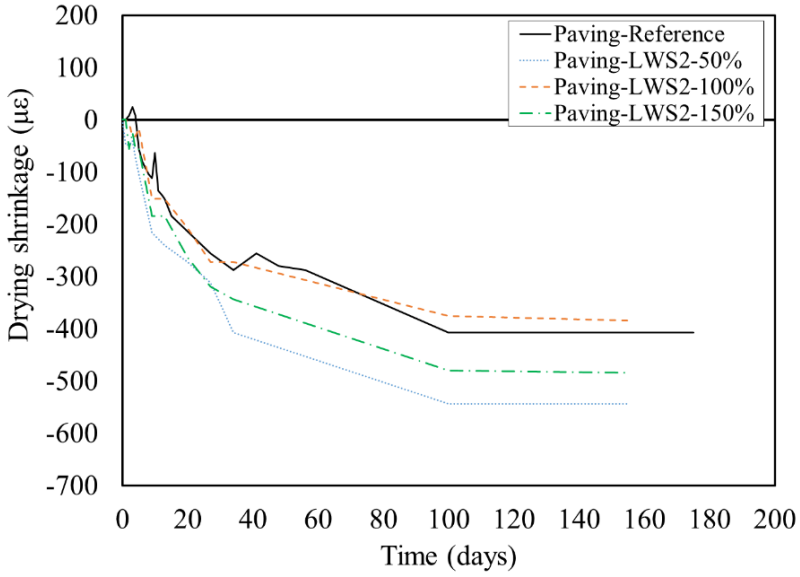

Figure 5.23: Drying shrinkage variations of paving concrete mixtures with different LWS2 contents under 3D curing condition

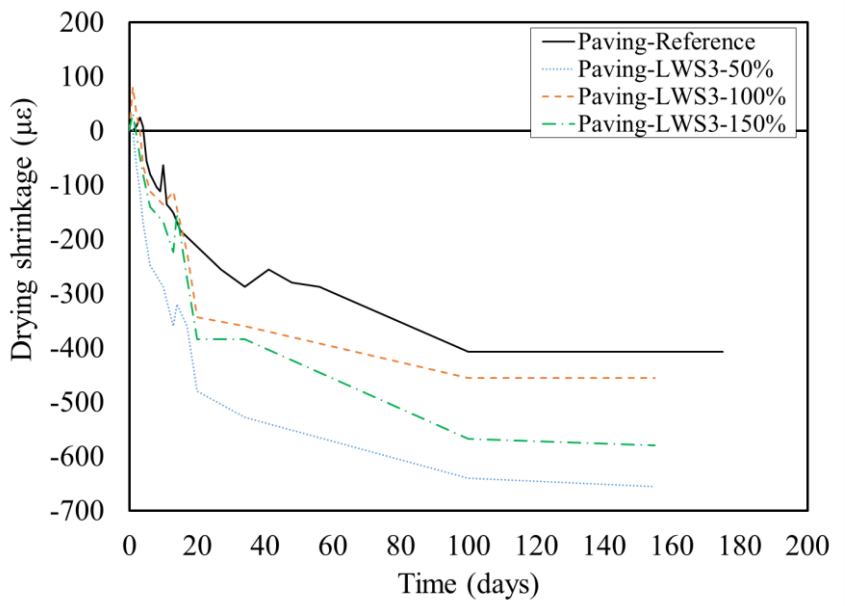

Figure 5.24: Drying shrinkage variations of paving concrete mixtures with different LWS3 contents under 3D curing condition

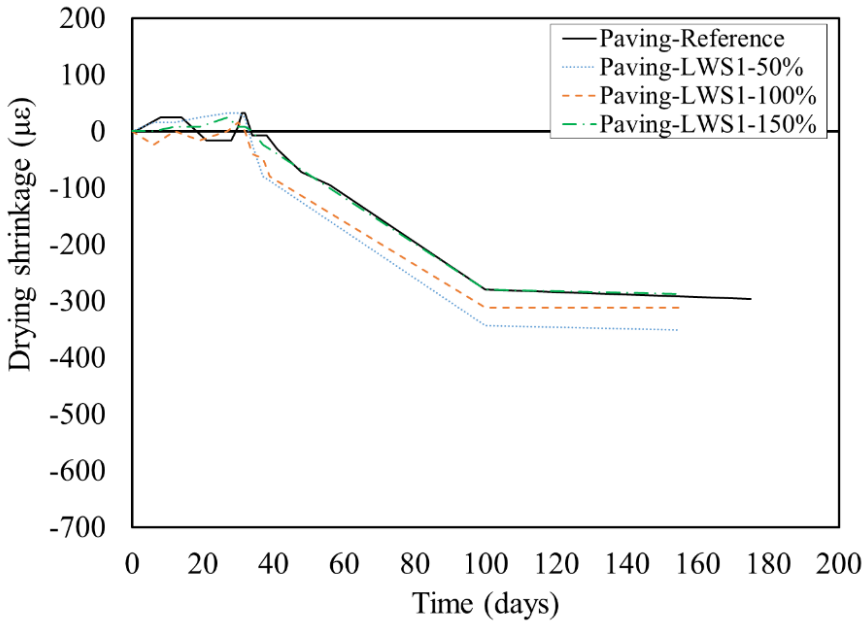

Figure 5.25: Drying shrinkage variations of paving concrete mixtures with different LWS1 contents under Standard curing condition (28 days of moist curing)

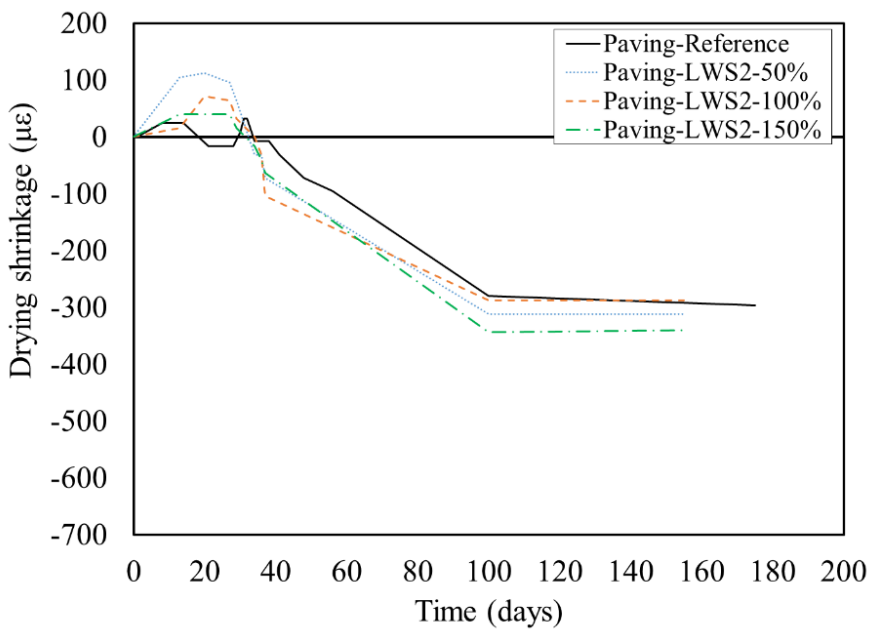

Figure 5.26: Drying shrinkage variations of paving concrete mixtures with different LWS2 contents under Standard curing condition (28 days of moist curing)

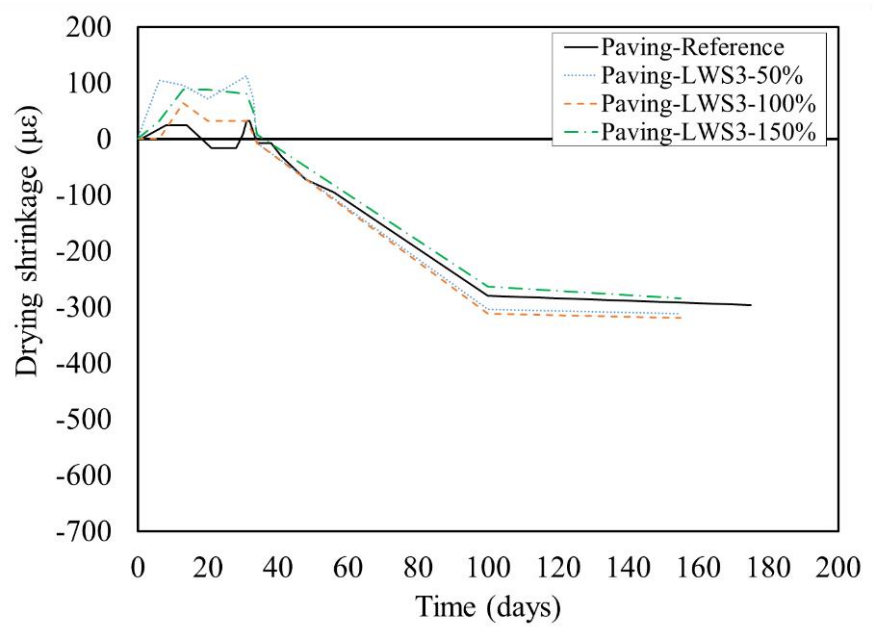

Figure 5.27: Drying shrinkage variations of paving concrete mixtures with different LWS3 contents under Standard curing condition (28 days of moist curing)

5.3 Summary

The effect of different LWS types and contents on mechanical properties, shrinkage, and durability were evaluated in this chapter. The results of the key properties of all investigated mixtures for the bridge deck concrete and paving concrete are compared in Tables 5.4 and 5.5, respectively. The results are normalized by the results obtained for the representative Reference mixtures made without any LWS. Therefore, enhancements of mechanical properties would be reflected in values greater than 100% and those of shrinkage would be reflected in values lower than 100%. Based on the test results, the following observations can be made:

(1) The 56-day compressive strengths of bridge deck mixtures made with 50%, 100%, and 150% LWS1 subjected to 3 days of moisture curing had 3, 3, and 10 MPa (435, 435, and 1,450 psi), respectively, greater values than the Bridge-Reference concrete. These values were 2, 1, and 8 MPa (290, 145, and 1,160 psi), respectively, under Standard curing condition.

(2) The bridge deck mixtures cured under 3D condition had up to 5 MPa (725 psi) higher 28-day compressive strength than those under Standard curing condition, regardless of the LWS type and content. In the case of paving mixtures, regardless of LWS type and content all mixtures subjected to 3 days of moist curing developed higher 28- and 56-day compressive strengths (up to 6 MPa (725 psi)) compared to those prepared under the Standard curing condition.

(3) For the bridge deck mixtures, the Bridge-LWS2-100% and Bridge-LWS1-50% mixtures exhibited the highest 56-day MOE of 42.5 GPa (6,615 ksi) under Standard curing compared to the other concrete mixtures. The Bridge-LWS2-150% subjected to 3D curing had a 56-day MOE of 27.5 GPa (3,990 ksi), which was the lowest MOE. Generally, the use of LWS reduces the MOE given the low MOE and density of LWS.

(4) The Bridge-LWS3-100% mixture cured under Standard condition (continuous moist curing) had the highest 56-day flexural strength of 5.5 MPa (800 psi). On the other hand, the Bridge-LWS2-150% mixture cured under 3D curing condition developed 4.2 MPa flexural strength, which was the lowest value. Applying Standard curing can, to some extent, improve the flexural properties. However, overall, the incorporation of LWS has a slightly negative effect on flexural properties.

(5) The mixtures prepared under 3D curing conditions exhibited significantly greater initial and secondary sorptivity values compared to those under Standard curing condition, regardless of the LWS type and content.

(6) The mixtures made with LWS2 presented the lowest sorptivity results, regardless of the curing condition and LWS content. This was in exception of concrete made with 50% LWS3 that showed slightly lower initial sorptivity compared to that made with LWS2 under 3D curing condition.

(7) The incorporation of LWS at the level of 150% resulted in significant reduction in autogenous shrinkage compared to the Reference mixtures, followed by 100% and 50% LWS, regardless of the LWS type. The Bridge-LWS2-150% exhibited the best performance in mitigating autogenous shrinkage with 160 micro-strain in expansion at 175 days.

(8) The lowest drying shrinkage at 175 days was obtained with the Bridge-LWS3-50% mixture (340 micro-strain) subjected to 28 days of moist curing. This was followed by the Bridge-LWS3-100% mixture (410 micro-strain) that received 3 days of moist curing.

(9) The lowest drying shrinkage at 155 days was obtained with the Paving-LWS3-150% mixture (265 micro-strain) subjected to 28 days of moist curing. This was followed by the Paving-LWS2-100% mixture (375 micro-strain) subjected to 3 days of moist curing.

(10) The incorporation of LWS1 slightly increased the surface and bulk resistivity, up 3 and 7 kΩ-cm (1.2 and 2.8 kΩ-in.), respectively, compared to the Reference mixture under the 3D curing condition. The highest surface and bulk resistivity values were obtained in mixtures containing 150% LWS1.

Table 5.4: Comparison of key properties of concrete with different type and content of LWS for bridge deck application (best performance is highlighted in **red**)

	3D curing condition			Standard curing condition			175-day autogenous shrinkage
	56-day compressive strength	56-day MOE	175-day drying shrinkage	56-day compressive strength	56-day MOE	175-day drying shrinkage	
Bridge-Reference	100%	100%	100%	100%	100%	100%	100%
Bridge-LWS1-50%	106%	92%	114%	104%	101%	83%	45%
Bridge-LWS1-100%	106%	97%	86%	103%	98%	78%	36%
Bridge-LWS1-150%	***120%***	***106%***	116%	***117%***	100%	69%	-23%
Bridge-LWS2-50%	112%	101%	106%	110%	98%	76%	64%
Bridge-LWS2-100%	117%	103%	102%	108%	***104%***	78%	2%
Bridge-LWS2-150%	115%	90%	124%	105%	93%	91%	***-38%***
Bridge-LWS3-50%	114%	94%	100%	107%	95%	***63%***	45%
Bridge-LWS3-100%	114%	93%	***84%***	107%	87%	71%	12%
Bridge-LWS3-150%	99%	75%	124%	96%	78%	79%	-2%

Table 5.5: Comparison of key properties of concrete with different type and content of LWS for paving application (best performance is highlighted in **red**)

	3D curing condition		Standard curing condition		175-day autogenous shrinkage
	56-day compressive strength	175-day drying shrinkage	28-day compressive strength	175-day drying shrinkage	
Paving-Reference	100%	100%	100%	100%	100%
Paving-LWS1-50%	116%	122%	115%	117%	41%
Paving-LWS1-100%	129%	110%	117%	107%	17%
Paving-LWS1-150%	***135%***	110%	***124%***	97%	-6%
Paving-LWS2-50%	121%	134%	111%	107%	31%
Paving-LWS2-100%	115%	***91%***	104%	100%	-5%
Paving-LWS2-150%	122%	117%	115%	119%	***-14%***
Paving-LWS3-50%	121%	156%	111%	107%	-
Paving-LWS3-100%	123%	111%	116%	107%	-
Paving-LWS3-150%	116%	139%	104%	***91%***	-

6. **References**

ACI Committee 213 (2014), "ACI 213R-14: Guide for Structural Lightweight-Aggregate Concrete" Manual of Concrete Practice, American Concrete Institute, Farmington Hills, MI.

Aïtcin, P.C. (2011). "High Performance Concrete." CRC Press.

Al-Khaiat, H., and Haque, M.N. (1998). "Effect of Initial Curing on Early Strength and Physical Properties of a Lightweight Concrete" Cement and Concrete Research, 28(6), pp. 859-866.

American Concrete Institute (2016), "ACI CR-16: Concrete Terminology" Manual of Concrete Practice, American Concrete Institute, Farmington Hills, MI.

ASTM Standard Volume C, ASTM International, West Conshohocken, PA.

Bangham, D. H. and Fakhoury, N. (1931), "The Translation Motion of Molecules in the Adsorbed Phase on Solids." Journal of the Chemical Society, pp. 1324-1333.

Bao, Y., Meng, W., Chen, Y., Chen, G., Khayat, K.H. (2015). "Measuring Mortar Shrinkage and Cracking by Pulse Pre-Pump Brillouin Optical Time Domain Analysis with a Single Optical Fiber" Material Letter, 145, pp. 344-346.

Bao, Y., Valipour, M., Meng, W., Khayat, K.H., Chen, G. (2017). "Distributed Fiber Optic Sensor-Enhanced Detection and Prediction of Shrinkage-Induced Delamination of Ultra-High-Performance Concrete Bonded over an Existing Concrete Substrate" Smart Materials and Structures, 26(8), 085009 (12 p).

Bentur, A., Igarashi, S., and Kovler, K. (2001). "Prevention of Autogenous Shrinkage in High-Strength Concrete by Internal Curing Using Wet Lightweight Aggregates" Cement and Concrete Research, 31, pp. 1587-1591.

Bentur, A., Igarashi, S., and Kovler, K. (1999). "Control of Autogenous Shrinkage Stresses and Cracking in High Strength Concretes" Proc. of 5th Int. Symp. of High Strength/High Performance Concrete Sandefjord, Norway, pp. 1017-1026.

Bentz, D.P. (2009). "Influence of Internal Curing Using Lightweight Aggregates on Interfacial Transition Zone Percolation and Chloride Ingress in Mortars" Cement and Concrete Composites, 31, pp. 285-289.

Bentz, D.P., Halleck, P.M., Grader, A.S., and Roberts, J.W. (2006). "Direct Observation of Water Movement during Internal Curing Using X-Ray Microtomography" Concrete International, 28 (10), pp. 39-45.

Bentz, D., Lura, P., and Roberts, J. (2005). "Mixture Proportioning for Internal Curing" Concrete International, 27 (2), pp. 35-40.

Bentz, D., and Weiss, J. (2011). "Internal Curing: A 2010 State-Of-The-Art Review" NISTIR 7765, U.S. Department of Commerce.

Bentz, D.P., and Snyder, K.A. (1999), "Protected Paste Volume in Concrete - Extension to Internal Curing Using Saturated Lightweight Fine Aggregate" Cement and Concrete Research, 29, pp. 1863-1867.

Bentz, D.P., and Stutzman, P.E. (2006), "Curing, Hydration, and Microstructure of Cement Paste" ACI Materials Journal, V. 103, No. 5, pp. 348-356.

Bentz, D.P., and Stutzman, P.E. (2008), "Internal Curing and Microstructure of High Performance Mortars" ACI SP-256, Internal Curing of High Performance Concretes: Laboratory and Field Experiences. Oct 1:81-90.

Beushausen, H., and Gillmer, M. (2014). "The Use of Superabsorbent Polymers to Reduce Cracking of Bonded Mortar Overlays." Cement and Concrete Composites, 52, pp. 1-8.

Bremner, T.W., and Holm, T.A. (1986). "Elastic Compatibility and the Behavior of Concrete." Journal of American Concrete International. 83, pp. 244-250.

Castro, J., Keiser, L., Golias, M., and Weiss, J. (2011). "Absorption and Desorption Properties of Fine Lightweight Aggregate for Application to Internally Cured Concrete Mixtures" Cement and Concrete Composites, 33(10), pp. 1001-1008.

Chia, K.S., and Zhang, M. (2002). "Water Permeability and Chloride Penetrability of High Strength Lightweight Aggregate Concrete" Cement and Concrete Research, 32, pp. 639-645.

Cohen, M.D., Olek, J., and Dolch, W.L. (1990). "On the Action of Capillary Pressure in Fresh Concrete" Cement and Concrete Research, 20, pp. 103-119.

Cusson, D., Lounis, Z., and Daigle, L. (2010). "Benefits of Internal Curing on Service Life and Lifecycle Cost of High-Performance Concrete Bridge Decks - a Case Study" Cement and Concrete Composites, 32, pp. 339-350.

De la Varga, I., and Graybeal, B. (2015), "Dimensional Stability of Grout-Type Materials Used as Connections between Prefabricated Concrete Elements" ASCE J. Mater. Civ. Eng. 27(9), 127 p.

EFNARC. (2002). "Specification and Guidelines for Self-Compacting Concrete" European Federation for Specialist Construction Chemicals and Concrete Systems, Norfolk, UK, English edition.

Ferraris, C. F. and Wittman, F. H. (1987), "Shrinkage Mechanisms of Hardened Cement Paste" Cement and Concrete Research, 17, pp. 453-464.

Geiker, M.R., Bentz, D.P., and Jensen, O.M. (2004). "Mitigating Autogenous Shrinkage by Internal Curing" in: J.P. Ries, T.A. Holm (Eds.), ACI SP-218, High Performance Structural Lightweight Concrete, American Concrete Institute, Farmington Hills, MI, pp. 143–154.

Greenspan, L. (1977). "Humidity Fixed Points of Binary Saturated Aqueous Solutions" Journal of Research of the National Bureau of Standards Section A: Physics and Chemistry, 81A(1), 89 p.

Habeeb, G.A., and Fayyadh, M.M. (2009). "Rice Husk Ash Concrete: the Effect of RHA Average Particle Size on Mechanical Properties and Drying Shrinkage" Australia Journal Basic Applied Science, 3(3), pp. 1616-1622.

Henkensiefken, R. (2008). "Internal Curing in Cementitious Systems Made Using Saturated Lightweight Aggregate" PhD Diss., Purdue University, 2008.

Henkenseifken, R., Castro, J., Bentz, D., Nantung, T., and Weiss, J. (2009). "Water Absorption in Internally Cured Mortar Made with Water-Filled Lightweight Aggregate" Cement and Concrete Research, 39, pp. 883-892.

Hiller, K. H. (1964). "Strength Reduction and Length Changes in Porous Glass Caused by Water Vapor Adsorption" Journal of Applied Physics, 35(5), pp. 1622-1628.

Holm, T.A., Ooi, O.S., and Bremner, T.W. (2003). "Moisture Dynamics in Lightweight Aggregate and Concrete" in: J.P. Ries, T.A. Holm (Eds.), Theodore Bremner Symp. on High-Performance Lightweight Concrete, Proc. 6th Int, Conf. on Durability of Concrete, Thessalonika, Greece, pp. 167-184.

Hooton, R.D., Mesic, T., and Beal, D.L. (1993). "Sorptivity Testing of Concrete as an Indicator of Concrete Durability and Curing Efficiency" Proc. of the 3rd Canadian Symp. On Cement and Concrete, Ottawa, Ont., Canada, pp. 264-275.

Hwang, S., Khayat, K.H., and Youssef, D. (2013). "Effect of Moist Curing and Use of Lightweight Sand on Characteristics of High-Performance Concrete" ACI Materials Journal, 46 (1-2), pp. 35-46.

Hwang, S.D., Lepesqueux, E., and Khayat, K.H. (2017). Effect of Lightweight Aggregate Volume on Key Properties of SCC Designated for Repair Applications, Jr. of Sustainable Cement-Based Materials, 15, pp. 1-20.

Jensen, O.M., and Hansen, P.F. (2001). "Water-Entrained Cement-Based Materials, I: Principles and Theoretical Background" Cement and Concrete Research, 31, pp. 647-654.

Jensen, O.M., and Hansen, P.F. (2002). "Water-Entrained Cement-Based Materials II: Experimental Observations" Cement and Concrete Research, 32, pp.973-978.

Jozwiak-Niedzwiedzka, D. (2005). "Scaling Resistance of High Performance Concretes Containing a Small Portion of Pre-Wetted Lightweight Fine Aggregate" Cement and Concrete Composites, 27, pp. 709-715.

Justs, J., Wyrzykoski, M., Winnefeld, F., Bajare, D., and Lura, P. (2014). "Influence of Superabsorbent Polymers on Hydration of Cement Pastes with Low Water-To-Binder Ratio" Journal of Thermal and Analytical Calorimetry, 115, pp. 425-432.

Justs, J., Wyrzykoski, M., Bajare, D., and Lura, P. (2015). "Internal Curing by Superabsorbent Polymers in Ultra-High Performance Concrete" Cement and Concrete Research, 76, pp. 82-90.

Lam, H., (2005), "Effects of Internal Curing Methods on Restrained Shrinkage and Permeability" M.Sc. Thesis, University of Toronto.

Lam, H., and Hooton, R.D., (2005), "Effects of Internal Curing Methods on Restrained Shrinkage and Permeability," in Proceedings of the 4th International Seminar: Self-Desiccation and Its Importance in Concrete Technology, B. Persson, D. Bentz, and L.-O. Nilsson, eds., Gaithersburg, MD, pp. 210-228.

Lura, P. and Bisschop, J. (2004). "On the Origin of Eigenstresses in Lightweight Aggregate Concrete" Cement and Concrete Composites, 26 (5), pp. 445-452.

Lura, P., Wyrzykowski, M., Tang, C., and Lehmann, E. (2014). “Internal Curing with Lightweight Aggregate Produced from Biomass-Derived Waste” Cement and Concrete Research, 59, pp. 24-33.

Lura, P., and van Breugel, K. (2000). “Moisture Exchange as a Basic Phenomenon to Understand Volume Changes of Lightweight Aggregate Concrete at Early Age” in: V. Baroghel-Bouny, P.C. Aitcin (Eds.), Proc. Int. Workshop on Shrinkage of Concrete Paris, pp. 533-546.

L'Hermite, R. G. (1960). “Volume Changes of Concrete” In Proceedings of the Fourth International Symposium on the Chemistry of Cement, Washington, D.C., Vol. II, pp. 659-694.

Maruyama, I., and Sato, R. (2005). “A Trial of Reducing Autogenous Shrinkage by Recycled Aggregate” Gaithersburg (MD), USA, in: B. Persson, D.P. Bentz, L.O. Nilsson (Eds.), Proc. 4th Int. Sem. on Self-Desiccation and Its Importance in Concrete Technology, pp. 264-270.

Mechtcherine, V., and Dudziak, L., and Hempel, S. (2009). “Internal Curing to Reduce Cracking Potential of Ultra High Performance Concrete by Means of Super Absorbent Polymers” Proc of 2nd International RILEM Workshop on Concrete Durability and Service Life Planning, (2009) pp. 31-38.

Mehta, P.K. (1986). “Concrete: Structure, Properties, and Materials” Prentice Hall.

Meng, W., and Khayat, K.H. (2017). “Mechanical Properties of Ultra-High-Performance Concrete Enhanced with Graphite Nanoplatelets and Carbon Nanofibers” Composite part B: Engineering, 107, pp. 113-122.

Meng, W., and Khayat, K.H. (2017). “Improving Flexural Performance of Ultra-High-Performance Concrete by Rheology Control of Suspending Mortar.” Composites part B: Engineering, 117, pp. 26-34.

Meng, W., Valipour, M., Khayat, K.H. (2017). “Optimization and Performance of Cost-Effective Ultra-High Performance Concrete” Materials and Structures, 50, 29 p.

Mindess, S., Young, J.F., and Darwin, D. (2003). “Concrete” Pearson Education, 2nd Edition.

Miller, A. E., Barrett, T. J., Zander, A. R., and Weiss, W. J. (2014). “Using a Centrifuge to Determine Moisture Properties of Lightweight Fine Aggregate for Use in Internal Curing” Advances in Civil Engineering Materials, 3(1).

Mindess, S., Young, J. F., and Darwin, D. (2003). Concrete (2nd ed.). Upper Saddle River, NJ: Pearson Education Inc.

Mohr, B.J., Premenko, L., Nanko, H., and Kurtis, K.E. (2005). “Examination of Wood-Derived Powders and Fibers for Internal Curing of Cement-Based Materials” Gaithersburg (MD), USA, in: B. Persson, D.P. Bentz, L.O. Nilsson (Eds.), Proc. 4th Int. Sem. on Self-Desiccation and Its Importance in Concrete Technology, pp. 229-244.

Nguyen, V.T. (2011). “Rice Husk Ash as a Mineral Admixture for Ultra High Performance Concrete” Ph.D. Dissertation, Delft University, Netherlands.

Paulini, P. (1992). “A Weighing Method for Cement Hydration” In 9th International Congress on the Chemistry of Cement: New Delhi, India, 1992 (pp. 248-254). New Delhi: National Council for Cement and Building Materials.

Powers, T. C., and Brownyard, T. L. (1946). "Studies of the Physical Properties of Hardened Portland Cement Paste." American Concrete Institute Journal Proceedings, 43 (9).

Powers, T.C. (1947). "A Discussion of Cement Hydration in Relation to the Curing of Concrete" In Proceedings of the Highway Research Board 27th Annual Meeting, Washington, D.C.. pp. 178-188.

Powers, T.C. (1960). "Physical Properties of Cement Paste" In Proceedings of the Fourth International Symposium on the Chemistry of Cement (Vol. II, pp.577-613). Washington, D.C.

Rockland, L. B. (1960). "Saturated Salt Solutions for Static Control of Relative Humidity between 5º And 40 ºC" Analytical Chemistry, 32(10), pp. 1375-1376.

RILEM TC-196 (2007). "Internal Curing of Concrete, State-Of-The-Art Report of RILEM Technical Committee 196-ICC" in: K. Kovler, O.M. Jensen (Eds.), RILEM Publications S.A.R.L, France, Bagneux, 139 p.

Schwesinger, P., and Sickert, G. (2000). "Reducing Shrinkage in HPC by Internal Curing by Using Pre-Soaked LWA." Proc. Int. Workshop on Control of Cracking in Early-Age Concrete, Tohoku University, Japan, pp. 313-318.

Wasserman, R., and Bentur, A. (1996). "Interfacial Interactions in Lightweight Aggregate Concretes and Their Influence on the Concrete Strength" Cement and Concrete Composites, 18, pp. 67-76.

Wei, Y. (2009). "Modeling of Autogenous Deformation in Cementitious Materials, Restraining Effect from Aggregate, and Moisture Warping in Slabs on Grade" (Doctoral dissertation, University of Michigan, 2008), Ann Arbor, MI: ProQuest LLC.

Wittman, F. H. (1976). "On the Action of Capillary Pressure in Fresh Concrete" Cement and Concrete Research, 6, pp. 49-56.

van Breugel, K., Outwerk, H., and de Vries, J. (2000). "Effect of Mixture Composition and Size Effect on Shrinkage of High Strength Concrete" in: V. Baroghel-Bouny, P.C. Aitcin (Eds.), Proc. Int. Workshop on Shrinkage of Concrete Paris, pp. 161-177.

Van, V.T.A., Rößler, C., Bui, D.D., and Ludwig, H.M. (2014) "Rice Husk Ash as both Pozzolanic Admixture and Internal Curing Agent in Ultra-High Performance Concrete" Cement and Concrete Composites. 53, pp. 270-278.

Yu, R., Spiesz, P., and Brouwers, H.J. (2014). "Mix Design and Properties Assessment of Ultra-High Performance Fiber Reinforced Concrete (UHPFRC)" Cement and Concrete Research, 28 (56), pp. 29-39.

Zhang, M.H., and Gjørv, O.E. (1990). "Microstructure of the Interfacial Zone Between Lightweight Aggregate and Cement Paste" Cement and Concrete Research, V. 20, 1990, pp. 610-618.

Zhang, M. and Gjørv, O.E. (1992). "Penetration of Cement Paste Into Lightweight Aggregate" Cement and Concrete Research, 22, pp. 47-55.

Zhang, T., Yu, Q., Wei, J., Gao, P., and Zhang, P. (2012) "Study on Optimization of Hydration

Process of Blended Cement" Journal of Thermal and Analytical Calorimetry. 107, pp. 489-498.

Zhutovsky, S., and Kovler, K. (2012) "Effect of Internal Curing on Durability-Related Properties of High Performance Concrete" Cement and Concrete Research, 42, pp. 20-26.

Zhutovsky, S., Kovler, K., and Bentur, A. (2002). "Autogenous Curing of High-Strength Concrete Using Pre-Soaked Pumice and Perlite Sand" Lund, Sweden, in: B. Persson, G. Fagerlund (Eds.), Proc. 3rd Int. Sem. on Self-Desiccation and Its Importance in Concrete. Technology, pp. 161-173.

Zhutovsky, S., Kovler, K., and Bentur, A. (2004). "Influence of Cement Paste Matrix Properties on the Autogenous Curing of High-Performance Concrete" Cement and Concrete Composites, 26, pp. 499-507.

Zhutovsky, S., Kovler, K., and Bentur, A. (2001). "Influence of Wet Lightweight Aggregate on Autogenous Shrinkage of Concrete at Early Ages" in: F.-J. Ulm, Z.P. Bazant, F.H. Wittmann (Eds.), Proc. 6th Int. Conf. Creep, Shrinkage and Durability Mechanics of Concrete and Other Quasi-Brittlematerials Cambridge (MA), USA, pp. 697-702.

Zhutovsky, S., Kovler, K., and Bentur, A. (2001). "Efficiency of Lightweight Aggregates for Internal Curing of High Strength Concrete to Eliminate Autogenous Shrinkage" Haifa, Israel, in: K. Kovler, A. Bentur (Eds.), Proc. RILEM Int. Conf. on Early Age Cracking in Cementitious Systems, pp. 365-374.